

**A STUDY ON ADAPTIVE ARRAY ANTENNA FOR OFDM MOBILE
RECEPTION**

PUBUDU SAMPATH WIJESENA

**THE UNIVERSITY OF ELECTRO-COMMUNICATIONS
MARCH 2006**

A STUDY ON ADAPTIVE ARRAY ANTENNA FOR OFDM MOBILE
RECEPTION

APPROVED BY SUPERVISORY COMMITTEE:

Chairperson: Professor Yoshio Karasawa
Member: Professor Takeshi Hashimoto
Member: Professor Masashi Hayakawa
Member: Professor Tadashi Fujino
Member: Professor Nobuo Nakajima

© Copyright 2006 by Pubudu Sampath Wijesena
All Rights Reserved

OFDM 移動体受信用アダプティブアレーアンテナに関する研究

ウィジェセーナ プブドゥ サンパトゥ

概要

携帯端末のマルチメディア化にともない、広帯域移動体通信への期待が高まっている。広帯域移動通信における主な課題として周波数選択性フェージングの対策と周波数領域の有効利用が挙げられる。これらの条件を満たす OFDM (Orthogonal Frequency Division Multiplexing) 変調方式が次世代の無線変調方式として採用されつつである。

OFDM はお互いに直交するサブキャリアを使うマルチキャリア変調方式であるため周波数変動が生じるような環境では受信特性が急激に悪化するという問題点がある。このため、移動受信によるドップラーシフトが伝送特性の劣化の原因となる。さらに、マルチパス信号が存在する環境では、各信号のドップラーシフト量も異なり、単一アンテナで構成される受信系ではその補正はかなり難しい。

本論文では、地上波放送の移動体受信を想定し、OFDM 変調方式の移動受信時のドップラーズプレッドによるキャリア間干渉に強い耐性を有するアダプティブアレーの提案、また、アダプティブアレーアンテナのアダプティブアレーアルゴリズム自身の高速化や高性能化を行っている。

本論文は 9 章から構成されており、主な内容は第 2 章の OFDM の基礎、第 3 章のアダプティブアレーアンテナの基礎、第 4 章の DTTB の基礎、第 5 章のビームスペースアレーアンテナによるドップラーズプレッドの抑圧、第 6 章の指向性アンテナによる DTTB の移動受信、第 7 章の高速に収束するアダプティブアルゴリズム、第 8 章の Fast-Fading 環境に適したアダプティブアレーアンテナの提案に大別される。

第 1 章は、序論であり、本論文の背景と目的について述べる。

第 2 章では、OFDM の基礎、またドップラーズプレッドによる OFDM キャリア間干渉について解説する。

第 3 章ではリニアアダプティブアレーアンテナの概念と、代表的なアダプティブアルゴリズムである MMSE アルゴリズムについて紹介する。

第4章では、日本の地上デジタルテレビ放送（DTTB）の概要を述べる。

第5章では、OFDMの移動受信にビームスペースアレーアンテナを用い、異なる到来角度で受信される信号を別々に取り出し、それらをビーム出力毎に位相補正した後、最大比合成することにより、ドップラースプレッドによる影響を低下させられることを提案し、シミュレーションによりその有効性を明らかにする。

第6章では、地上デジタルテレビの移動受信に指向性素子から構成されるアダプティブアレーアンテナの使用を提案する。本章の前半では無指向性素子と指向性素子から構成される4素子アダプティブアレーを地上デジタルテレビの移動受信に用いた場合の特性評価を行い、両方の場合ほぼ同程度の結果が得られることをシミュレーションにより示す。後半では、指向性アンテナを用い、ドップラー補正を行うことが大幅な特性改善につながることを示し、最後に2素子アダプティブアレーを用いる場合、指向性アンテナ素子を車の左右に設置するよりも前後に設置したほうが望ましいことを示す。

第7章では、多数の素子数から構成されるアダプティブアレーアンテナの受信信号を固有値分解により、少数の直交成分に分けることから、アダプティブアレーアンテナの収束を高速化するアダプティブアルゴリズムとしてED-RLSアルゴリズムを提案し、計算機シミュレーションによりその有効性を示し、最後にOFDMに適用する場合のシステムについて述べる。

第8章では、Post-FFT型OFDMアダプティブアレーに適用可能な蓄積信号処理型アダプティブアルゴリズムを提案する。提案方式では各アンテナの受信信号を一時的に蓄積し、現在と過去の中間点を仮想的な現在とみなすことにより、この時点で見た過去と未来の受信信号を元に、現時点のウェイトベクトルを計算する。ウェイトベクトルの計算に未来の情報を用いることから高速移動体においても時間遅れなく正確にウェイトを求めることができる。このアルゴリズムは原理的に常時存在するパイロット信号に対して追従することができるのみで、シングルキャリア通信方式のアダプティブアレーには適さないが、その特徴は、制御用サブチャネルとデータ用サブチャネルを並列に持つことができるOFDM方式、特に高速移動体を対象とするOFDM移動通信に適用が可能である。本論文は計算機シミュレーションを用い、ドップラースプレッドや同一周波数干渉信号が存在する過酷な環境においても提案方式が安定したSINRを保持することを示し、提案方式の有効性を明らかにする。

第9章では、本研究で得られた結論をまとめるとともに、今後の課題について述べる。

A Study on Adaptive Array Antenna for OFDM Mobile Reception

Pubudu Sampath Wijesena

Abstract

The demand for broadband multimedia communication over mobile terminals is growing exponentially. One of the major obstacles to realize broadband wireless communication is frequency selective fading due to multipath propagation. Further the efficient use of the electromagnetic frequency spectrum would be an additional requirement when implementing broadband wireless communications, as the electromagnetic spectrum is limited.

Orthogonal Frequency Division Multiplexing (OFDM) is being considered as one of the promising approaches to overcome those obstacles and has been applied in many broadband wireless communication systems such as Digital Video Broadcasting (DVB), Digital Audio Broadcasting (DAB), Wireless Local Area Network (WLAN) and Digital Terrestrial Television Broadcasting in Japan (DTTB). Further OFDM has also been considered as the modulation system for the fourth generation mobile communication systems with the success it has achieved in previous applications.

However, as OFDM uses mutually orthogonal subcarriers in order to maximize the electromagnetic spectrum efficiency, it is more sensitive to frequency offsets. Frequency offset of the received signal in OFDM system destroys the orthogonal property among the subcarriers and causes Inter Carrier Interference (ICI). This is one of the primary disadvantages of OFDM modulation system, which declines the possibility of OFDM for mobile communication applications, where significant Doppler frequency shifts occur.

In our work, firstly we examine the ICI due to Doppler spread in OFDM mobile reception and propose the use of Beam-Space Adaptive Array antenna (BSAAA) and Directional-Element Adaptive Array Antenna for moving receivers in order to overcome ICI due to Doppler spread. In the proposed schemes, multipath signals are separated into number of beams according to their Direction of Arrival (DOA) and then despread the Doppler frequency shift of each beam signal considering the beam direction, and combine the corrected beam signals using Maximal Ratio Combining (MRC).

Introducing two types of Adaptive Array Antenna (AAA) to suppress the Doppler spread in OFDM mobile reception is our first work, and the second work is concentrated on improvement of the performance of adaptive algorithm in OFDM Adaptive Array Antenna (OFDM-AAA). We introduce two types of adaptive algorithms, which can be

applicable to Post-FFT type OFDM-AAA in order to achieve a rapid convergence and to increase the adoptability to fast fading environments. First one, namely, Eigenvalue-Decomposition-based Recursive Least-Squares (ED-RLS), adaptive algorithm gives a fast convergence rate in AAA which are used in environments where one strong interference source, but any number of multipaths of desired and interference signals exist. The other is the adaptive algorithm based on accumulated signal processing, which gives improved performance in fast fading conditions. The application of these two algorithms to OFDM mobile communication system too is discussed.

Finally a discussion on overall results and future work too are presented in the paper.

Acknowledgements

Firstly I would like to express my deepest gratitude to my advisor Prof. Yoshio Karasawa for the guidance and the encouragement I gained through out the research work. I believe that it is a great fortune of me to be supervised by an advisor who is so matured in both research field and as a person. I also would like to pay my respect to my supervisor for the support given to me in my personal life during the work. I owe many thanks to Prof. Yoshio Karasawa for my progress as a researcher as well as a person. I am also grateful for my second advisor Prof. Takeshi Hashimoto for his guidance and valuable comments on this work. Further I would like to thank other member committees for their helpful comments on this work. I would also like to thank Dr. Tetsuki Taniguchi for the valuable discussions during the course of work.

Moreover I would like to thank the members of Karasawa Laboratory for the useful discussions, the support, and the good times I had while working together. Also my special thank goes to Mr. Atsushi Takemoto for the great support rendered to me through out the work.

Further I would like to thank The Ministry of Education, Culture, Sports, Science and Technology Japan (MEXT), Tokyu Scholarship Foundation and Honjo Scholarship Foundation for the financial assistance that I received during my studies. It is not an exaggeration to say that this work would have been impossible without this financial support.

Finally, I would like to express my gratitude to my parents for guiding me through best educational opportunities. I am also thankful to my wife Nuradha, darling son Thenuk, for their understanding, endless patience and encouragement when it was most required.

Table of Contents

CHAPTER 1 INTRODUCTION.....	1
1.1 CONTEXT OF WORK	1
1.2 ORIGINAL CONTRIBUTIONS.....	3
1.3 THESIS OVERVIEW	3
CHAPTER 2 FUNDAMENTALS OF OFDM	6
2.1 INTRODUCTION	6
2.2 OFDM SIGNAL	7
2.3 FREQUENCY SPECTRUM OF OFDM.....	9
2.4 GUARD INTERVAL WITH CYCLIC PREFIX.....	10
2.5 INTER CARRIER INTERFERENCE DUE TO DOPPLER SPREAD	11
2.5.1 <i>Doppler Frequency Shift due to Mobile Reception</i>	11
2.5.2 <i>Inter Carrier Interference in OFDM Signal</i>	12
2.5.3 <i>Doppler Spread due to Multipath Reception</i>	13
CHAPTER 3 FUNDAMENTALS OF ADAPTIVE ARRAY ANTENNA.....	15
3.1 INTRODUCTION	15
3.2 UNIFORMLY SPACED LINEAR ARRAY	15
3.3 BEAMFORMING	17
3.4 CRITERIA FOR WEIGHT CALCULATION.....	18
3.4.1 <i>Minimum Mean-Squared Error (MMSE) Criterion</i>	19
3.4.2 <i>Maximum Signal to Noise Ratio (MSN) Criterion</i>	20
3.5 ADAPTIVE ALGORITHMS FOR BEAMFORMING	21
3.5.1 <i>Least Mean Square (LMS) Algorithm</i>	22
3.5.2 <i>Sample Matrix Inversion (SMI) Algorithm</i>	22
3.5.3 <i>Recursive Least-Squares (RLS) Algorithm</i>	24
CHAPTER 4 DIGITAL TERRESTRIAL TELEVISION BROADCASTING.....	25
4.1 INTRODUCTION	25
4.2 ISDB-T STANDARD	26
4.3 ATTRACTIVE FEATURES OF DTTB	28
4.3.1 <i>High Definition Television (HDTV)</i>	28
4.3.2 <i>Mobile Reception</i>	28
4.3.3 <i>Copyright Protection</i>	28

CHAPTER 5 BEAM-SPACE ADAPTIVE ARRAY ANTENNA FOR SUPPRESSING THE DOPPLER SPREAD IN OFDM MOBILE RECEPTION.....	29
5.1 INTRODUCTION	29
5.2 BASIC CONFIGURATION	30
5.3 BEAM-SPACE ARRAY (MULTIBEAM FORMATION).....	31
5.4 MAXIMAL RATIO COMBINING (MRC).....	36
5.5 SIMULATIONS.....	37
5.5.1 <i>System Parameters for Simulation</i>	37
5.5.2 <i>Optimizing MRC</i>	39
5.5.3 <i>Performance Evaluation</i>	42
5.6 SUMMARY	47
CHAPTER 6 DIRECTIONAL-ELEMENT ADAPTIVE ARRAY ANTENNA FOR MOBILE RECEPTION OF DIGITAL TERRESTRIAL TELEVISION	49
6.1 INTRODUCTION	49
6.2 ARRAY CONFIGURATION AND ADAPTIVE ALGORITHM	50
6.2.1 <i>Omni-directional-Element Adaptive Array Antenna</i>	50
6.2.2 <i>Directional- Element Adaptive Array Antenna</i>	51
6.2.3 <i>Despreading Doppler Frequency Shift for Directional-Element Arrays</i>	52
6.2.4 <i>Maximal Ratio Combining</i>	55
6.3 SIMULATIONS.....	57
6.3.1 <i>Propagation Environment</i>	57
6.3.2 <i>Assumed OFDM Scheme</i>	57
6.4 PERFORMANCE EVALUATION	58
6.4.1 <i>Optimizing the despreading factor</i>	58
6.4.2 <i>Four-Element Adaptive Array</i>	59
6.4.3 <i>Two-Element Adaptive Array</i>	62
6.5 SUMMARY	62
CHAPTER 7 EIGENVALUE-DECOMPOSITION-BASED RECURSIVE LEAST-SQUARES ALGORITHM FOR OFDM COMMUNICATIONS OVER FAST TIME-VARYING CHANNELS.	64
7.1 INTRODUCTION	64
7.2 EIGENVALUE DECOMPOSITION BASED RLS	65
7.3 SIMULATION RESULTS	66
7.3.1 <i>Simulation Conditions</i>	66
7.3.2 <i>Simulation Results</i>	66
7.4 ED-RLS BASED OFDM COMMUNICATION	68
7.4.1 <i>Transmitted OFDM Signal</i>	68

7.4.2 <i>Receiving Scheme of OFDM Application</i>	68
7.5 SUMMARY	69
CHAPTER 8 ADAPTIVE ALGORITHM BASED ON ACCUMULATED SIGNAL PROCESSING FOR FAST FADING CHANNELS WITH APPLICATION TO OFDM MOBILE RADIO	71
8.1 INTRODUCTION	71
8.2 ADAPTIVE ALGORITHM BASED ON ACCUMULATED SIGNAL PROCESSING.....	72
8.3 SIMULATION CONDITIONS AND RESULTS	75
8.3.1 <i>Simulation Conditions</i>	75
8.3.2 <i>Simulation Results</i>	76
8.4 OFDM APPLICATION	81
8.4.1 <i>OFDM Symbol</i>	81
8.4.2 <i>Receiving Scheme of OFDM Application</i>	82
8.4.3 <i>Weight Interpolation</i>	84
8.4.4 <i>Simulation Conditions and Results</i>	85
8.5 SUMMARY	87
CHAPTER 9 CONCLUSIONS AND FUTURE WORK	88
9.1 CONCLUSIONS	88
9.2 FUTURE WORK.....	89

List of Figures

FIG. 2-1 THEORETICAL WAY OF GENERATING THE OFDM SIGNAL	8
FIG. 2-2 BLOCK DIAGRAM OF A BASIC OFDM COMMUNICATION SYSTEM	8
FIG. 2-3 FREQUENCY SPECTRUM OF THE OFDM SIGNAL	9
FIG. 2-4 INSERTION OF GUARD INTERVAL AND SUBCARRIER SIGNALS OF DIRECT AND DELAYED PATHS.....	10
FIG. 2-5 DOPPLER SHIFT DUE TO MOVING OF RECEIVER	11
FIG. 2-6 INTER CARRIER INTERFERENCE DUE TO DOPPLER SHIFT	13
FIG. 2-7 DOPPLER FREQUENCY SPREAD DUE TO MULTIPATH RECEPTION.....	13
FIG. 2-8 INTER CARRIER INTERFERENCE DUE TO DOPPLER SPREAD.....	14
FIG. 3-1 UNIFORMLY SPACED LINEAR ARRAY ANTENNA WITH A PLANE WAVE INCIDENTS FROM DIRECTION θ	17
FIG. 3-2 NARROWBAND BEAMFORMER	19
FIG. 5-1 PROPOSED BSAAA SCHEME FOR OFDM MOBILE RECEPTION.....	31
FIG. 5-2 BEAM-SPACE ARRAY ANTENNA IN THE MOBILE TERMINAL (A) ANTENNA ARRANGEMENT (B) MULTI-BEAM PATTERN FOR $d = \lambda/2$, $M = 8$ (C) MULTI-BEAM PATTERN FOR $d = 3\lambda/8$, $M = 8$	34
FIG. 5-3 RADIATION PATTERN OF BEAM 5	35
FIG. 5-4 MRC OF AN M -ELEMENT BSAA RECEIVER.....	36
FIG. 5-5 TIME VARIATION OF THE RECEIVED SIGNAL POWER AT $f_d T_s = 0.15$, $SNR = 20dB$	38
FIG. 5-6 BER AS A FUNCTION OF SNR OF THE RECEIVED SIGNAL FOR $M = 8$	41
FIG. 5-7 BER AS A FUNCTION OF NORMALIZED DOPPLER FREQUENCY WHERE RECEIVED SIGNAL $SNR = 10dB$, $M = 8$	42
FIG. 5-8 BER AS A FUNCTION OF SNR OF THE RECEIVED SIGNAL FOR $M = 4$	44
FIG. 5-9 BER AS A FUNCTION OF NORMALIZED DOPPLER FREQUENCY, $SNR = 10dB$, $M = 4$	44
FIG. 5-10 BER AS A FUNCTION OF SNR $f_d T_s = 0.0, 0.15, 0.30$ FOR $M = 1, 4, 8$	45
FIG. 5-11 BER AS A FUNCTION OF NORMALIZED DOPPLER FREQUENCY $M = 1, 4, 8$ AND $Q = 3$	46
FIG. 5-12 BER AS A FUNCTION OF NORMALIZED DOPPLER FREQUENCY AT A PROPAGATION CONDITION WHERE 50 MULTIPATH SIGNALS RECEIVED, $M = 1, 4, 8$, $Q = 3$ AND $SNR = 20dB$	47
FIG. 6-1 ANTENNA INSTALLMENT.....	51
FIG. 6-2 ADAPTIVE ARRAY ANTENNA	53
FIG. 6-3 DOPPLER POWER SPECTRUM	54
FIG. 6-4 DOPPLER DESPREADING FOR COSINE-GAIN ELEMENT ADAPTIVE ARRAY ANTENNA	55
FIG. 6-5 MAXIMAL RATIO COMBINING (MRC).....	56
FIG. 6-6 PROPAGATION ENVIRONMENT (A DISCRETE TYPE EXPONENTIAL DELAY PROFILE)	57
FIG. 6-7 DOPPLER DESPREADING EFFECT ($SNR = 30dB$, $f_d T_s = 0.05$)	59
FIG. 6-8 BER vs. SNR	60

FIG. 6-9 BER vs. DOPPLER FREQUENCY SPREAD.....	61
FIG. 6-10 PERFORMANCE COMPARISON BETWEEN THE USE OF ELEMENT 2,4 AND 1,3 (SNR = 40dB).....	62
FIG. 7-1 BASIC CONFIGURATION OF ED-RLS ALGORITHM	65
FIG. 7-2 OFDM MOBILE COMMUNICATIONS SYSTEM.....	67
FIG. 7-3 CONVERGENT CHARACTERISTIC FOR RLS AND ED-RLS ALGORITHM.....	67
FIG. 7-4 TRANSMITTED OFDM SYMBOL	68
FIG. 7-5 RECEIVING SCHEME OF THE PROPOSED OFDM SYSTEM	69
FIG. 8-1 ADAPTIVE ALGORITHM BASED ON ACCUMULATED SIGNAL PROCESSING.....	73
FIG. 8-2 SIMULATION ENVIRONMENT.....	75
FIG. 8-3 TIME VARIANT OF THE REAL PART OF THE FIRST ELEMENT WEIGHT AT $f_d T_s = 0.033$ AND $\beta = 1.0$	78
FIG. 8-4 TIME VARIANT OF SINR AT $f_d T_s = 0.033$ AND $\beta = 0.85$	79
FIG. 8-5 CUMULATIVE DISTRIBUTION OF SINR AT $f_d T_s = 0.033$ AND $\beta = 0.85$	79
FIG. 8-6 SINR AS A FUNCTION OF NUMBER OF UTILIZED PRE- AND POST-RECEIVED SYMBOLS ($p = q$).....	80
FIG. 8-7 SINR AS A FUNCTION OF DOPPLER FREQUENCY SHIFT ($\beta = 0.85$).....	81
FIG. 8-8 OFDM SYMBOL	82
FIG. 8-9 RECEIVING SCHEME OF OFDM APPLICATION	83
FIG. 8-10 INTERPOLATION OF WEIGHT VECTORS.....	84
FIG. 8-11 AVERAGED SINR OF EACH SUBCHANNEL.....	86

List of Tables

TABLE 4-1 <i>DIGITAL TERRESTRIAL BROADCASTING SYSTEMS IN THE WORLD</i>	26
TABLE 4-2 <i>SEGMENT PARAMETERS FOR ISDB-T (6 MHz)</i>	27
TABLE 5-1 <i>SYSTEM PARAMETERS</i>	39
TABLE 5-2 <i>PROPAGATION ENVIRONMENT</i>	39
TABLE 6-1 <i>SYSTEM PARAMETER</i>	58
TABLE 7-1 <i>SYSTEM PARAMETER</i>	66
TABLE 8-1 <i>SIMULATION ENVIRONMENT</i>	75
TABLE 8-2 <i>SYSTEM PARAMETERS</i>	76
TABLE 8-3 <i>OFDM SYSTEM PARAMETERS</i>	85

List of Abbreviations

AAA	Adaptive Array Antenna
ADSL	Asymmetric Digital Subscriber Line
AWGN	Additive White Gaussian Noise
BSAAA	Beam Space Adaptive Array Antenna
BER	Bit Error Rate
BPSK	Binary Phase Shift Keying
BS	Base Station
BST-OFDM	Band Segmented Transmission OFDM
CDMA	Code Division Multiple Access
CMA	Constant Modulus Algorithm
CMP	Constrained Minimization of Power
DAB	Digital Audio Broadcasting
DFT	Discrete Fourier Transformation
DOA	Direction of Arrival
DTTB	Digital Terrestrial Television Broadcasting
DVB	Digital Video Broadcasting
ED-RLS	Eigenvalue Decomposition based Recursive Least Squares
FDMA	Frequency Division Multiple Access
FFT	Fast Fourier Transformation
HDTV	High Definition Television
ICI	Inter Carrier Interference
IDFT	Inverse Discrete Fourier Transformation
IFFT	Inverse Fast Fourier Transformation
ISDB-C	Integrated Service Digital Broadcasting for Cable broadcasting
ISDB-S	Integrated Service Digital Broadcasting for Satellite broadcasting
ISDB-T	Integrated Service Digital Broadcasting for Terrestrial broadcasting
ISI	Inter Symbol Interference
LMS	Least Mean Squares
MC-CDAM	Multicarrier CDMA

MMSE	Minimum Mean Squared Error
MRC	Maximal Ratio Combining
MS	Mobile Station
MSN	Maximum Signal to Noise Ratio
OFDM	Orthogonal Frequency Division Multiplexing
OFDMA	Orthogonal Frequency Division Multiple Access
PSK	Phase Shift Keying
QPSK	Quadrature Phase Shift Keying
RLS	Recursive Least Squares
SINR	Signal to Interference plus Noise Ratio
SMI	Sample Matrix Inversion
SNR	Signal to Noise Ratio
TDMA	Time Division Multiple Access
WLAN	Wireless Local Area Network

Chapter 1

Introduction

1.1 Context of Work

The growing demand for multimedia communication over mobile terminals increases the expectations for broadband wireless communications. The main obstacles to overcome towards this goal are frequency selective fading due to multipath propagation and efficient use of electromagnetic frequency spectrum. Recently, Orthogonal Frequency Division Multiplexing (OFDM) as a modulation system, and Adaptive Array Antenna (AAA) as mobile receivers have gained enormous interest in order to fulfill the requirements for realizing broadband mobile wireless communications.

OFDM, having the ability of combating against multipath delay propagation as a multicarrier modulation system along with its frequency usage efficiency which is almost similar to single carrier modulation system [1, 2], is highly assessed and been applied in many broadband wireless communication systems such as Digital Video Broadcasting (DVB), Digital Audio Broadcasting (DAB), Wireless Local Area Network (WLAN) and Digital Terrestrial Television Broadcasting in Japan (DTTB) [3, 4]. Further OFDM is being considered as a modulation system for the fourth generation mobile communication systems with the success it has achieved in previous applications [5, 6].

However, as OFDM uses mutually orthogonal subcarriers in order to maximize the electromagnetic spectrum efficiency, it is more sensitive to frequency offsets. Frequency offset of the received signal in OFDM system destroys the orthogonal characteristic among the subcarriers and causes Inter Carrier Interference (ICI) [7-9]. This is one of the primary disadvantages of OFDM modulation system, which declines the possibility of OFDM for mobile communications applications, where significant Doppler frequency shifts occur.

A number of methods have been proposed to reduce this sensitivity to frequency offset, including windowing of the transmitted signal [10], self-ICI cancellation [11] and space domain interpolation [12]. However, all these methods give very less performance improvement compared to their high complexity in implication. Particularly, [10] and [11] reduce the frequency usage efficiency. Further in [13], it has been proposed to reduce the Doppler spread by limiting the receiving range of the antenna, which will disuse some of multipaths and reduce the power efficiency.

Motivated by having no reasonable method to suppress the ICI due to Doppler frequency spread in OFDM mobile reception, in the first part of our work we introduce Beam-Space Adaptive Array Antenna (BSAAA) to OFDM mobile communication

systems, where the Doppler spread is suppressed by separating and revising Doppler frequency shift of each multipath. The proposed scheme suppresses Doppler spread almost perfectly with 8-element BSAAA. A further discussion on using directional element AAA in order to achieve the same goal in much easier manner is also presented in our work.

Working along AAA in related to OFDM, we noticed that AAA has been introduced to OFDM in order to increase the adaptability of system for mobile communication systems because of the ability of AAA in increasing the system capacity without increasing the transmitted power or bandwidth [14-18]. However, an AAA consisting of a large number of elements along with a fast convergence rate would be an essential requirement to implement OFDM-based mobile radio systems such as MC-CDMA and OFDMA in fast time-varying channels. Even the fastest among MMSE adaptive algorithms, Recursive Least-Squares Algorithm (RLS), which takes 3,4 times of steps of the number of weights it has to update to be converged [19], would not be suitable for such AAA applications with a large number of elements.

With our experience of that Maximal Ratio Combining (MRC) can be performed sufficiently by only referring to previous three samples [18], and hinted by [20], where Eigenvalue Decomposition has been introduced to AAA systems in the purpose of reducing the total computational load, we propose an adaptive algorithm called Eigenvalue-Decomposition-based Recursive Least-Squares (ED-RLS), where eigenvalue decomposition is been used to achieve a fast convergence rate in AAA. Particularly we could gain an essential convergence in the seventh step in a 16-element array configuration, in an environment with -10dB of SNR and 10dB interference signal power, where more than 30 steps were taken corresponding to conventional RLS algorithm.

Working further with OFDM adaptive array antenna, we understood that, steering AAA would be a challenging task in OFDM based mobile communication system since the propagation environment of mobile radio system is more complicated with the existence of delay spread, Doppler spread and interference signals, compared to the propagation environments of WLAN, where only delay spread but no Doppler spread, and DTTB, where both delay spread and Doppler spread exist but no interference signal. We confirm that we can overcome this difficulty, simply and successfully with an adaptive algorithm based on accumulated signal processing. The proposed algorithm could be applicable to Post-FFT-type OFDM adaptive array antennas and will keep the system performance in fast fading channels. Proposed scheme calculates the weight of each element at a particular instant t , by considering both -post and pre-received symbols. The proposed algorithm improves the performances under fast fading conditions since the scheme utilizes additional forthcoming information on channel behavior to the weight-calculating scheme.

Further, considering that the Post-FFT-type OFDM AAA has gained a particular concern, compared to Pre-FFT-type OFDM AAA [17, 18, 21], regardless of its high computational load since it increases the robustness against frequency selective fading,

and the availability of number of methods to reduce the high computational load of Post-FFT-type OFDM adaptive array [22, 23], we discuss on applying our proposed ED-RLS and accumulated signal processing based adaptive algorithm to Post-FFT-type OFDM-AAA.

The original contribution of our work is presented in the next section.

1.2 Original Contributions

Several contributions on OFDM adaptive array antenna and its applications have been made in this work. The following list summarizes our main contributions within the scope of this work.

1. First, the chapter 5 describes the introduction of Beam-Space Adaptive Array Antenna in order to suppress the Doppler spread in OFDM mobile reception. This work is published in the *IEICE Transactions of Communications, vol.E87-B, no.1, Jan.2004* and also presented at *2002 Interim International Symposium on Antennas and Propagation, November, Yokosuka Research Park, Japan.*
2. Second is the evaluation of directional-element adaptive array antenna in OFDM mobile reception, given in chapter 6. The work is presented at *2005 Interim International Symposium on Antennas and Propagation, August, Seoul, Korea.*
3. Third is the proposing of ED-RLS adaptive algorithm which faster the convergence rate of adaptive array antenna. This is described in chapter 7 and presented at *2003 IEEE Topical Conference on Communication Technology Conference, October, Hawaii, USA.*
4. An accumulated signal processing based adaptive algorithm to improve the system performance in fast fading condition is presented in chapter 8. This work is published in the *IEICE Transactions of Communications, vol.E88-B, no.2, Feb.2005* and also presented at *2004 Interim International Symposium on Antennas and Propagation, August, Sendai, Japan.*

1.3 Thesis Overview

The thesis contains 9 chapters and is organized as follows.

Chapter 2 gives an introduction on OFDM including the process of generating OFDM signal, the overlapping frequency spectrum of OFDM, and the cyclic prefix guard interval used in OFDM modulation. Secondly the chapter describes the major weakness of OFDM

that focused in our work, Inter Carrier Interference (ICI) due to Doppler frequency spread in mobile reception of OFDM modulated signal.

Chapter 3 presents the basic of adaptive array antenna. The discussion is focused on uniformly spaced linear adaptive array, and MMSE adaptive algorithm.

Chapter 4 gives a brief introduction on Digital Terrestrial Television Broadcasting (DTTB) in Japan.

Chapter 5 proposes the use of Beam-Space Adaptive Array Antennas (BSAAA) for moving receivers in order to suppress ICI due to Doppler spread in OFDM mobile reception. In the proposed system, firstly we separate multipath signals into a number of multi-beams according to their incident directions, then correct the Doppler frequency shift of each beam signal, considering the beam direction, and finally combine the corrected beam signals based on MRC. Further this chapter clarifies the excellent performance of the proposed system in suppressing the influence of Doppler spread by carrying out computer simulation. Particularly, it was certified that it is possible to suppress the influence of the Doppler spread efficiently for all the receiving directions by using 8-element BSAAA with element spacing of $(3/8)\lambda$, and referring 3 past symbols when calculating the weight vector of MRC.

Chapter 6 proposes the use of directional-element AAA on the reception of OFDM based DTTB in vehicles. Firstly the paper evaluates the mobile receiving quality of DTTB of Post-FFT-type OFDM-AAA consisting of omni-directional- and directional-element with computer simulation and confirms that similar performance to omni-directional-element AAA can be achieved with the use of directional-element AAA. Secondly, the paper shows that remarkable performance improvement can be achieved in directional-element AAA mobile reception by the application of Doppler despreading. The chapter also confirms that allocating directional elements on the front and the rear sides of the vehicle instead of the left and right sides, gives better receiving quality.

Chapter 7 introduces an adaptive algorithm called Eigenvalue-Decomposition-based Recursive Least-Squares (ED-RLS) to reduce the convergence time of AAA. The proposed adaptive algorithm gives performance improvement in an environment where less number of interference sources along with any number of multipath signals of desired and interference signal exist. Further a method of applying the proposed adaptive algorithm to Post-FFT-type OFDM-AAA is presented.

Chapter 8 proposes an adaptive algorithm based on accumulated signal processing, which could be applicable to Post-FFT-type OFDM-AAA. Proposed scheme calculates the weight of each element at a particular instant t , by considering both post- and pre-received symbols. Because of the use of additional forthcoming information on channel behavior in the weight calculation scheme, one can expect an improved performance in fast fading conditions by using the proposed adaptive algorithm. This chapter also discusses the application of the proposed adaptive algorithm to OFDM-AAA. In OFDM application, a few subchannels are being used to transmit pilot symbols, and at the

receiver, the proposed adaptive algorithm is applied to those pilot subchannels, and interpolates the weights for the data subchannels which are allocated between the pilot subchannels. Finally, the system performance improvement with the application of the proposed adaptive algorithm is verified by computer simulation.

Finally, chapter 9 summarizes the main results of work and concludes the thesis.

Chapter 2

Fundamentals of OFDM

This chapter firstly gives an introduction on Orthogonal Frequency Division Multiplexing (OFDM) including the process of generating the OFDM signal, the overlapping frequency spectrum of OFDM, and the cycle prefix guard interval used in OFDM modulation. Secondly the chapter describes the major weakness of OFDM that focused in our work, Inter Carrier Interference (ICI) due to Doppler frequency spread in mobile reception of OFDM modulated signal.

2.1 Introduction

OFDM is a special case of multicarrier transmission, where a single datastream is transmitted over a number of lower rate subcarriers. In classical multicarrier modulation system, the total signal frequency band is divided into a number of nonoverlapping frequency subchannels to eliminate Inter Carrier Interference (ICI). However, this leads to inefficient use of the available electromagnetic frequency spectrum. The specialty of OFDM is that it uses mutually orthogonal subcarriers and realizes overlapped-subcarrier FDM to maximize the efficiency of frequency usage.

The concept of using parallel data transmission and frequency division multiplexing has published in the mid-1950s and the first OFDM schemes were presented in the mid-1960s [24]. But the practicability of the concept was questioned, as it was required to generate thousands of orthogonal subcarriers precisely to realize the scheme. But with the proposal of the Discrete Fourier Transform (DFT) based OFDM in 1970s, OFDM became more practical [2]. Finally the high growth of the signal processing devices, such as FFT processors and AD converters, steered OFDM to one of the leading modulation systems nowadays.

The OFDM transmission scheme has the following key advantages:

- ✓ OFDM is an efficient way to deal with multipath; for a given delay spread, the implementation complexity is significantly lower than that of a single carrier system with an equalizer.
- ✓ Data rate for each subcarrier can be set separately according to the signal-to-noise ratio (SNR) of that particular subcarrier. This will enhance the system capacity significantly.

- ✓ OFDM is robust against narrowband interference, because such interference affects only a small percentage of the subcarriers.
- ✓ OFDM makes Single Frequency Networks (SFN) possible, which is especially attractive for broadcasting applications.

On the other hand, OFDM also has some drawbacks compared with single-carrier modulation:

- ✓ OFDM is more sensitive to frequency offset and phase noise.
- ✓ OFDM has a relatively large peak-to-average power ratio (PAPR), which tends to reduce the power efficiency of the RF amplifier.

Because of its robustness against frequency selective fading, and the efficient use of the frequency spectrum, OFDM has become one of the promising modulation systems and have been successfully applied to following broadband digital communication applications:

- ✓ Digital Audio Broadcasting (DAB)
- ✓ Digital Video Broadcasting (DVB)
- ✓ Asymmetric Digital Subscriber Line (ADSL)
- ✓ Wireless Local Area Network (WLAN)
- ✓ Digital Terrestrial Television Broadcasting (DTTB) in Japan

2.2 OFDM Signal

Figure 2-1 illustrates the theoretical way to generate the OFDM signal. As shown in the figure, OFDM signal is made of N subcarrier signals. It should be noted that each subcarrier has an exact integer number of cycles in the OFDM symbol period T_s , and remain zero outside the symbol period. This property accounts for the orthogonal characteristic between the subcarriers, which allows the demodulator to demodulate each subcarrier without ICI. Here we can see that the OFDM modulated signal is equivalent to the Inverse Fourier Transform (IFT) of the input complex original data symbols (e.g. QAM, PSK modulated symbols). As this is an efficient way to implement OFDM modulation, in practice, Inverse Discrete Fourier Transformation (IDFT) or Inverse Fast Fourier Transformation (IFFT) has been used as the OFDM modulator.

Figure 2-2 illustrates the structure of a basic OFDM communication system. As shown in the block diagram, OFDM divides the serial data stream into a parallel data stream and modulates them by performing IDFT. After adding the guard interval to

eliminate Inter Symbol Interference (ISI), it again converts the parallel data stream into a serial data stream. The baseband signal at the output of the OFDM transmitter is given by

$$S(k) = \sum_{n=0}^{N-1} d_n \cdot \exp(j2\pi nk / N) \quad , \quad k = 0,1,\dots, N-1 \quad (2.1)$$

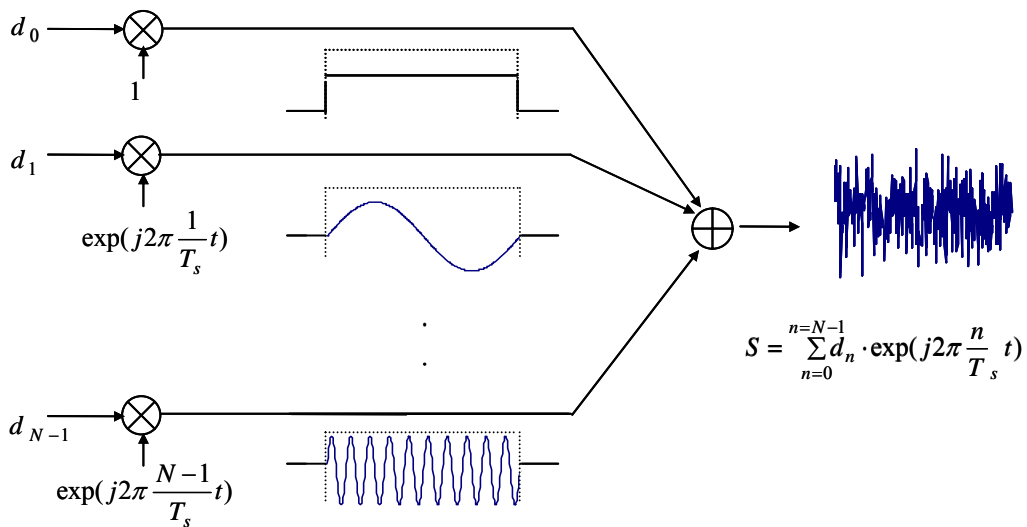


Fig. 2-1 Theoretical way of generating the OFDM signal

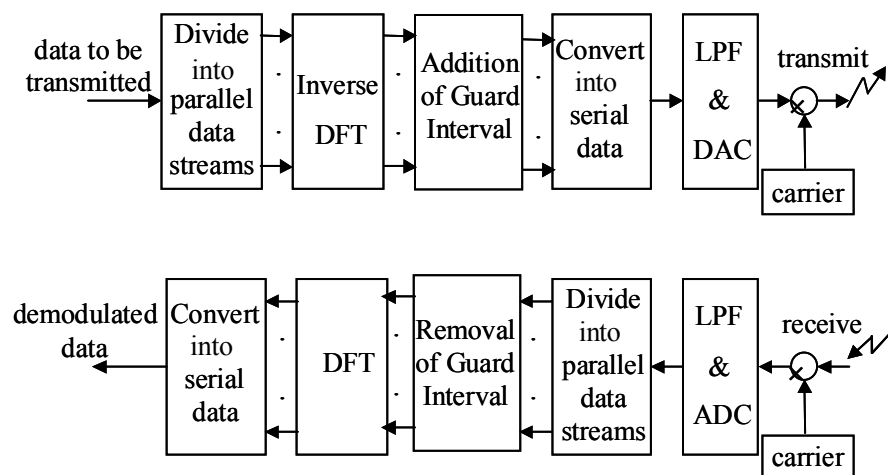


Fig. 2-2 Block diagram of a basic OFDM communication system

where N denotes the number of subcarriers and d_0, d_1, \dots, d_{N-1} are the N complex original data symbols (e.g. PSK), which modulate the subcarriers of the OFDM symbol. At the receiver *visa versa* is been applied to demodulate the signal.

2.3 Frequency Spectrum of OFDM

As we discussed in the previous section, OFDM symbol consists of N different subcarriers. When considering the frequency spectrum of these subcarriers, the frequency spectrum of the n^{th} subcarrier, which has $n-1$ cycles during the OFDM symbol period T_s , is equal to $\text{sinc}(\pi(n-1)/T_s)$. Hence the OFDM signal consists of these N subcarriers, the frequency spectrum of the OFDM signal can also be expressed by the sum of their frequency spectrums. Fig.2-3(a), (b), and (c) illustrate the modulated signal of the subcarrier number 2, the frequency spectrum of subcarrier number 2 and the frequency spectrum of the OFDM signal, respectively.

From Fig.2.3 (c), we can see that at the maxima of each subcarrier spectrum, all the other subcarrier spectra are zero. Therefore the receiver can demodulate each subcarrier free from any interference of the other subcarriers, if it samples the spectrum values at those points that correspond to the maxima of individual subcarriers. This characteristic displays the orthogonal property among the subcarriers, which is been used to realize overlapping multicarrier modulation system in order to increase the frequency usage efficiency.

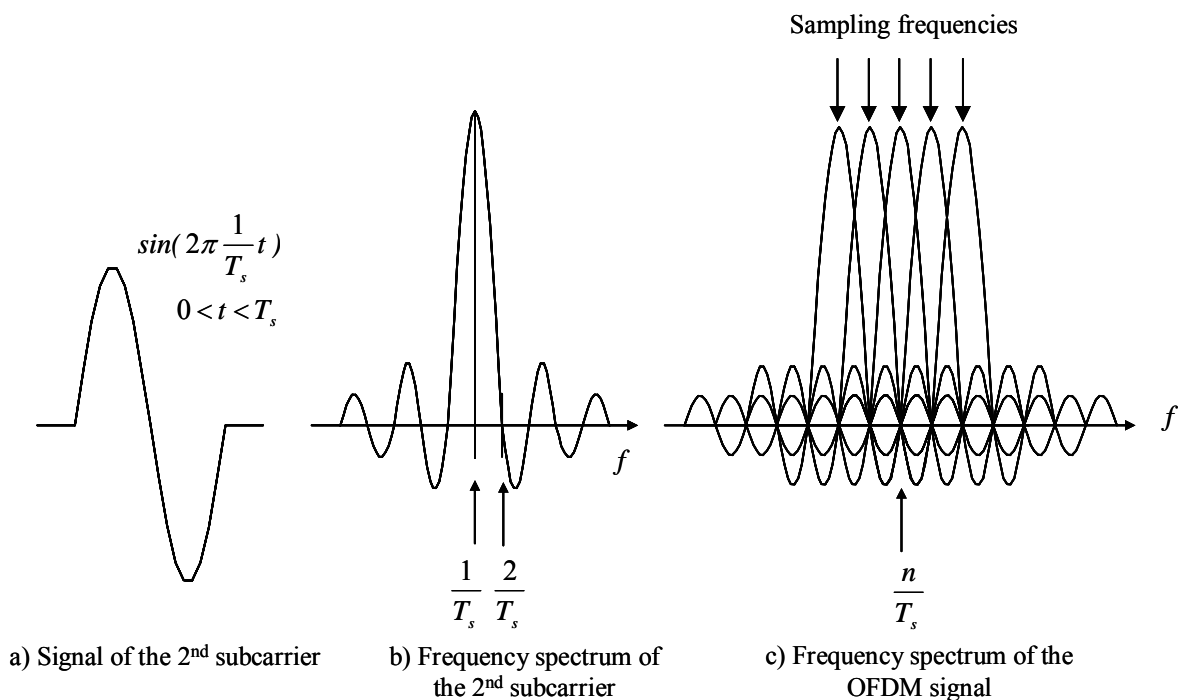


Fig. 2-3 Frequency spectrum of the OFDM signal

On the other hand this also signifies that ICI would occur if the sampling frequency is dislocated from the corresponding maximal values and this will be discussed in section 2.5.

2.4 Guard Interval with Cyclic Prefix

OFDM is resilient to ISI because its symbol duration is long compared with data symbol in single carrier data stream. Moreover, to reduce the ISI further, a guard interval is inserted at the beginning of each OFDM symbol before the transmission, and removed at the receiver before the DFT operation.

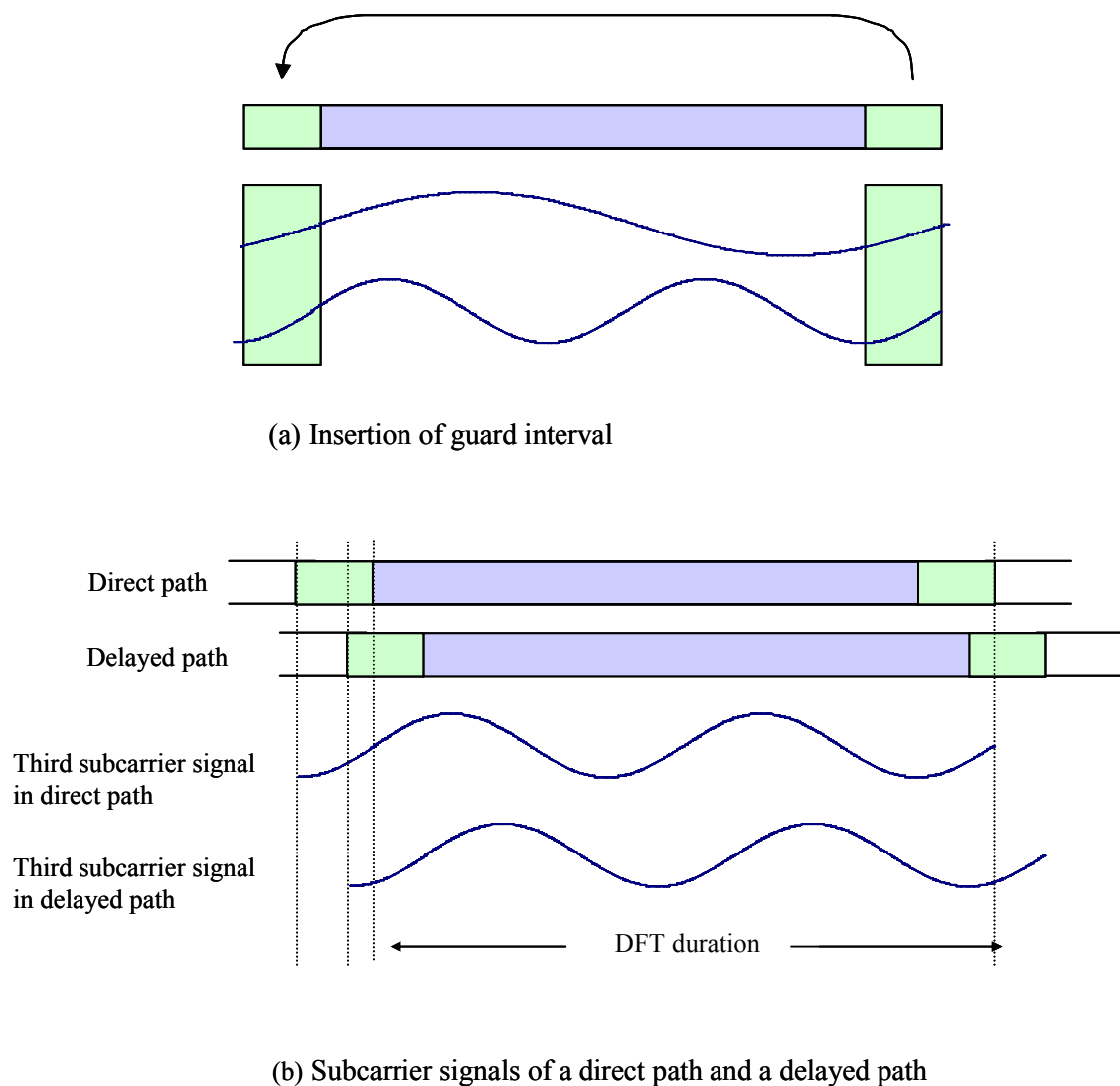


Fig. 2-4 Insertion of guard interval and subcarrier signals of direct and delayed paths

Fig.2-4 (a) illustrates the way of performing the insertion of guard interval. In order to preserve orthogonal characteristic among subcarriers, the guard interval is inserted by cyclically extending an OFDM symbol. Fig.2-4 (b) shows third subcarrier signals of a direct path signal and a delayed path signal, on which delay is less than the guard interval. It is clear for both the paths, an exact integer number of cycles (in this case 2) are included in the DFT duration, which signifies that cyclic prefix guard interval not only eliminate ISI, but also ICI by protecting the orthogonal characteristic between the subcarriers.

2.5 Inter Carrier Interference due to Doppler Spread

ICI due to Doppler spread is known as one of the major problems to overcome in mobile reception of OFDM modulated signals.

2.5.1 Doppler Frequency Shift due to Mobile Reception

When the transmitter or the receiver is in motion, frequency of the received signal shifts from the original frequency f , so-called Doppler frequency shift. The degree of frequency shift depends on the spatial angle between the direction of arrival of the signal and the direction of vehicular motion, the original frequency of the signal and the velocity of the receiver.

If a vehicle is moving at a constant speed v as shown in Fig.2-5, the Doppler frequency shift f_d of the received plane-wave component can be given by

$$f_d = (v / \lambda) \cos(\theta) \quad (2.2)$$

where λ and θ denote the carrier wavelength and the arrival angle of the received plane-wave component measured from the direction of the vehicular motion, respectively.

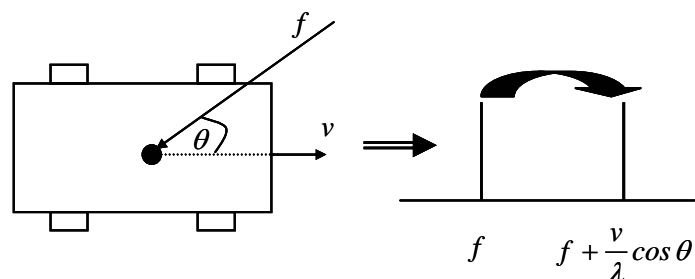


Fig. 2-5 Doppler shift due to moving of receiver

2.5.2 Inter Carrier Interference in OFDM Signal

When a moving receiver receives an OFDM modulated signal, the frequency of the received signal is shifted from the original signal given in Equation (2.1). Therefore the received symbol can be given by

$$S' = \sum_{n=0}^{N-1} d_n \cdot \exp(j2\pi(\frac{n}{NT} + f_d)iT) \quad i = 0,1,\dots,N-1 \quad (2.3)$$

where T , N and f_d denote the original data symbol duration, the number of subcarriers and the Doppler frequency shift, respectively. Here it should be noted that efficient OFDM symbol duration T_s could be expressed by

$$T_s = T \cdot N \quad (2.4)$$

When demodulating this received signal by using a basic OFDM demodulator, received complex value of the k^{th} subcarrier, d'_k can be obtained as

$$d'_k = \frac{1}{N} \sum_{i=0}^{N-1} \sum_{n=0}^{N-1} \left\{ d_n \exp(i2\pi \left[\frac{n}{NT} + f_d - \frac{k}{NT} \right] iT) \right\} \quad (2.5)$$

According to Equation (2.5), d'_k retains at d_k only when f_d is equal to zero. When f_d gains a validity, d'_k consist of ingredients of all the N complex values that modulate the subcarriers of the OFDM symbol. Therefore Equation (2.5) verifies that the Doppler frequency shift causes ICI.

ICI can also be demonstrated in the frequency domain. When the frequency of the received signal is shifted, the sampling frequencies of each subcarrier will not remain at the points that correspond to the maximal spectrum values of individual subcarriers. As a result, ingredients of the other subcarriers will also be sampled and this will lead to ICI as shown in Fig.2-6.

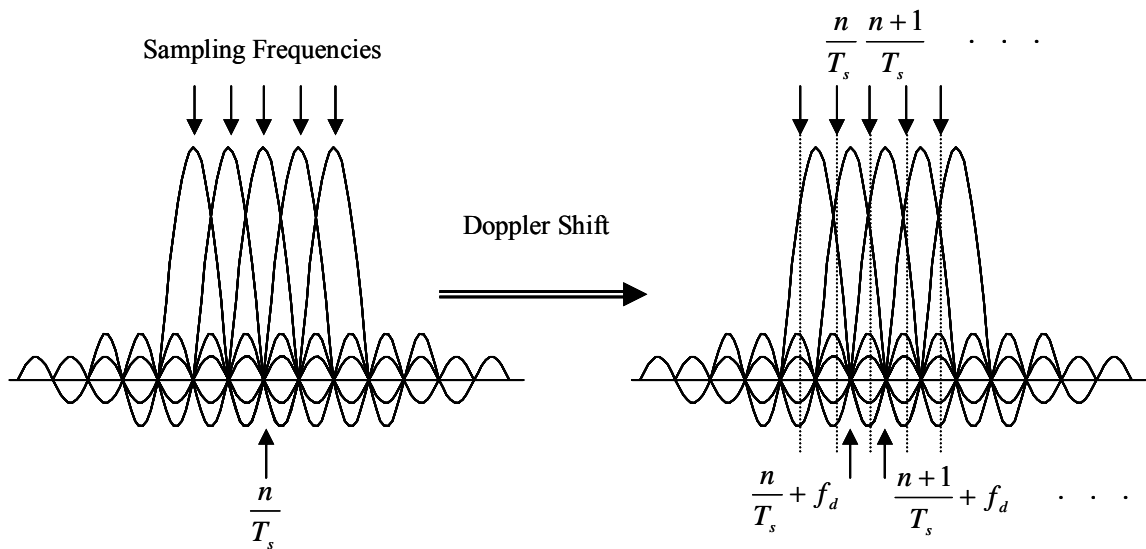


Fig. 2-6 Inter Carrier Interference due to Doppler Shift

2.5.3 Doppler Spread due to Multipath Reception

Under multipath propagation condition, as the direction of arriving of each multipath differs, the Doppler frequency shift for each path differs from each other as shown in Fig.2-7. Hence, the comprehensive frequency spectrum of the OFDM signal will be spread out, so-called Doppler frequency spread. This is shown in Fig.2-8. In such an environment, cancellation of ICI becomes more difficult. To realize high quality reception under multipath propagation condition where Doppler effect is significant, it is required to separate these multipath signals on their spatial directions and correct their frequency shifts individually.

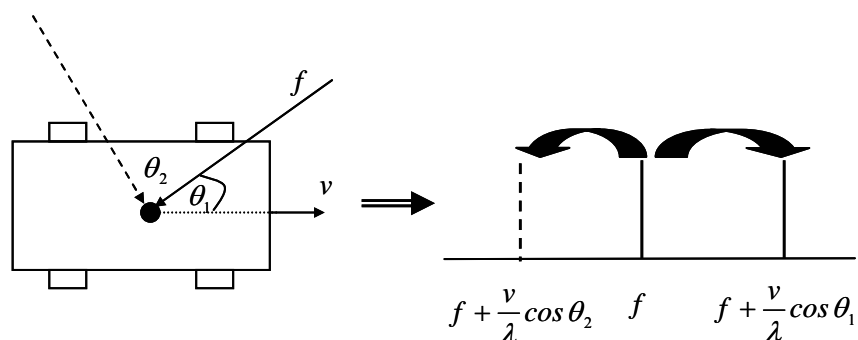


Fig. 2-7 Doppler frequency spread due to multipath reception

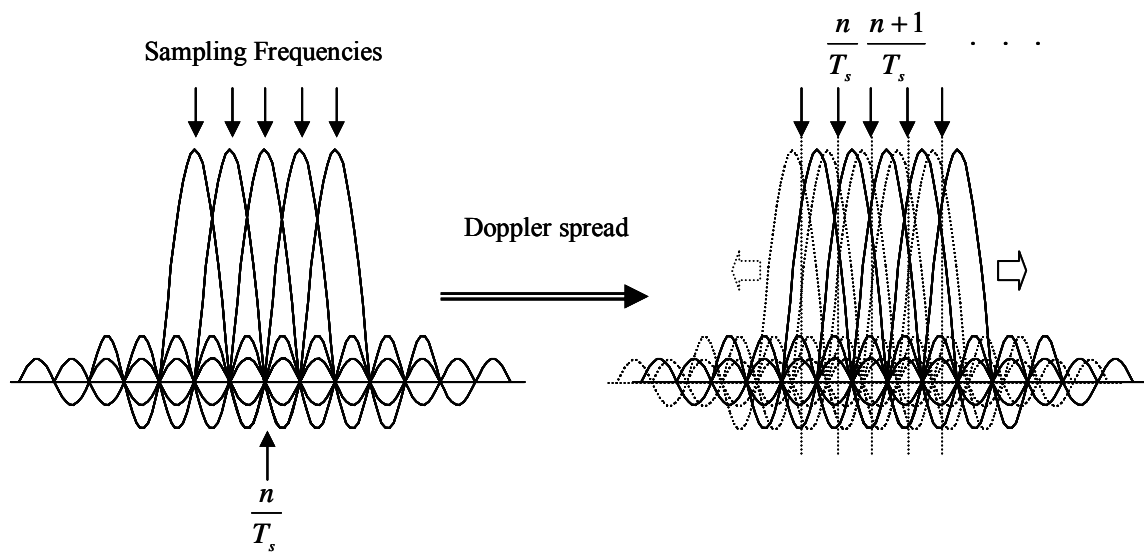


Fig. 2-8 *Inter Carrier Interference due to Doppler Spread*

Chapter 3

Fundamentals of Adaptive Array Antenna

This chapter gives a brief introduction on Adaptive Array Antenna (AAA). The discussion is focused on uniformly spaced linear adaptive array, and Minimum Mean Square Error (MMSE) adaptive algorithm.

3.1 Introduction

Adaptive array antenna (AAA) has gained enormous attention due to its ability to combat against frequency selective fading and to increase the channel capacity without expanding the bandwidth or the transmit power. AAA are mainly used to extract a desired signal out of interfering signals, which leads to higher capacity and reduced power consumption.

In an AAA implemented system, antenna array is located to sample the wavefront simultaneously on several places and the received signal of the antenna array is combined using a certain criterion so called beamforming in order to make efficient suppression of noise and interference.

The antenna elements of an antenna array can be arranged in various geometries, with linear, circular and planar array being very common. Uniformly spaced linear array, in which antenna elements are spaced equally along a straight line, is discussed here.

3.2 Uniformly Spaced Linear Array

Figure 3-1 illustrates a uniformly spaced linear array with M identical isotropic elements, with the rightmost element as the reference element. Assuming the signal source is located far apart from the antenna array, the received signal at the antenna array can be considered to be a plane wave incident at an angle θ with respect to the array normal. According to Fig.3.1, the plane wave first reaches the element number #1, which is the reference element, and propagates all the way to M^{th} antenna element. The propagation delay from the first to second element can be given by

$$\tau = \frac{d \sin \theta}{c} \quad (3.1)$$

where d and c denote the element spacing and the speed of the light, respectively. Assuming the bandwidth of the signal is narrow compared to the carrier frequency, the received complex envelope representation of the element number #2 can be given by

$$E_2(t) = E_1(t) \cdot \exp(-j2\pi f_c \tau) \quad (3.2)$$

where $E_1(t)$ and f_c represent the complex envelope representation of the element number #1 and the carrier frequency of the signal, respectively. As the antenna elements are uniformly distributed across the antenna array, the propagation delay along any two consecutive elements is the same and therefore the received signal at the m^{th} antenna element can be expressed as

$$E_k(t) = E_1(t) \cdot \exp(-j \frac{2\pi}{\lambda} d[m-1] \sin \theta) \quad (3.3)$$

where λ and θ represent the wavelength of the plane wave component and the incident direction of the plane wave component, respectively. Therefore the received array signal can be expressed in vector notation as

$$\mathbf{X}(t) = \mathbf{a}(\theta) \cdot E_0(t) \quad (3.4)$$

where $\mathbf{a}(\theta)$ is known as the array response vector or the steering vector and given by

$$\mathbf{a}(\theta) = [1, \exp(-j \frac{2\pi}{\lambda} d \sin \theta), \dots, \exp(-j \frac{2\pi}{\lambda} (m-1)d \sin \theta)] \quad (3.5)$$

Assuming the channel is Additive White Gaussian Noise (AWGN) and there are L number of signals reaching the antenna array at the same time and at the same frequency such as delayed multipaths of the desired signal as well as interfering signals, the complex envelope representation of the received signal can be expressed by

$$\mathbf{X}(t) = \sum_{l=1}^L \mathbf{a}(\theta_l) \cdot E_1^l(t) + \mathbf{n}(t) \quad (3.6)$$

where L , θ_l , $E_1^l(t)$ and $\mathbf{n}(t)$ denote the number of signals, the direction of arrival (DOA) for the l^{th} signal, the received signal of the reference element of the l^{th} signal and the noise

vector at the array elements, respectively. As mentioned in section 3.1, beamforming is performed to extract the desired signal from the array received signal by suppressing the interference and noise components.

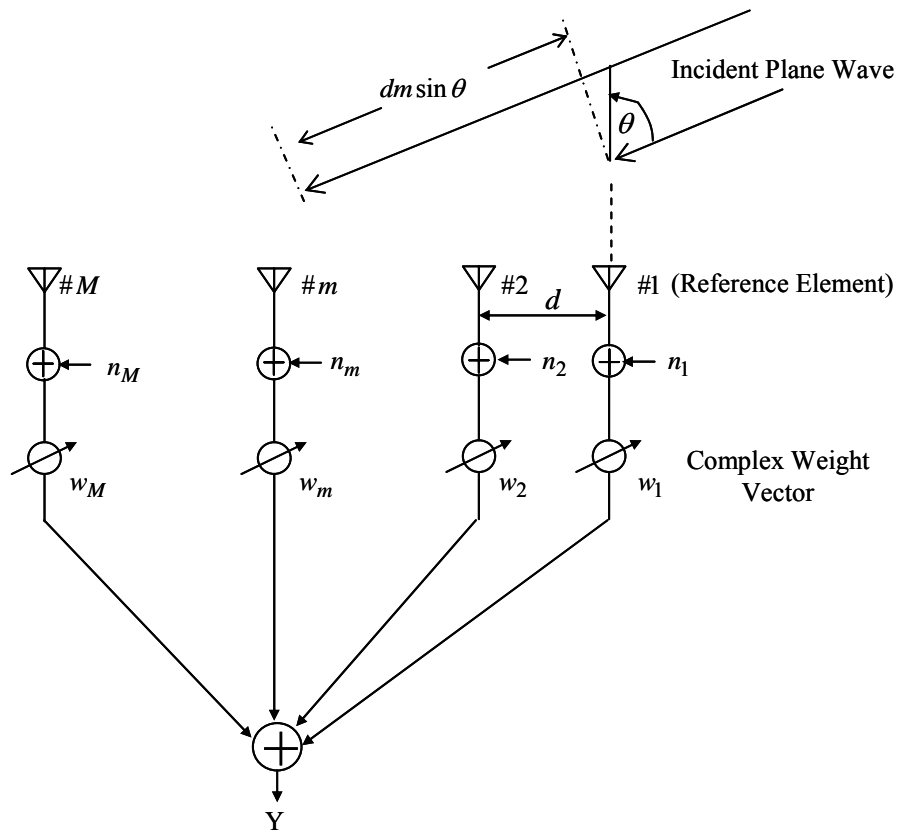


Fig. 3-1 Uniformly spaced linear array antenna with a plane wave incidents from direction θ

3.3 Beamforming

Beamforming is the algorithm that is used to separate the desired signal spatially from interfering signals which have the same frequency but different DOAs. There are two types of beamformers, one for narrowband signals and the other for wideband signals. Narrowband beamformer is focused in our discussion. Referring to Fig.3-2, which illustrates the basic concept of narrowband beamformer, the output signal of the beamformer can be given by

$$Y(t) = E_1(t) \sum_{m=1}^M A_m \exp(-j \frac{2\pi}{\lambda} (d-1)m \sin \theta + j\phi_m) \quad (3.7)$$

where the complex weight that applied to the m^{th} element is given by

$$w_m = A_m + j\delta_m \quad (3.8)$$

It should be noted that by setting the phase factor of the weight as

$$\delta_m = \frac{2\pi}{\lambda}(d-1)m \sin \theta_0 \quad (3.9)$$

the receiving gain for the direction of θ_0 is maximized as the phase of the received signal of each element for that direction is equaled. Like this, adaptive array antenna maximizes the antenna gain in the desired signal direction and simultaneously place minimal radiation pattern in the directions of interferes, by optimizing the weight vector. This is the basic concept of beamforming and there are several criteria to update the weight vector as the receiving direction of the desired signal might be unknown or a time varying factor in real communication. The output of the beamformer at time n can be given in vector form as

$$Y(n) = \mathbf{W}^H \cdot \mathbf{X}(n) \quad (3.10)$$

where H denoted the Hermitian (complex conjugate) transpose and

$$\mathbf{W} = [w_1, w_2, \dots, w_M]^T \quad (3.11)$$

is the complex weight vector.

3.4 Criteria for Weight Calculation

In order to maximize the SNR at the beamformer output, the adaptive beamformer adjust the weight on each element based on the statistics of the array data and places nulls in the directions of interfering signals. As the statistics of the array data may not be known and may time varying, adaptive algorithms are typically employed to determine the weights. Most adaptive beamforming algorithms involve iteration process to adjust the weights until a certain performance criterion is met. Generally used criteria are Minimum Mean Square Error (MMSE), Maximum Signal to Noise Ration (MSN), Constrained Minimization of Power (CMP), and Constant Modulus Algorithm (CMA). Here is brief discussion on the first two criteria, which are used in our research work.

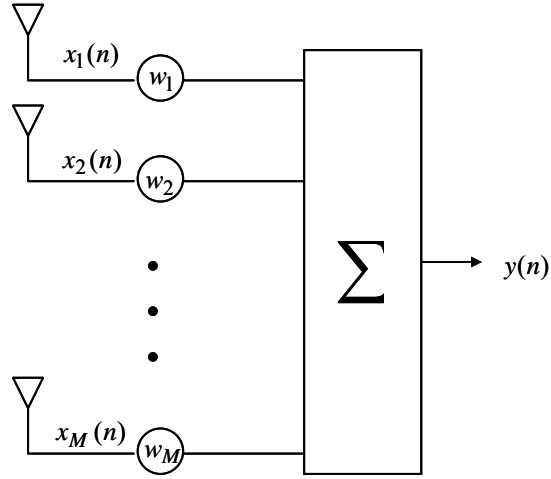


Fig. 3-2 *Narrowband beamformer*

3.4.1 Minimum Mean-Squared Error (MMSE) Criterion

The objective of the MMSE criterion is to minimize the mean-squared error between the received signal $Y(n)$ and the reference (desired) signal $r(n)$. Mathematically, the cost function to be minimized is

$$Err = E[|r(n) - y(n)|^2] \quad (3.12)$$

where $E[\cdot]$ denotes the ensemble average operator. Substituting Equation (3.10) into Equation (3.12), we have

$$E[|Err(n)|^2] = E[|d(n)|^2] - \mathbf{W}^T \cdot \mathbf{r}_{xr}^* - \mathbf{W}^H \cdot \mathbf{r}_{xr} + \mathbf{W}^H \cdot \mathbf{R}_{xx} \cdot \mathbf{W} \quad (3.13)$$

where \mathbf{R}_{xx} and \mathbf{r}_{xr} denote the correlation matrix of the array element input, given in Equation (3.14), and correlation vector between the reference signal $r(n)$, and the array element input given in Equation (3.15), respectively.

$$\mathbf{R}_{xx} = E[\mathbf{X}(n) \cdot \mathbf{X}^H(n)] \quad (3.14)$$

$$\mathbf{r}_{xr} = E[\mathbf{X}(n) \cdot r^*(n)] \quad (3.15)$$

In order to minimize the error given in Equation (3.13), we take the gradient of the function with respect w and set to zero. By solving this, we have the optimum weight vector so called Wiener solution, given by

$$\mathbf{W}_{opt} = \mathbf{R}_{xx}^{-1} \cdot \mathbf{r}_{xr} \quad (3.16)$$

In this section we described the MMSE criteria for calculation the optimum weight vector. Since the propagation conditions are usually unknown and changes over time, adaptive beamforming algorithms are employed to estimate them and update the weight vector over time. In section 3.5, we will discuss on those adaptive algorithms.

3.4.2 Maximum Signal to Noise Ratio (MSN) Criterion

In this criterion, weights are chosen to maximize the SNR of the output signal. Recalling the Equation (3.10), the output signal of the beamformer can be expressed by

$$y(n) = \mathbf{W}^T \mathbf{X}(n) \quad (3.17)$$

It should be noted that ingredients of noise, interference as well as desired signal are included in the received signal vector \mathbf{X} . Defining the components of desired signal, interference signal and noise inside \mathbf{X} by

$$\begin{aligned} S(n) &= [s_1(n), s_2(n), \dots, s_M(n)]^T \\ U(n) &= [u_1(n), u_2(n), \dots, u_M(n)]^T \\ N(n) &= [n_1(n), n_2(n), \dots, n_M(n)]^T \end{aligned} \quad (3.18)$$

,respectively. The power of each component in the output signal can be given by

$$\begin{aligned} P_S(n) &= \mathbf{W}^H \mathbf{R}_{ss} \mathbf{W} \\ P_U(n) &= \mathbf{W}^H \mathbf{R}_{uu} \mathbf{W} \\ P_N(n) &= P_n \mathbf{W}^H \mathbf{W} \end{aligned} \quad (3.19)$$

where R_{ss} , R_{uu} and P_n are given by

$$\begin{aligned}
\mathbf{R}_{ss} &= E[\mathbf{S}(n)\mathbf{S}^H(n)] \\
\mathbf{R}_{uu} &= E[\mathbf{U}(n)\mathbf{U}^H(n)] \\
P_n &= E[|n_m(n)|^2]
\end{aligned} \tag{3.20}$$

The SNR of the output signal can be defined by

$$SNR = \frac{P_s}{P_U + P_N} = \frac{\mathbf{W}^H \mathbf{R}_{ss} \mathbf{W}}{\mathbf{W}^H \mathbf{R}_{mm} \mathbf{W}} \tag{3.21}$$

where \mathbf{R}_{mm} expresses the correlation matrix of interference-plus-noise and given by

$$\mathbf{R}_{mm} = \mathbf{R}_{uu} + P_n \mathbf{I} \tag{3.22}$$

In order to maximize the SNR, we take the gradient of the function with respect w and set to zero. By solving this, we have the optimum weight vector so called Wiener solution, given by

$$\mathbf{W}_{opt} = \mathbf{R}_{mm}^{-1} \mathbf{V}_s \tag{3.23}$$

where \mathbf{V}_s expresses the steering vector of the adaptive array antenna.

3.5 Adaptive Algorithms for Beamforming

We discussed criterions to calculate the optimum weight vector in the previous section. Since it is needed to know the second-order statistics on the channel, which are subjected to be changed over the time or sometimes remains unknown, adaptive beamforming algorithms are employed to estimate and update the weight vector over time. The weights are being iteratively adjusted until the performance of the beamformer satisfies the desired criterion. In this section some of the adaptive algorithms that are used in MMSE adaptive array algorithm are discussed.

3.5.1 Least Mean Square (LMS) Algorithm

LMS algorithm avoids the correlation matrix inverse operation by using the instantaneous gradient vector (∇_w) to update the weight vector. Weight vector for the $(n+1)^{th}$ step can be expressed using the weight vector for the n^{th} step in LSM algorithm by

$$\mathbf{W}(n+1) = \mathbf{W}(n) - \frac{\mu}{2} \nabla_w E[|e(n)|^2] \quad (3.24)$$

where μ is the convergence factor which controls the speed of convergence and its value is usually between 0 and 1. $\nabla_w E[|e(n)|^2]$ can be calculated as

$$\begin{aligned} \nabla_w E[|e(n)|^2] &= -2\mathbf{r}_{xr} + 2\mathbf{R}_{xx} \mathbf{W}(n) \\ &= -2E[\mathbf{X}(n)\mathbf{r}^*(n)] + 2E[\mathbf{X}(n)\mathbf{X}^H(n)]\mathbf{W}(n) \\ &= -2E[\mathbf{X}(n)\{\mathbf{r}^*(n) - \mathbf{X}(n)\mathbf{W}(n)\}] \\ &= -2E[\mathbf{X}(n)\{\mathbf{r}^*(n) - Y^*(n)\}] \\ &= -2E[\mathbf{X}(n)e^*(n)] \end{aligned} \quad (3.25)$$

Inserting Equation (3.25) into Equation (3.23) we can get the weight vector as

$$\mathbf{W}(n+1) = \mathbf{W}(n) + \mu\mathbf{X}(n)e^*(n) \quad (3.26)$$

Further, it is known that the convergence factor should satisfy

$$0 < \mu < \frac{1}{\lambda_{\max}} \quad (3.27)$$

in order to converge. Here λ_{\max} denotes the largest eigenvalue of the correlation matrix \mathbf{R}_{xx} .

3.5.2 Sample Matrix Inversion (SMI) Algorithm

The idea of SMI algorithm is to estimate the correlation matrix \mathbf{R}_{xx} and the cross-correlation vector \mathbf{r}_{xr} based on the array input in an observation interval and calculates the optimized weight vector by inserting them into Weiner solution, which is given in Equation (3.16). The correlation matrix and the correlation vector are given by

$$\mathbf{R}_{xx} = \frac{1}{n} \sum_{i=1}^n \mathbf{X}(i) \mathbf{X}^H(i) \quad (3.28)$$

and

$$\mathbf{r}_{xr} = \frac{1}{n} \sum_{i=1}^n \mathbf{r}^*(n) \mathbf{X}(n) \quad (3.29)$$

, respectively. Then the optimum weight is calculated using the Weiner solution that is given in Equation (3.16). Further, estimating the correlation matrix and correlation vector for the $(n+1)^{th}$ step using that of for the n^{th} step is used more generally in order to reduce the calculation weight. The equations for the estimation are given by

$$\begin{aligned} \mathbf{R}_{xx}(0) &= \delta \mathbf{I} \quad ; \quad \delta > 0 \\ \mathbf{R}_{xx}(n+1) &= \beta^n \mathbf{R}_{xx}(n) + (1-\beta) \sum_{i=1}^n \beta^n \mathbf{X}(i) \mathbf{X}^H(i) \end{aligned} \quad (3.30)$$

and

$$\begin{aligned} \mathbf{r}_{xr}(1) &= \mathbf{X}(1) \mathbf{r}^*(1) \\ \mathbf{r}_{xr}(n+1) &= \beta \mathbf{r}_{xr}(n) + (1-\beta) \mathbf{X}(n) \mathbf{r}^*(n) \end{aligned} \quad (3.31)$$

, respectively. Here, β and \mathbf{I} denote the forgetting factor, which gives more weight to the recent samples and unit matrix. It should be noted that the inverse matrix of the correlation matrix is required in the process to calculate the optimum weight and to avoid matrix inversion of the correlation matrix, the matrix inversion lemma can be applied, which is given by

$$\begin{aligned} \mathbf{R}_{xx}^{-1}(0) &= \delta^{-1} \mathbf{I} \\ \mathbf{R}_{xx}^{-1}(n+1) &= \frac{1}{\beta} \mathbf{R}_{xx}^{-1}(n) - \frac{(1-\beta) \mathbf{R}_{xx}^{-1}(n) \mathbf{X}(n+1) \mathbf{X}^H(n+1) \mathbf{R}_{xx}^{-1}(n)}{\beta^2 + \beta(1-\beta) \mathbf{X}^H(n+1) \mathbf{R}_{xx}^{-1}(n) \mathbf{X}(n+1)} \end{aligned} \quad (3.32)$$

3.5.3 Recursive Least-Squares (RLS) Algorithm

In RLS algorithm, both correlation matrix of array input signals and the correlation matrix between the array inputs and reference signal are estimated by weighted sum as given below.

$$\mathbf{R}_{xx}(n+1) = \sum_{i=1}^n \alpha^n \mathbf{X}(i) \cdot \mathbf{X}^H(i) \quad (3.33)$$

$$\mathbf{r}_{xr}(n) = \sum_{i=1}^n \alpha^n \mathbf{X}(i) \cdot \mathbf{r}^*(i) \quad (3.34)$$

where $0 < \alpha < 1$ is the weighting factor which determines how quickly the previous data are de-emphasized, and n is the observation interval. The optimum weight obtained by subjecting the gradient of the error with respect to w to zero can be given by

$$\mathbf{W}_{opt}(n) = \mathbf{R}_{xx}^{-1}(n) \cdot \mathbf{r}_{xr}(n) \quad (3.35)$$

By further calculation, we can update the weight vector as follows

$$\mathbf{W}(n+1) = \mathbf{W}(n) + \gamma \mathbf{R}_{xx}^{-1}(n) \mathbf{X}(n+1) e^*(n+1) \quad (3.36)$$

where $e(n+1)$ and γ are defined by

$$e(n+1) = r(n+1) - \mathbf{W}^H(n) \mathbf{X}(n+1) \quad (3.37)$$

and

$$\gamma = \frac{1}{\alpha + \mathbf{X}^H(n+1) \mathbf{R}_{xx}^{-1}(n) \mathbf{X}(n+1)} \quad (3.38)$$

, respectively.

Chapter 4

Digital Terrestrial Television Broadcasting

This chapter gives a brief introduction on Digital Terrestrial Television Broadcasting (DTTB) in Japan, which is introduced in three major metropolitan areas in December 2003 and scheduled to be extended to nationwide coverage by 2011.

4.1 Introduction

Terrestrial television broadcasting introduced in Japan in 1953, thereafter it has developed to the fundamental media in Japan. Now there are more than 48 million households and 120 million television sets. In December 2003, Japan's terrestrial television broadcasting moved another step forward by introducing DTTB in three major cities and scheduled to be extended to a nationwide coverage by 2011. Following are the main attractions of DTTB.

- ✓ High picture quality
- ✓ High sound quality
- ✓ The ability of communicating in both ways
- ✓ Data broadcasting
- ✓ Efficient use of frequency
- ✓ Extinguishment of ghost
- ✓ Robust against noise
- ✓ Improvement of mobile reception

As summarized in Table 4-1, basically there are three major standards for digital broadcasting in the world. After Advanced Television Systems Committee (ATSC), the American standard and Terrestrial Digital Video Broadcasting (DVB-T), the European standard, Japan developed Integrated Services Digital Broadcasting (ISDB) which is suitable for the environment in Japan as well as to expand the flexibility across the physical layer regardless of whether it is applied to satellite or terrestrial broadcasting [25-27]. Although there are some commonalities with DVB-T, ISDB-T has many unique

factors such as segment structure, time interleaving and Transmission and Multiplexing Configuration Control (TMCC). There are three kinds of ISDB systems, ISDB-S for Satellite broadcasting, ISDB-T for Terrestrial broadcasting and ISDB-C for Cable broadcasting. A further discussion on ISDB-T is done in the next section.

Table 4-1 Digital terrestrial broadcasting systems in the world

Systems	ISDB-T	DVB-T	ATSC
Transmission	Multicarrier (OFDM) (BSD-OFDM) (OFDM)		Single carrier (8VSB)
Modulation	DQPSK/QPSK/16QAM /64QAM	QPSK/16QAM /64QAM	8VSB
Error Control	Convolution code / RS		Trellis code + RS
Characteristic	SFN capability Effective against ghost Segmented OFDM Time interleaving	SFN capability	Analog based format
Bandwidth	6/7/8 MHz		
Area	Japan	Europe	USA

4.2 ISDB-T Standard

Japan, as a country that has cities surrounded by mountains as well as high rise buildings, a modulation system which is robust against multipath fading and with high efficiency in frequency usage was given the priority when choosing a modulation system for DTTB. As a result, a multicarrier modulation system, Orthogonal Frequency Division Multiplexing (OFDM), which is also used in DVB-T, is adopted for ISDB-T. ISDB-T separates the 5.6MHz bandwidth into 13 segments of 429 KHz. Because of this special characteristic of dividing the bandwidth into a number of segments, the OFDM modulation system which is used in ISDB-T is particularly called Band Segmented Transmission-OFDM (BST-OFDM). This feature makes it possible to broadcast multi programs simultaneously using these 13 segments flexibly. For an instant, it can broadcast one HDTV (12 segments) with mobile service (1 segment) or 3 SDTV (3*4 segments) + mobile service (1 segment). Also it should be noted that the transmission parameters of the modulation scheme of OFDM carriers, the coding rates of inner code, and the length of the time interleaving can be independently specified for each data segment. The maximum of 3 layers can be transmitted in a channel at the same time. Table 4-2 shows the main segment parameters for 6MHz ISDB-T.

Table 4-2 Table 4-2 Segment Parameters for ISDB-T (6 MHz)

Mode		Mode 1		Mode 2		Mode 3	
Bandwidth		428.57 kHz					
Carrier spacing		3.968 kHz		1.984 kHz		0.992 kHz	
Number of carriers	Total	108	108	216	216	432	432
	Data	96	96	192	192	384	384
	SP ₁	9	0	18	0	36	0
	CP ₁	0	1	0	1	0	1
	TMCC ₂	1	5	2	10	4	20
	AC ₁ ₃	2	2	4	4	8	8
	AC ₂ ₃	0	4	0	9	0	19
Carrier modulation		16QAM 64QAM QPSK	DQPSK	16QAM 64QAM QPSK	DQPSK	16QAM 64QAM QPSK	DQPSK
Number of symbol per frame		204					
Effective symbol duration		252 μs		504 μs		1008 μs	
Guard interval		63 μs, 31.5 μs, 15.75 μs, 7.875 μs		126 μs, 63 μs, 31.5 μs, 15.75 μs		252 μs, 126 μs, 63 μs, 31.5 μs	
Frame duration		64.26ms, 57.834ms, 54.621ms, 53.0145ms		128.52ms, 115.668ms, 109.242ms, 106.029ms		257.04ms, 231.336ms, 218.464ms, 212.058ms	
FFT sample cock		8.12693.. MHz					
Inner code		Convolution code (1/2, 2/3, 3/4, 5/6, 7/8)					
Outer code		RS (204, 188)					

1: SP (Scattered Pilot) and CP (Continual Pilot) can be used for frequency synchronization and channel estimation

2: TMCC (Transmission and Multiplexing Configuration Control) carries information on transmission parameters

3: AC (Auxiliary Channel) carries ancillary information for network operation

4.3 Attractive Features of DTTB

4.3.1 High Definition Television (HDTV)

The government has required the broadcasters to ensure more than 50% of programs to be broadcasted in HDTV format. Although the technical requirement to be called HDTV is 720p, DTTB uses 1080i.

4.3.2 Mobile Reception

ISDB-T has allocated one segment to transmit a 16QAM modulated 639kbps stream for mobile receivers and scheduled to be commenced service from 2005. MPEG4 will be used as the video compression standard for this segment. Although this will provide enough picture quality for mobile terminals such as mobile phones and PDAs, many researches have been conducted in order to receive 12-segment high quality broadcast from vehicles.

4.3.3 Copyright Protection

One of major advantages of digital signals is that it allows to achieve a copy as same as the master in quality. On the other hand, this will harm the program rights and leads to introduction of a copy right protection to DTTB in STDB-T. The viewer is allowed to make a single copy of a program, and the first copy will be automatically erased once it is copied to another media.

Chapter 5

Beam-Space Adaptive Array Antenna for Suppressing the Doppler Spread in OFDM Mobile Reception

This chapter proposes the use of Beam-Space Adaptive Array Antennas (BSAAA) for moving receivers in order to suppress Inter Carrier Interference (ICI) due to Doppler frequency spread in Orthogonal Frequency Division Multiplexing (OFDM) mobile reception. In the proposed system, firstly we separate the multipath signals into multi-beams according to their incident directions, then correct the Doppler frequency shift of each beam signal considering the beam direction, and finally combine the corrected beam signals based on Maximal Ratio Combining (MRC). Further this chapter clarifies the excellent performance of the proposed system in suppressing the influence of Doppler frequency spread by carrying out computer simulation. Particularly, it was certified that it is possible to suppress the influence of the Doppler frequency spread efficiently for all the receiving directions by using eight-element BSAA antenna with element spacing of $(3/8)\lambda$, and referring only three past symbols when calculating the weight vector of MRC.

5.1 Introduction

Over the past few years, OFDM has been successfully applied to a wide variety of digital communication applications such as Digital Video Broadcasting (DVB), Digital Audio Broadcasting (DAB), Asymmetric Digital Subscriber Line (ADSL), Wireless Local Area Network (WLAN) and Digital Terrestrial Television Broadcasting in Japan (DTTB) [3, 4]. Further OFDM has been considered as a modulation system for the fourth generation mobile communication systems with the success it has achieved in previous applications [5, 6]. One of the main reasons for the use of OFDM is to increase the robustness against frequency selective fading due to multipath propagation or narrowband interference. In a single-carrier system, a signal fade or interfere can cause the entire link to fail, but in a multicarrier system, only a small percentage of the subcarriers will be affected. However, conventional multicarrier systems are paid less attention due to its inefficient use of the available spectrum. But by using an overlapping multicarrier modulation technique such as OFDM, one can increase the efficiency of the frequency usage. In order to realize the overlapping multicarrier technique, crosstalk between subcarriers needs to be reduced. This means subcarriers must be mutually orthogonal, which lead OFDM more sensitive to frequency offsets [7-9].

It is well known, under such conditions of a moving source or a receiver, the frequency observed by the receiver will be shifted from the original frequency so-called

Doppler Shift. The frequency shift is related to the spatial angle between the receiving direction of the signal and the direction of vehicular motion [28]. Therefore in an environment where multipath signals exist, it would lead to Doppler spread. Doppler spread causes a number of impairments including ICI and reduction of signal amplitude in the output of the filters matched to each of the carriers [9]. The impairment due to the Doppler spread is one of the major problems to overcome in mobile reception of DTTB, where the symbol period and the moving speed of the receiver are comparatively high.

A number of methods have been proposed to reduce this sensitivity to frequency offset, including windowing of the transmitted signal [10], self-ICI cancellation [11] and space domain interpolation [12]. However, all these methods give very less performance improvement comparing to their complexity in implication. Further in [13], it has been proposed to reduce the Doppler spread by limiting the incoming angle of the received signal, which will disuse some multipaths and reduce the power efficiency. Motivated by having no reasonable method to suppress the ICI due to Doppler frequency spread; in this work we introduce Beam-Space Adaptive Array Antenna to OFDM mobile communication systems.

In our proposed scheme, firstly we separate the multipath signals into number of multibeam according to their incident directions, then correct the frequency shift of each beam signal considering their beam directions and finally combine the corrected beam signals based on Maximal Ratio Combining. Here we have used a similar method given in [13] to calculate the phase shift for a given direction when compensating the Doppler shift. Further we have evaluated and verified the performance of the proposed scheme by computer simulation. Particularly, it has been shown the possibility of efficient Doppler spread suppression for all incident angles by the use of 8-element BSAAA with element spacing of $(3/8)\lambda$ and considering only 3 past symbols when calculating the weight vector of MRC.

5.2 Basic Configuration

Figure 5-1 shows the basic configuration of the proposed receiver scheme of a mobile terminal in OFDM system. This scheme will be applicable to mobile reception of DTTB. The following is the step-by-step procedure of the proposed scheme.

- Step1: Separate the multipath signals on their incident directions to a number of groups (beams), using BSAAA.
- Step2: Correct the frequency shift due to Doppler effect of each beam signal considering its beam direction.
- Step3: Convert the serial data stream into a parallel data stream and demodulate the corrected signals of each beam by performing Discrete Fourier Transformation (DFT).

Step4: Combine the demodulated beam signals using Maximal Ratio Combiner (MRC).

Step5: Convert the parallel data stream back into a serial data stream.

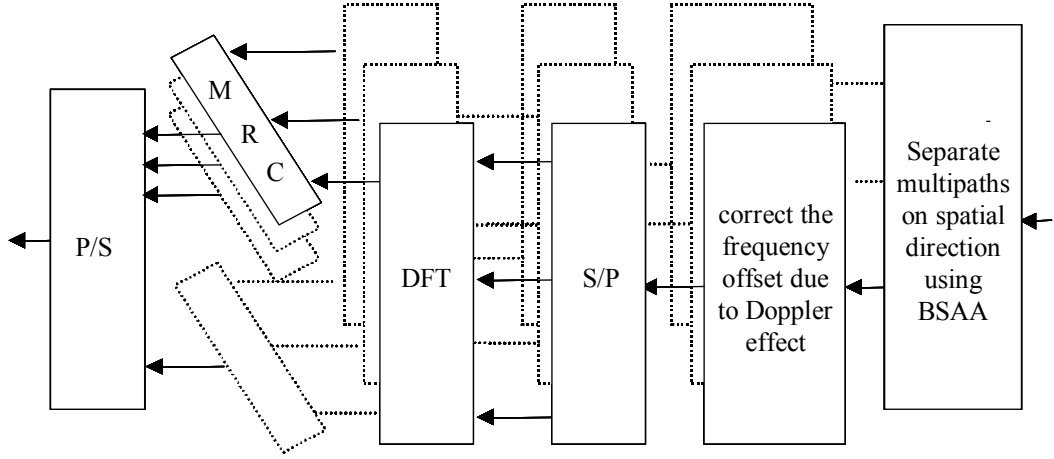


Fig. 5-1 Proposed BSAA Scheme for OFDM Mobile Reception

5.3 Beam-Space Array (Multibeam formation)

In the above proposed scheme, we have suggested the use of a linear array antenna that consists of M components at the mobile terminal in order to separate multipath signals by their incident directions as shown in Fig.5-2(a). The received signal of the array antenna is given by

$$\mathbf{R} = \sum_{l=1}^L a_l \begin{bmatrix} 1, \exp(-j2 \frac{\pi}{\lambda} d \cos \theta_l), \exp(-j4 \frac{\pi}{\lambda} d \cos \theta_l), \\ \dots, \exp(-j2(M-1) \frac{\pi}{\lambda} d \cos \theta_l) \end{bmatrix}^T \quad (5.1)$$

where d , L , θ_l and a_l denote the inter-element space of the array antenna, the number of multipath signals, the incident direction of the l^{th} multipath signal and the amplitude of the l^{th} multipath signal, respectively. It should be noted that the element of the linear array antenna is placed in parallel to the moving direction of the receiver.

Performing DFT in space domain for the received array signal forms the multibeam pattern. The received signal of the m^{th} beam pattern is given by

$$B_m = \sum_{i=0}^{M-1} R_i \cdot \exp(-j2\pi im / M), \quad m = 0, 1, \dots, M-1 \quad (5.2)$$

where R_i denotes the complex amplitude of the i^{th} element of the array antenna. Fig.5-2(b) illustrates the multibeam pattern of the eight-element beam-space array, where inter-element space d is $\lambda/2$. As shown in Fig.5-2(b), beam number 4 (B_4) receives signals from the front and rear sides of the vehicle, where Doppler frequency shifts are v/λ and $-v/\lambda$, respectively. Therefore B_4 receives signals with two different Doppler shifts.

When considering the other beams, for example B_6 , it receives both signals in the direction of $\theta = |\cos^{-1}(2/3)|$ and $\theta = -|\cos^{-1}(2/3)|$. But it should be noted that the magnitude of the Doppler frequency shift for both directions are the same. This signifies that the beams except B_4 contain signals with nearly the same frequency shift. This also implies that we can maximize the efficiency of separating multipath signals by the use of linear array antenna placed parallel to the direction of movement. For instance we could divide the space in to 12 beams for the purpose of canceling Doppler frequency spread by using only 8-element linear array antenna. This is shown in Fig.5-2(c).

By setting the inter-element space to $(3/8)\lambda$ of the eight-element array, one can direct B_5 in the direction of the vehicle movement and B_3 in the opposite direction of the vehicle movement as illustrated in Fig.5-2(c). The radiation pattern of beam 5 (B_5) at $d = \lambda/2$ and $d = 3\lambda/8$ are illustrated in Fig.5-3. Therefore, we can receive signals from all directions with only using other beams except B_4 , which receives signals with different Doppler frequency shift. Furthermore the array antenna arrangement can be made compact by reducing the inter-element spacing. However, the mutual coupling between the array elements becomes larger when the element-spacing decreases. Nonetheless we believe that mutual coupling would not be a serious problem as the task of the proposed BSAAA is only to divide the multipath signals in to a number of beams, but not to estimate the Direction of Arriving (DOA) of the multipath signals accurately. Moreover two schemes to compensate the mutual coupling between the array elements called, Re-defined Mutual Impedance Matrix scheme and Reference Signal scheme have been introduced in [29]. Therefore, problems associated with mutual coupling can be overcome by implementing one of the above mentioned schemes if necessary.

In four-element array, covering the entire space with beams except B_2 , which receives signals with different Doppler shift can be done by setting the inter-element space to $\lambda/4$. However, this may not be in practice due to the high mutual coupling between the array elements.

In each beam, signals received have nearly the same Doppler shift. Accordingly, by compensating each Doppler shift beam-by-beam, Doppler spread can be despread. If λ and v are known, it is possible to calculate the degree of Doppler frequency shift for each beam direction. Calculated Doppler shift canceling vector for eight-element array receiver is given by

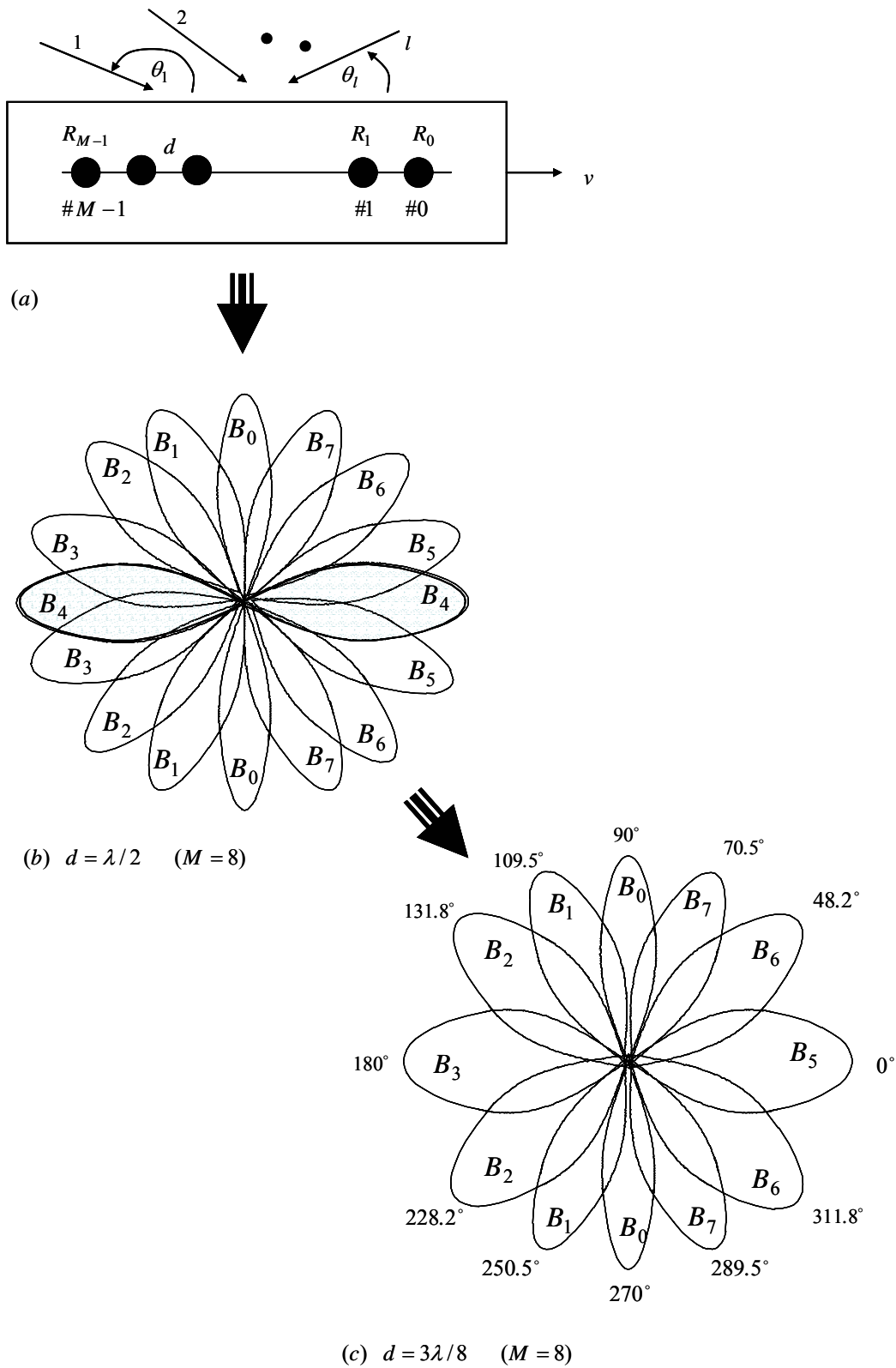
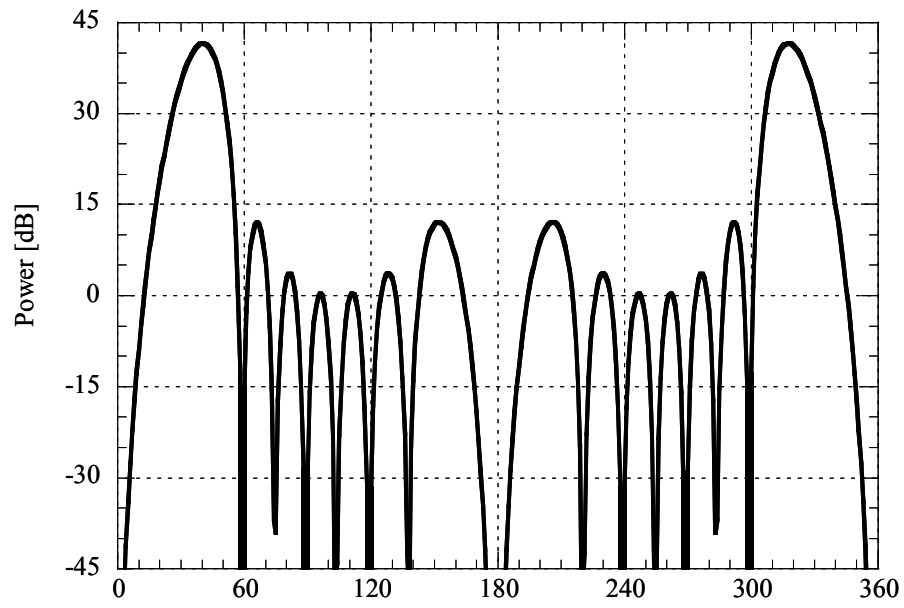
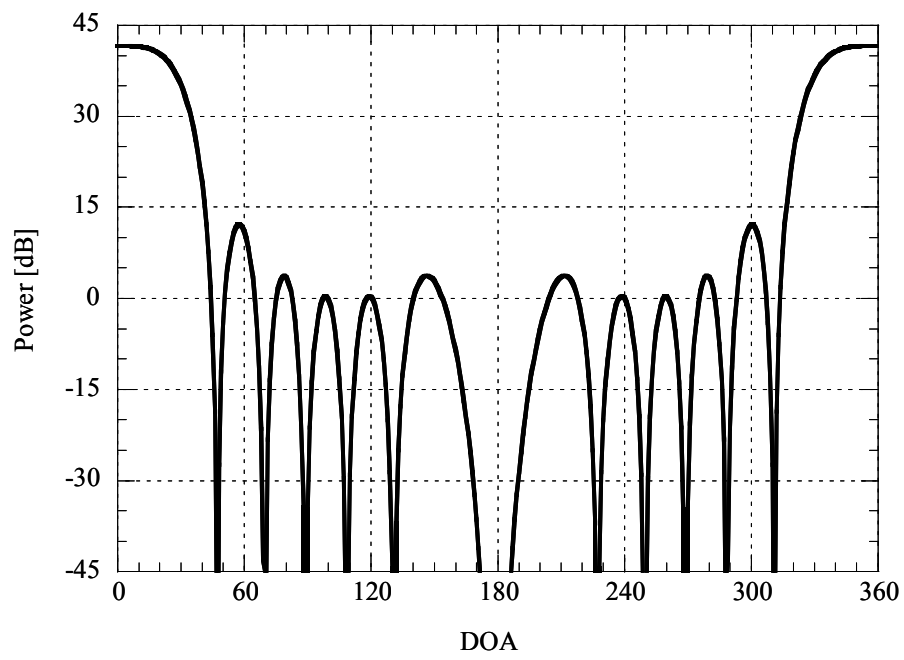


Fig. 5-2 Beam-Space Array Antenna in the mobile terminal (a) antenna arrangement (b) multi-beam pattern for $d = \lambda/2$, $M = 8$ (c) multi-beam pattern for $d = 3\lambda/8$, $M = 8$



(a) $d = \lambda/2$



(b) $d = 3\lambda/8$

Fig. 5-3 Radiation pattern of beam 5

5.4 Maximal Ratio Combining (MRC)

After correcting the Doppler frequency shift of each beam signal, we demodulate and combine them using Maximal Ratio Combiner (MRC). This is carried out for each subchannel individually to maximize the Signal to Noise Ratio (SNR) of the combined signal. The configuration of MRC is illustrated in Fig.5-4.

When calculating the correlation matrix of the beam output signals, the sliding average of past Q samples have been considered. Correlation matrix for k^{th} subchannel is given by

$$\mathbf{R}_{xx}^{(k)}(t) = \frac{1}{Q} \sum_{i=0}^{Q-1} \mathbf{X}^{(k)}(t - iT_s) \mathbf{X}^{(k)H}(t - iT_s) \quad (5.6)$$

where T_s denotes the efficient OFDM symbol duration, and $\mathbf{X}^{(k)}(t - iT_s)$ denotes the k^{th} subchannel signal of past i^{th} OFDM symbol of each beam and given by

$$\mathbf{X}^{(k)}(t - iT_s) = \begin{bmatrix} X_{(0)}^{(k)}(t - iT_s), X_{(1)}^{(k)}(t - iT_s), \dots \\ X_{(M/2-1)}^{(k)}(t - iT_s), X_{(M/2+1)}^{(k)}(t - iT_s), \\ \dots, X_{(M-1)}^{(k)}(t - iT_s) \end{bmatrix}^T \quad (5.7)$$

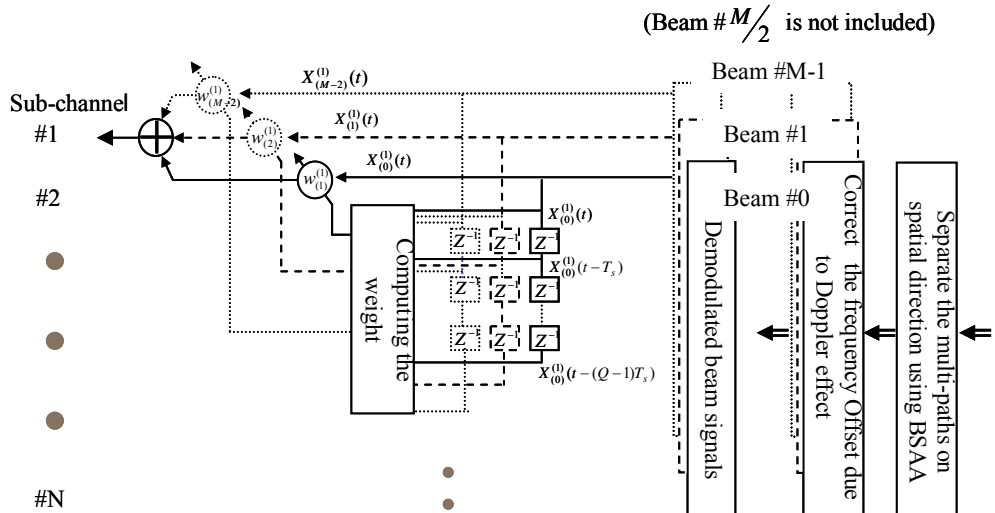


Fig. 5-4 MRC of an M -element BSAA receiver

Subsequently, we carried out MRC by using the eigenvector $\mathbf{e}_{\max}^{(k)}(t)$, for the maximum eigenvalue $\lambda_{\max}^{(k)}(t)$, of the $\mathbf{R}_{xx}^{(k)}(t)$ as the weight vector for the k^{th} sub-channel.

$$\mathbf{w}^{(k)}(t) = \mathbf{e}_{\max}^{(k)}(t) \quad (5.8)$$

Fig.5-5 illustrates the time variation of the received signal power for single antenna receiver, simply adding of the beam signals of BSAAA, and MRC based BSAAA receivers in (a), (b) and (c), respectively.

Here it can be seen that the time variation of the received power can be decelerated by dividing multipath signals on their incident direction with the use of beam space array antenna and combine them after correcting the Doppler frequency shift. Furthermore Fig.5-5(c) verifies that the propagation characteristic of the receiver can be improved significantly by applying MRC when combining the beam signals of BSAAA. This result hints the excellence performance of BSAAA and further evaluation is done by Bit Error Rate (BER).

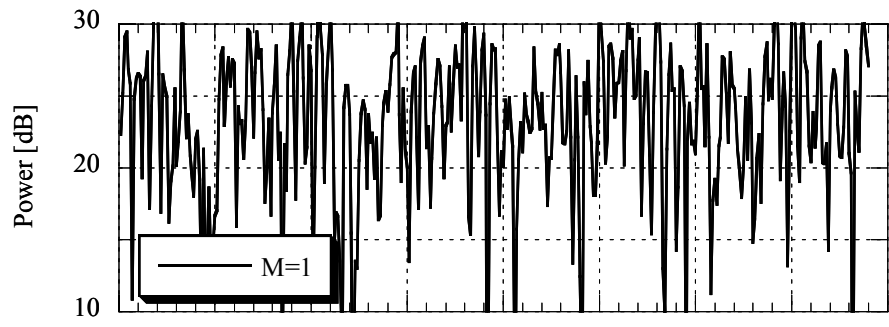
5.5 Simulations

To demonstrate the performance of the proposed scheme, computer simulations have been carried out and the system performance is measured by the BER, which is averaged over 1 million bits. Before presenting the simulation results, we first describe the parameters of the OFDM simulation system and the propagation environment.

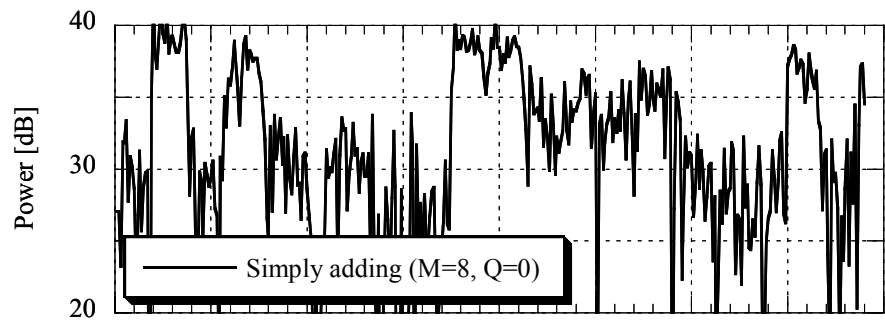
5.5.1 System Parameters for Simulation

The assumed OFDM system is identical to mode 3 of DTTB when considering the influence of Doppler frequency shift but the number of subcarriers is being reduced in order to simplify the simulation. Single omni-directional antenna, 4-element and 8-element BSAAA are used as the receivers. A propagation environment with 5 multipath signals is assumed. Multipath signals are placed inside the guard interval.

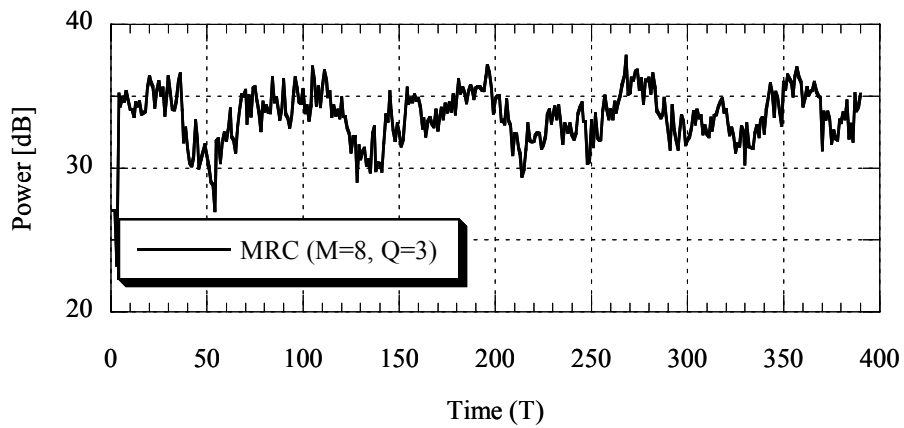
System parameters are set as shown in Table 5-1 and carried out simulation to optimize the number of past OFDM symbols that considered when carrying out MRC, and to evaluate the performance of the proposed scheme. Table 5-2 shows the propagation environment assumed here.



(a) Results for single antenna



(b) Results for simply adding of the beam signals



(c) Results for MRC of the beam signals

Fig. 5-5 Time variation of the received signal power at $f_d T_s = 0.15$, $SNR = 20dB$

Table 5-1 System Parameters

Number of bits transmitted	1,000,000	
Number of sub-carriers (N)	256	
Symbol period (without GI) ($T_s = 256 \times T$)	1 ms	
Modulation system	DQPSK	
Guard interval (GI)	$8T$	
Number of elements of linear array antenna (M)	1,4,8	
Inter-element spacing	$M = 4$	$\frac{\lambda}{4}$
	$M = 8$	$\frac{3\lambda}{8}$

Table 5-2 Propagation Environment

Path	Angle	Amplitude	Delay
1	30°	1.0	$1T$
2	45°	1.0	$2T$
3	120°	1.0	$3T$
4	235°	1.0	$5T$
5	290°	1.0	$7T$

5.5.2 Optimizing MRC

In this section the performance is evaluated as a function of the number of past data considered when calculating $\mathbf{R}_{xx}^{(k)}(t)$ in 4-element and 8-element BSAAA. For comparison, results for the simple addition of multibeam outputs are also given.

(a) 8-Element Beam-Space Array Receiver

Figures 5-6(a), (b) and (c) show the BER versus total signal power to noise ratio of the received signal, for various Q s, and $M = 8$ at normalized Doppler frequencies of $f_d T_s = 0$, 0.15 and 0.30, respectively. From Fig.5-6(a), it can be seen that the BER improves as the value of Q increases, though there is no remarkable improvement for Q over 3, in an environment where Doppler spread does not exist.

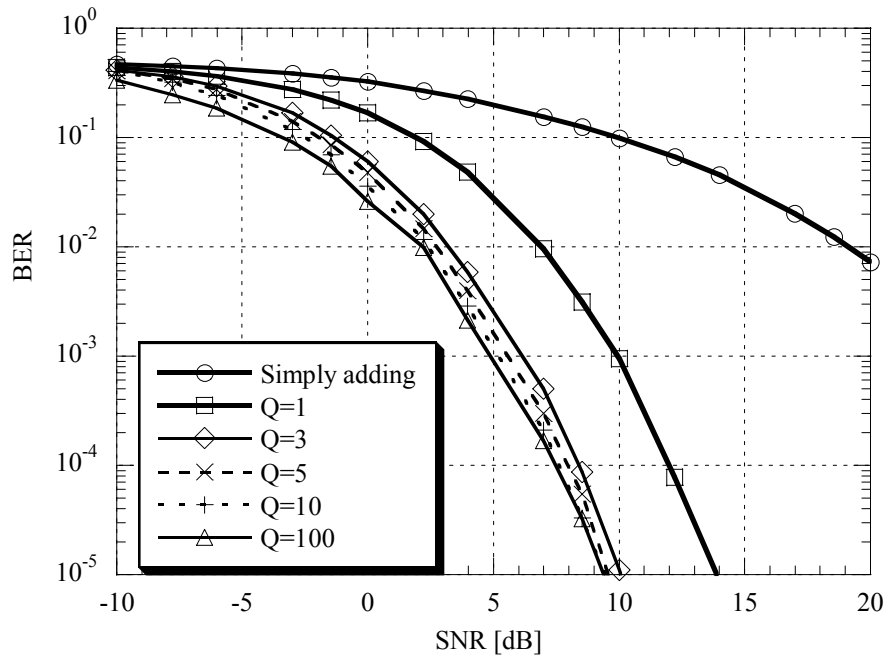
Figure 5-6(b), was obtained at $f_d T_s = 0.15$ of normalized Doppler spread. Here it can be seen an improvement in the BER with increasing Q and the best BER at $Q=5$. However, further increase in Q deteriorates the achievable BER. Although similar system performance can be predicted for $Q=3, 5$ and 10, the BER characteristic for $Q=100$ has deteriorated very sharply due to the Doppler spread.

Figure 5-6(c) illustrates the BER characteristic for $f_d T_s = 0.30$, which is considerably large. Here we have achieved the best performances for $Q=3$ and 5. The performance for $Q=10$ has deteriorated compared to its performance for $f_d T_s = 0.15$.

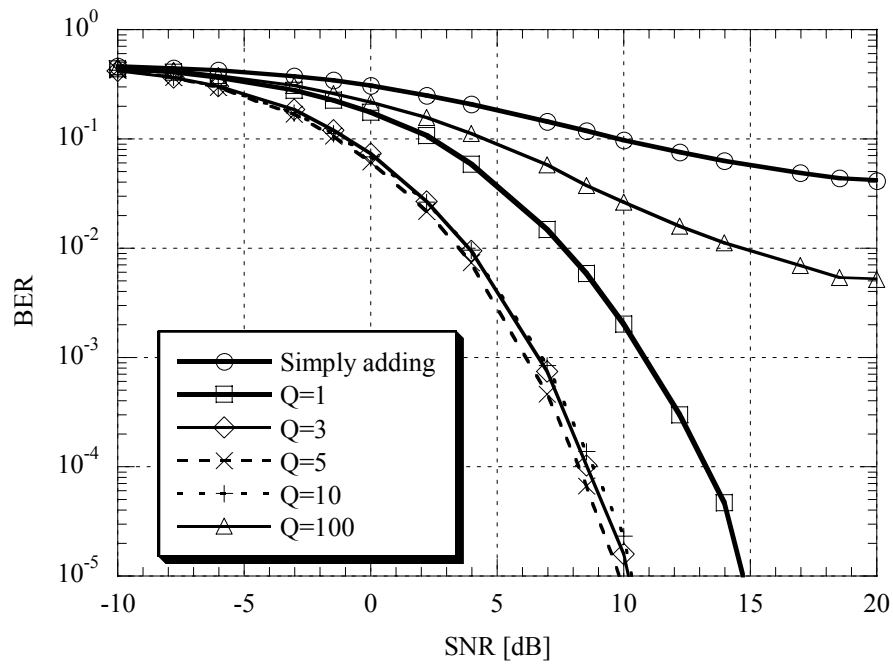
By considering these 3 results, Fig.5-6(a) suggests that the influence of the noise to the weight vector of the MRC can be reduced by considering a large number of past data when calculating the weight vector. On the other hand, Fig.5-6(b) and 5-6(c) explain that, under a time varying propagation condition, weight vector is mislead, when a large number of past data is been considered.

Further we have illustrated how the BER varies as a function of Doppler frequency, where the total signal power to noise ratio of the received signal is 10dB in Fig.5-7. This also verifies, by setting the Q to a very large number such as 100, or a considerably large number such as 10, gives better accuracy for only small Doppler spreads. On the other hand by setting Q to a very small number such as 1, does not improve the system performance considerably. However, by setting Q to a small number such as 3 or 5, we can achieve an excellent system performance for any amount of Doppler spread.

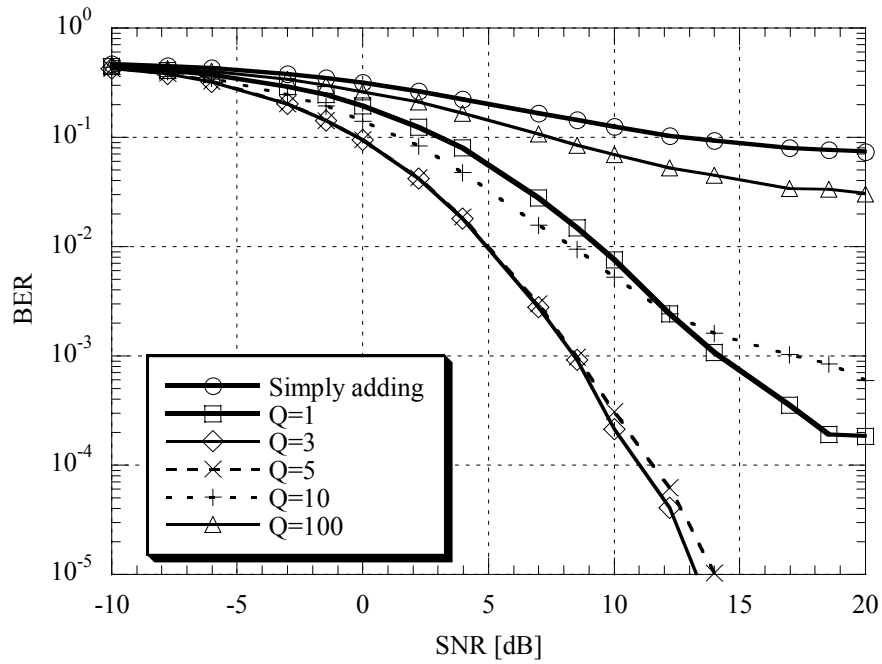
After considering results, illustrated in Figs.5-6 and 5-7, it is clear that we can achieve the best BER performance by setting Q to a small number such as 3 or 5. Furthermore, by considering the calculation time and due to similar performances in systems with $Q=3$ and $Q=5$, we can identify that $Q=3$ is sufficient to suppress the inter carrier interference (ICI) due to Doppler spread in 8-element beam-space array receiver.



(a) $f_d T_s = 0$



(b) $f_D T_s = 0.15$



(c) $f_D T_s = 0.30$

Fig. 5-6 BER as a function of SNR of the received signal for $M = 8$

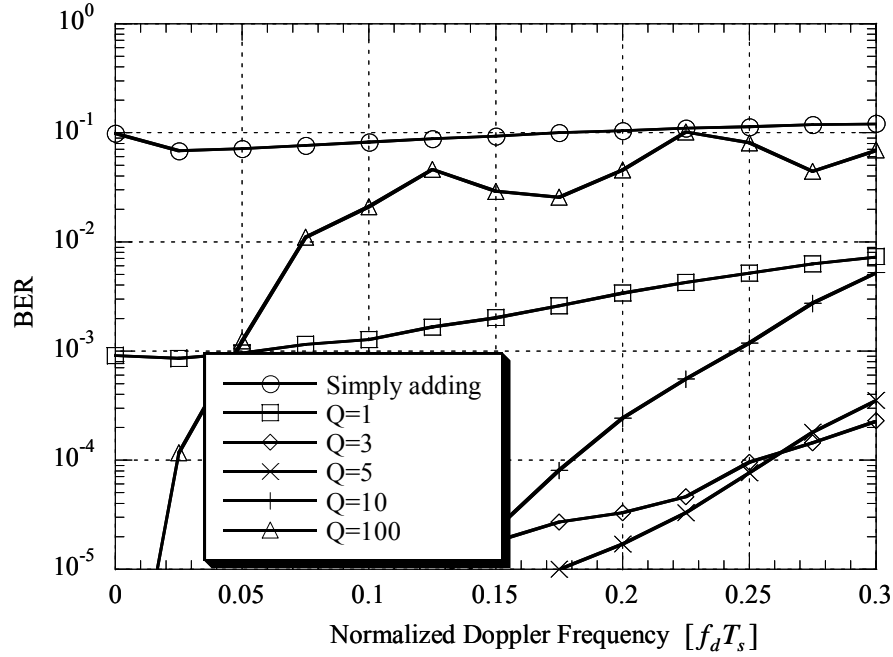


Fig. 5-7 BER as a function of normalized Doppler frequency where received signal SNR = 10dB ,
 $M = 8$

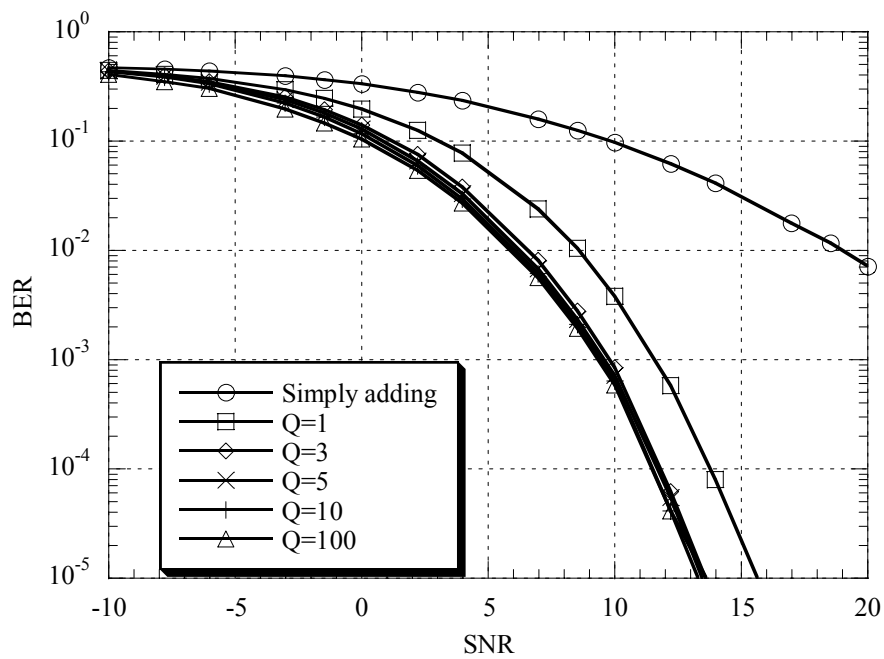
(b) 4-Element Beam-Space Array Receiver

We have also performed similar simulations to examine the most suitable Q for 4-element beam-space array receiver, which has three different beam patterns. Results from simulations are shown in Figs.5-8 and 5-9. Here too we could justify that $Q=3$ is sufficient to suppress the inter carrier interference (ICI) due to Doppler spread in 4-element beam-space array receiver.

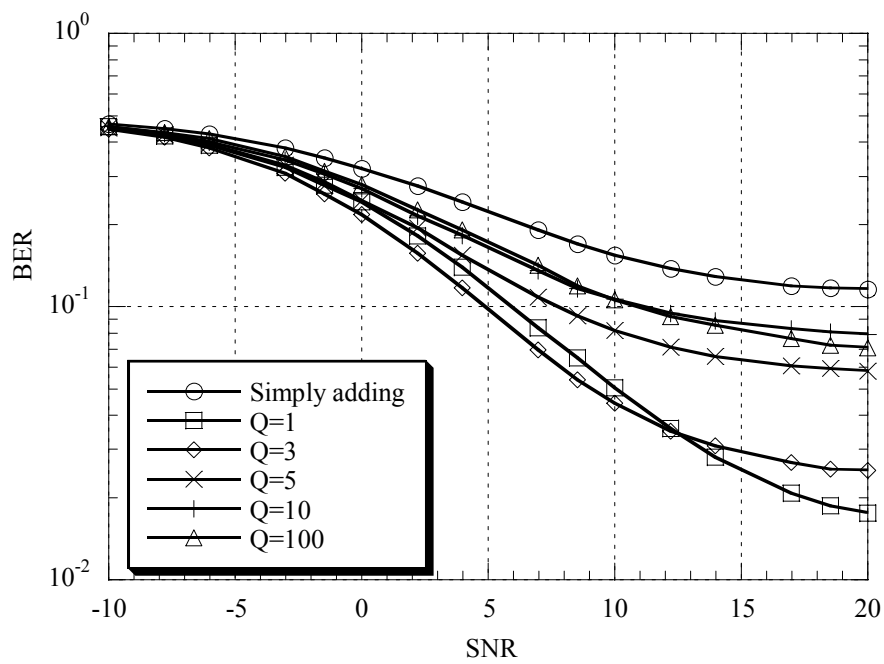
5.5.3 Performance Evaluation

In this section, the performances of single omni-directional antenna receiver, 4-element simply adding BSAA receiver, 4-element MRC BSAA receiver, 8-element simply adding BSAA receiver and 8-element MRC BSAA receiver are evaluated.

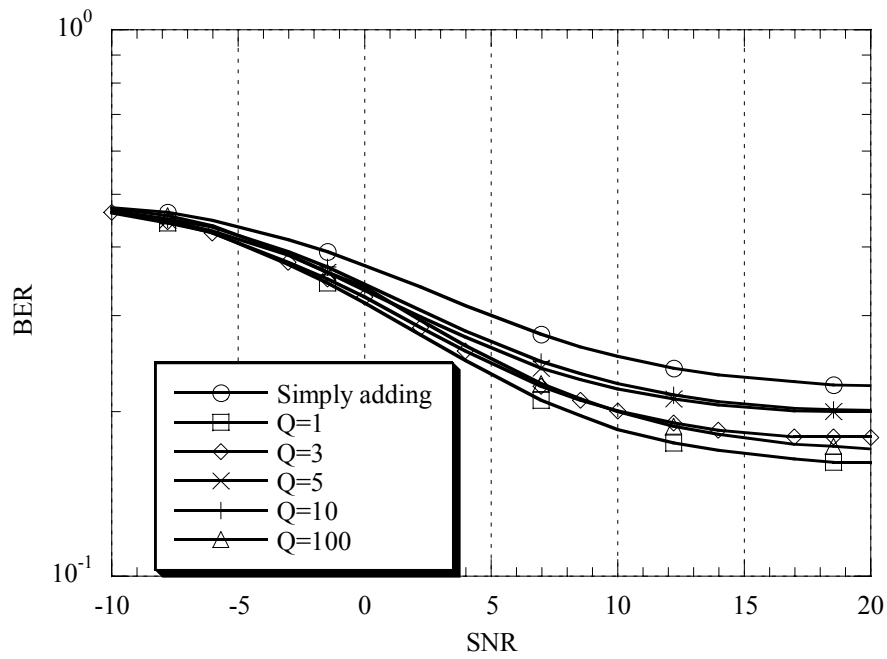
Figure 5-10 illustrates the BER versus total signal power to noise ratio (SNR) of the received signal, for M of 1, 4 and 8 at $f_d T_s = 0.0$, $f_d T_s = 0.15$ and $f_d T_s = 0.3$. Here $Q=3$, the most suitable value for Q , has been used when performing MRC. It can be seen that the BER improves for higher values of M . Particularly, 8-element BSAA combined with MRC gives the best system performance for any degree of noise.



(a) $f_D T_s = 0$



(b) $f_D T_s = 0.15$



(c) $f_d T_s = 0.30$

Fig. 5-8 BER as a function of SNR of the received signal for $M = 4$

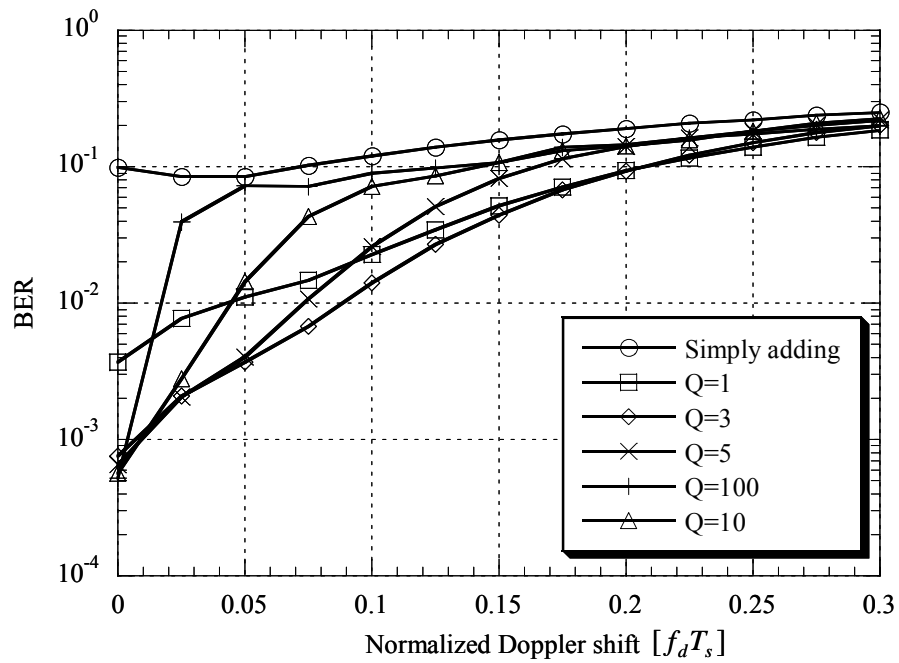


Fig. 5-9 BER as a function of normalized Doppler frequency, $SNR = 10dB$, $M = 4$

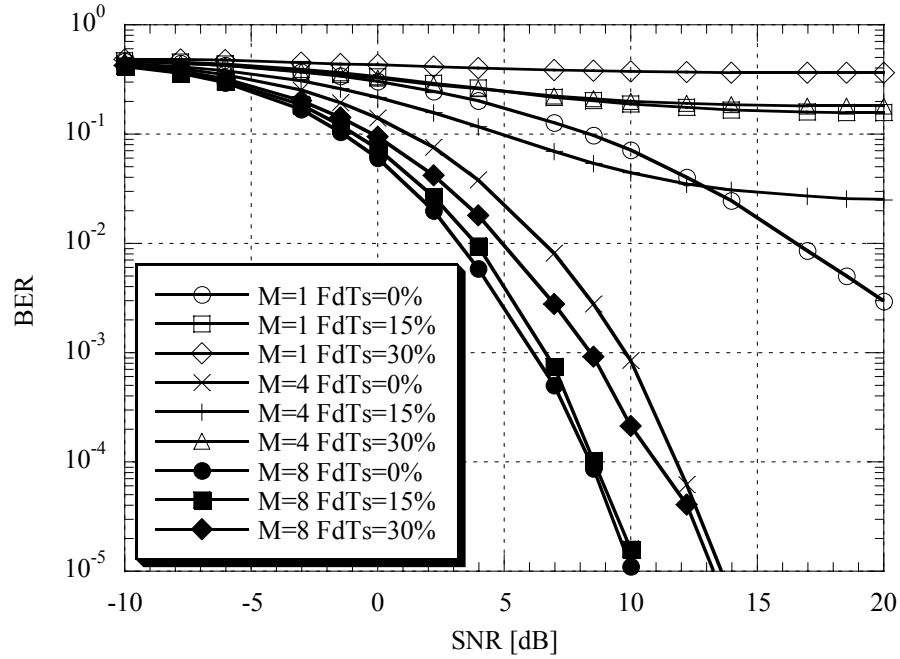
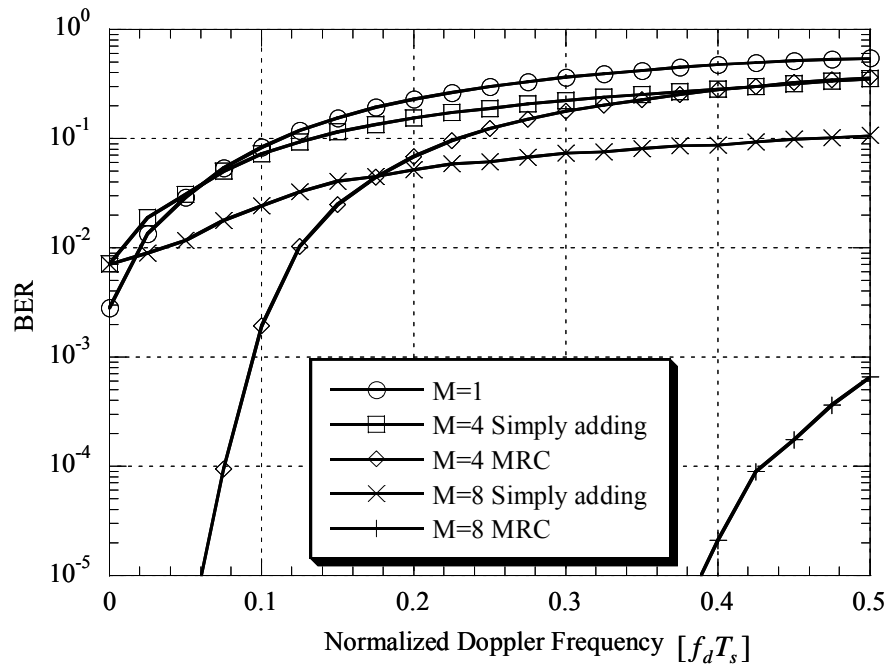


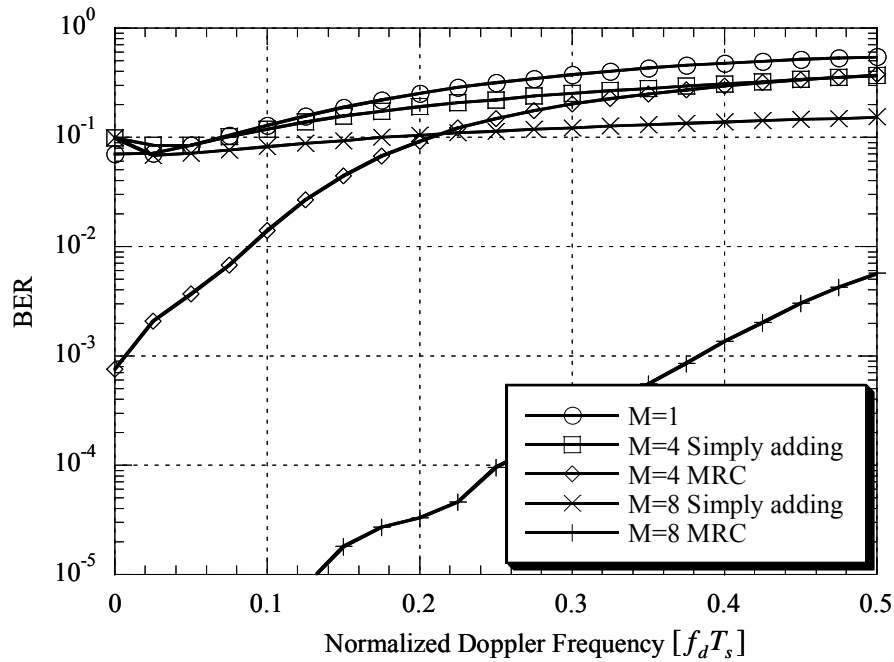
Fig. 5-10 BER as a function of SNR $f_d T_s = 0.0, 0.15, 0.30$ for $M = 1, 4, 8$

Fig.5-11(a) shows the bit error rate as a function of normalized Doppler frequency shift for M of 1, 4 and 8, for both the systems where MRC ($Q = 3$) and simply adding is performed to combine the beam signals. Here the total signal power to noise ratio of the received signal was set to 20dB. We can see that the BER improves with increasing M . This signifies the possibility of BSAA to suppress the BER due to Doppler frequency spread. Furthermore it should be noted that application of MRC improves the BER sharply. The reason for this improvement can be explained as follows. Bit errors occur due to Doppler spread and white noise. When applying MRC to combine the beam signals, the power of the received signal is been increased as well as the propagation characteristic is improved. Therefore reduce the bit errors that occur due to white noise. Particularly, we could maintain the BER less than 10^{-5} with the use of eight-element BSAAA combined with MRC even for the normalized Doppler frequency of 0.38.

The simulation result for the SNR at 10dB is given in Fig.5-11(b). Here the BER characteristics for all receivers have deteriorated compared to the values obtained in Fig.5-11(a). However, we could attain BER less than 10^{-3} up to the normalized Doppler spread is 0.38, with the use of eight-element BSAAA combined with MRC.



(a) SNR = 20dB



(b) SNR = 10dB

Fig. 5-11 BER as a function of normalized Doppler frequency $M = 1, 4, 8$ and $Q = 3$

Finally, we assumed a more multipath-rich propagation condition around a mobile station. In this case 50 multipath signals arriving from omni-directional angles, with 20dB of total signal power to noise ratio, and a delay spreading within the guard interval. The simulation result is illustrated in Fig.5-12. As it can be seen we could obtain an excellent improvement in the performance with the use of eight-element beam-space array antenna combined with MRC

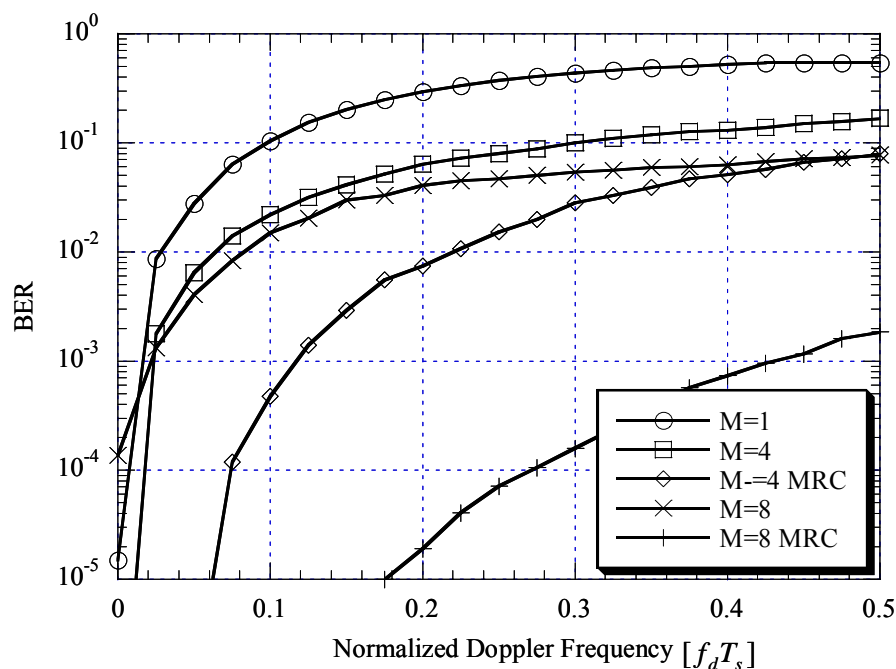


Fig. 5-12 BER as a function of normalized Doppler frequency at a propagation condition where 50 multipath signals received, $M = 1, 4, 8$, $Q = 3$ and $SNR = 20dB$

The results given in Figs.5-10 to 5-12 verify the possibility of the proposed scheme to eliminate the influence of the Doppler frequency spread completely, with sufficient number of antenna elements. On the other hand, these results also suggest that the receiver requires minimum of four elements to give sufficient performance, which limits the location of the antenna to such as the roof of a vehicle.

5.6 Summary

In this chapter we have proposed to use BSAAA for OFDM mobile reception. It was verified by computer simulation that the proposed system efficiently suppress the ICI due to the Doppler spread.

In the performance evaluation, we assumed a propagation condition around a mobile station where a number of multipath waves arrive from omni-directional angles and have delay spreading, and adopted eight-element BSAAA with element spacing of $(3/8)\lambda$.

We could gain a visible performance improvement in the system by implementing MRC to combine beam-spaced signals.

Further we have evaluated the influence of the iterative numbers (Q) of the past OFDM symbols, when calculating the correlation matrix among the beam output signals for each subchannel in BSAA-based OFDM mobile receiver, and it was verified by computer simulation that $Q = 3$ is sufficient to suppress the ICI due to Doppler spread.

Chapter 6

Directional-Element Adaptive Array Antenna for Mobile Reception of Digital Terrestrial Television

This chapter proposes the use of directional-element adaptive array antennas on the reception of Orthogonal Frequency Division Multiplexing (OFDM) based Digital Terrestrial Television Broadcasting (DTTB) in vehicles. Firstly this chapter evaluates the mobile receiving quality of DTTB of Post-FFT-type OFDM adaptive array antenna consisting of omni-directional- and directional-element with computer simulation and confirms that similar performance to omni-directional-element adaptive array antenna can be achieved with the use of directional-element adaptive array antenna. Secondly, this chapter shows that remarkable performance improvement can be achieved in directional-element adaptive array antenna mobile reception by the application of Doppler despreading. This chapter also confirms that allocating directional elements on the front and the rear sides of the vehicle instead of the left and right sides, gives better receiving quality.

6.1 Introduction

Reception of DTTB in vehicles has become a new research interest with the introduction of OFDM based DTTB in Japan. Although OFDM has the ability of combating against intersymbol interference (ISI) and frequency selective fading, its sensitivity to Doppler frequency spread is known as the main problem in OFDM mobile reception [7-9]. Though several methods have been introduced to overcome this problem only with signal processing such as windowing of the transmitted signal [10], self-ICI cancellation [11], recently, adaptive array antennas have been considered energetically in order to suppress the influence of Doppler frequency spread and frequency-selective fading as well as to increase the system capacity without increasing the transmitted power or bandwidth [12, 13, 16, 18]. Particularly, Post-FFT-type OFDM adaptive array antenna has gained more concern regardless of its high computational load since it increases the robustness against frequency selective fading due to multipath delay spreading. Moreover, considering the outward appearance, installing antennas on windows, instead of the roof of vehicles has attracted more attention though it restricts the array elements to directional ones [30].

This chapter, firstly evaluates the mobile receiving quality of DTTB of Post-FFT-type OFDM adaptive array antenna consisting of omni-directional as well as directional elements. Simulation results confirm that similar performance to omni-directional-element adaptive array antenna can be achieved with the use of directional-element

adaptive array antenna. Secondly, the paper shows that remarkable performance improvement can be achieved in directional-element adaptive array antenna mobile reception by the application of Doppler despreading. The paper also confirms that allocating directional elements on the front and the rear sides of the vehicle instead of the left and right sides, improves the receiving quality.

The second section of the chapter discusses the array configuration, the characteristics of the elements that are used in the adaptive array antenna, despreading Doppler spread and the maximal ratio combining of the array element signal. In section 6-3 assumed propagation environment is explained. After discussing the simulation results in section 6-4, remarks and conclusions are given in section 6-5.

6.2 Array Configuration and Adaptive Algorithm

Considering the recent trend of installing antennas on windows instead of the roof, the antenna elements are allocated in four sides of the vehicle as shown in Fig.6-1, where l and w denote the inter-element spacing between element #1 and #3, and #2 and #4, respectively. It should be noted that the direction of arrival (DOA) of receiving multipaths is measured referring the moving direction of the vehicle. Omni-directional as well as directional elements are considered as elements of the adaptive array antenna. Two types of amplitude characteristics are evaluated for directional elements, one, receiving signals with equal gain irrelevant to the DOA and the other with cosine amplitude characteristic which are referred as equal-gain-element and cosine-gain-element, respectively in the later part. The radiation pattern of each element is illustrated in Fig.6-2 (a). It should be noted that directional elements receive signals only from -90° to 90° , which is measured assuming the element is directed to 0° direction. Finally, the received signals of each adaptive array antenna element are combined using a Post-FFT-type maximal ratio combiner (MRC).

6.2.1 Omni-directional-Element Adaptive Array Antenna

Four omni-directional elements are used in the adaptive array antenna as illustrated in Fig.6-2(b). The received signal of omni-directional element adaptive array antenna is given by

$$\mathbf{R}_{OMNI} = \sum_{i=1}^I a_i \begin{bmatrix} \exp(j2 \frac{\pi}{\lambda} \frac{l}{2} \cos \theta_i), \exp(j2 \frac{\pi}{\lambda} \frac{w}{2} \sin \theta_i), \\ \exp(-j2 \frac{\pi}{\lambda} \frac{l}{2} \cos \theta_i), \exp(-j2 \frac{\pi}{\lambda} \frac{w}{2} \sin \theta_i) \end{bmatrix}^T \quad (6-1)$$

where I, λ, θ_i and a_i denote the number of multipath signals, wavelength of the DTTB signal, incident direction of the i^{th} multipath and the complex amplitude of the i^{th} multipath, respectively. The center of the antenna array is being used as the phase reference point when calculating the received signal of each element.

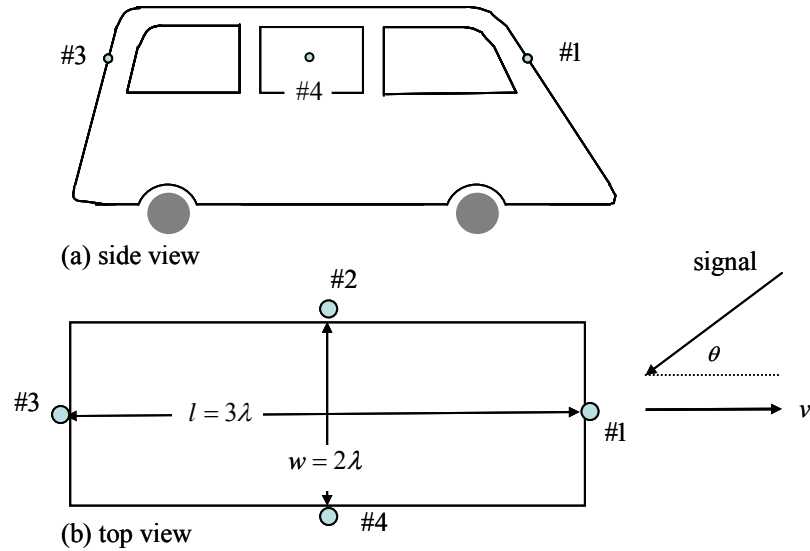


Fig. 6-1 Antenna installment

6.2.2 Directional- Element Adaptive Array Antenna

Equal-gain-element and cosine-gain-element adaptive array antennas are shown in Fig.6-2(c) and Fig.6-2(d), respectively. The received signal of directional element adaptive array antenna is given by

$$\mathbf{R}_{DIR} = \sum_{i=1}^I \begin{bmatrix} a_i^1 \cdot \exp(j2 \frac{\pi}{\lambda} \frac{l}{2} \cos \theta_i), a_i^2 \cdot \exp(j2 \frac{\pi}{\lambda} \frac{w}{2} \sin \theta_i), \\ a_i^3 \cdot \exp(-j2 \frac{\pi}{\lambda} \frac{l}{2} \cos \theta_i), a_i^4 \cdot \exp(-j2 \frac{\pi}{\lambda} \frac{w}{2} \sin \theta_i) \end{bmatrix}^T \quad (6-2)$$

where a_i^m for equal-gain-element adaptive array antenna is given by

$$\begin{aligned}
a_i^1 &= \begin{cases} \sqrt{2}a_i & -90^\circ < \theta_i \leq 90^\circ \\ 0 & \text{else} \end{cases}, \quad a_i^2 = \begin{cases} \sqrt{2}a_i & 0^\circ < \theta_i \leq 180^\circ \\ 0 & \text{else} \end{cases}, \\
a_i^3 &= \begin{cases} \sqrt{2}a_i & 90^\circ < \theta_i \leq 270^\circ \\ 0 & \text{else} \end{cases}, \quad a_i^4 = \begin{cases} \sqrt{2}a_i & 180^\circ < \theta_i \leq 360^\circ \\ 0 & \text{else} \end{cases}
\end{aligned} \tag{6-3}$$

and that for cosine gain element adaptive array antenna is given by

$$\begin{aligned}
a_i^1 &= \begin{cases} 2a_i \cos(\theta_i) & -90^\circ < \theta_i \leq 90^\circ \\ 0 & \text{else} \end{cases}, \\
a_i^2 &= \begin{cases} 2a_i \sin(\theta_i) & 0^\circ < \theta_i \leq 180^\circ \\ 0 & \text{else} \end{cases}, \\
a_i^3 &= \begin{cases} 2a_i \cos(\pi - \theta_i) & 90^\circ < \theta_i \leq 270^\circ \\ 0 & \text{else} \end{cases}, \\
a_i^4 &= \begin{cases} 2a_i \sin(\pi - \theta_i) & 180^\circ < \theta_i \leq 360^\circ \\ 0 & \text{else} \end{cases}
\end{aligned} \tag{6-4}$$

It should be noted that the radiation pattern of each element has been normalized by

$$\int_{-\pi}^{\pi} a^2(\theta) \cdot d\theta = 2\pi \tag{6-5}$$

where, $a(\theta)$ denotes the amplitude radiation pattern. Here too the center of the antenna array is being used as the reference point.

6.2.3 Despreading Doppler Frequency Shift for Directional-Element Arrays

When the reception is done from a moving object, the complex amplitude of each multipath experience a phase shift due to Doppler effect. Phase shifted complex amplitude of i^{th} multipath is given by

$$a_i(t) = a_{i0}(t) \cdot \exp(j2\pi f_D [\cos \theta_i] t) \tag{6-6}$$

where a_{i0} and f_D denote the complex amplitude of i^{th} multipath before the Doppler frequency shift is applied and the maximum Doppler frequency shift, which is defined by

$$f_D = \frac{v}{\lambda} \tag{6-7}$$

, respectively. Here v denotes the velocity of the vehicle.

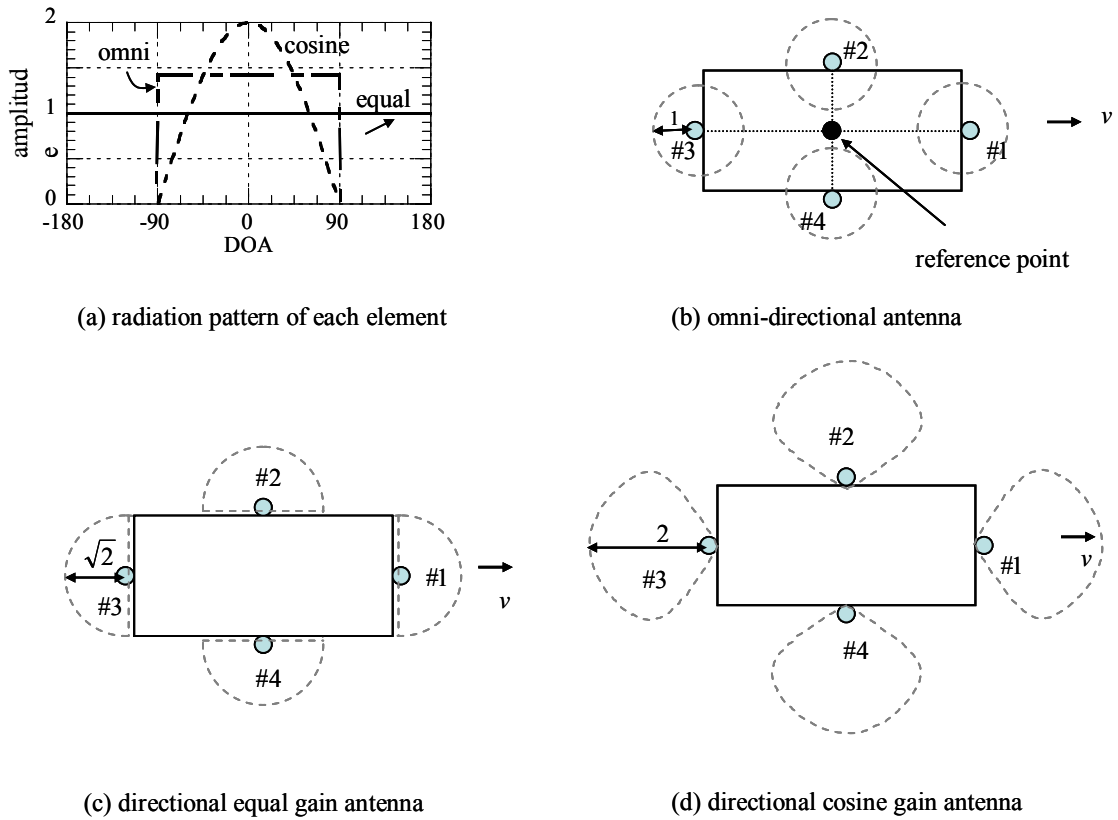


Fig. 6-2 Adaptive array antenna

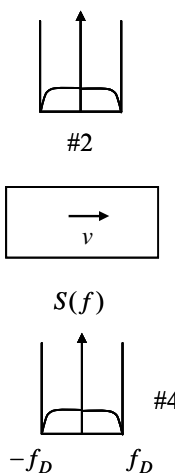
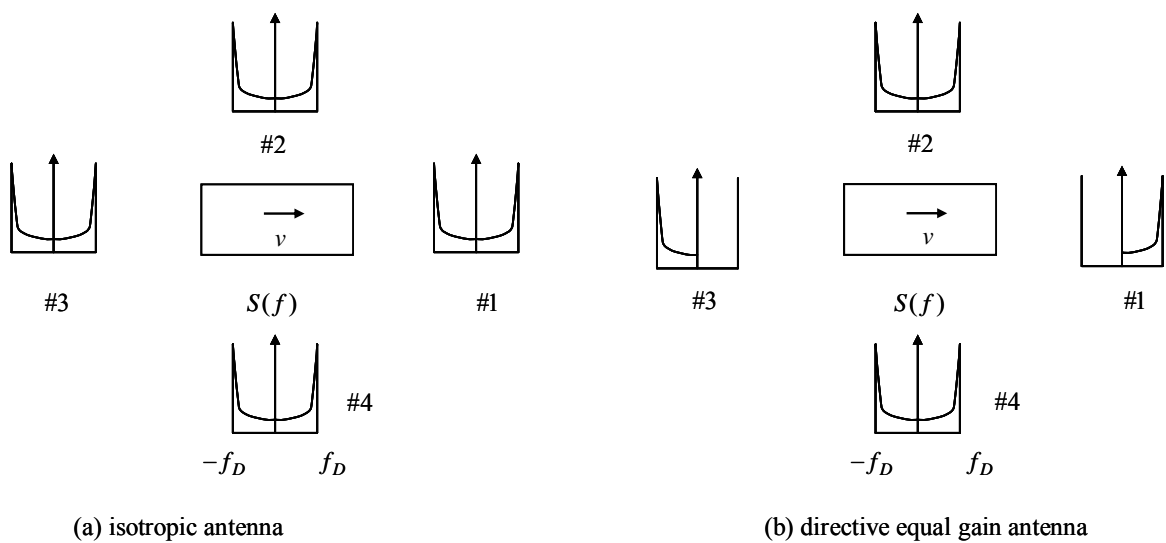
The Doppler power density function for multipath components uniformly distributed environment is known as Jakes PSD [31] and given by

$$S(f) = \frac{P_R}{\pi f_D \sqrt{1 - (f/f_D)^2}} \tag{6-8}$$

where, P_R denotes the averaged received power. It should be noted that the derivation of Jakes PSD is based on the assumption of that omni-directional antennas are deployed in both ends of the link. Referring [32], where a study on the PSD function for moving

directional receivers is done, the Doppler power spectrum of each element of adaptive array antenna is illustrated in Fig.6-3. As shown in Figure for directional-element adaptive array antenna, element #1 receives signals only with positive Doppler frequency shift while the received signal of the element #3 contains only negative Doppler frequency shifted signals. This suggests the application of despreading Doppler frequency spread that introduced in our previous work, [18] for the elements #1 and #3, since the average Doppler frequency shift for them is not zero. Doppler despread signal can be given by

$$\mathbf{X} = \text{diag} [R_{DIR}] \cdot \mathbf{P} \quad (6-9)$$



(c) directive cosine gain antenna

Fig. 6-3 Doppler power spectrum

where, \mathbf{P} denotes Doppler despreading vector given by

$$\mathbf{P} = [\exp(-j2\pi\Delta f), 1, \exp(j2\pi\Delta f), 1]^T \quad (6-10)$$

where, Δf denotes the degree of Doppler despreading, which is a proportional to the maximum Doppler frequency shift and will be optimized in the later part of the chapter.

On the other hand element #2 and #4 in directional-element adaptive array antenna and all the elements of omni-directional-element adaptive array have zero average Doppler frequency shifts and cannot be despread. Doppler despreading process for cosine-gain element adaptive array antenna is illustrated in Fig.6-4.

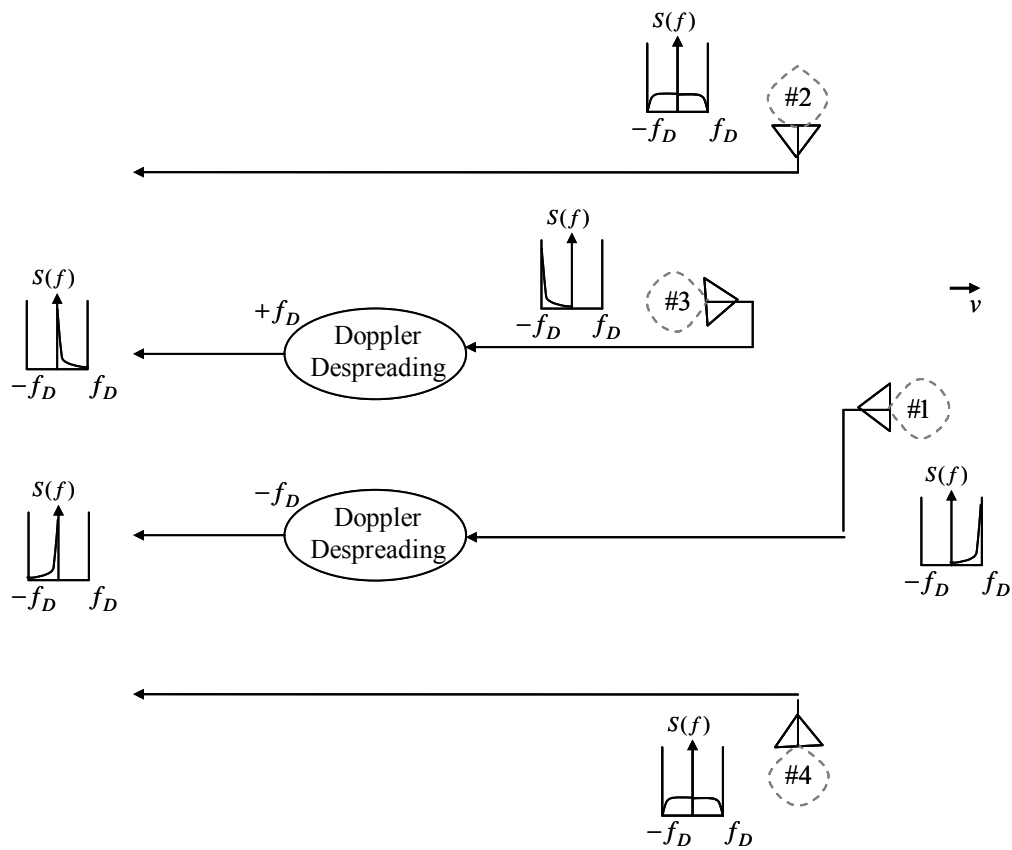


Fig. 6-4 Doppler Despreading for cosine-gain element adaptive array antenna

6.2.4 Maximal Ratio Combining

After despreading Doppler frequency spread and OFDM demodulation, a Post-FFT-type maximal ratio combiner, shown in Fig.6-5, is used to combine the element signals of

adaptive array antenna as discussed in our previous work [18]. When performing MRC, firstly, the correlation matrix among the received signals of array elements is calculated by taking the sliding average of past Q samples. Corresponding to the result we achieved in [33] $Q = 5$ is used in this scheme. Correlation matrix for k^{th} sub-channel is given by

$$\mathbf{R}_{xx}^{(k)}(t) = \frac{1}{Q} \sum_{q=0}^{Q-1} \mathbf{X}^{(k)}(t - qT_s) \mathbf{X}^{(k)H}(t - qT_s) \quad (6-11)$$

where T_s and $\mathbf{X}^{(k)}(t - qT_s)$ denote the OFDM symbol duration, and the k^{th} sub-channel signal of past q^{th} OFDM symbol of adaptive array antenna and given by

$$\mathbf{X}^{(k)}(t - qT_s) = \begin{bmatrix} X_{(1)}^{(k)}(t - qT_s), X_{(2)}^{(k)}(t - qT_s), \\ X_{(3)}^{(k)}(t - qT_s), X_{(4)}^{(k)}(t - qT_s) \end{bmatrix}^T \quad (6-12)$$

where $X_{(m)}^{(k)}(t - qT_s)$ denotes the k^{th} sub-channel signal of past q^{th} OFDM symbol of m^{th} element. Then MRC is carried out by using the eigenvector $\mathbf{e}_{\max}^{(k)}(t)$, for the maximum eigenvalue $\lambda_{\max}^{(k)}(t)$, of $\mathbf{R}_{xx}^{(k)}(t)$ as the weight vector for the k^{th} sub-channel.

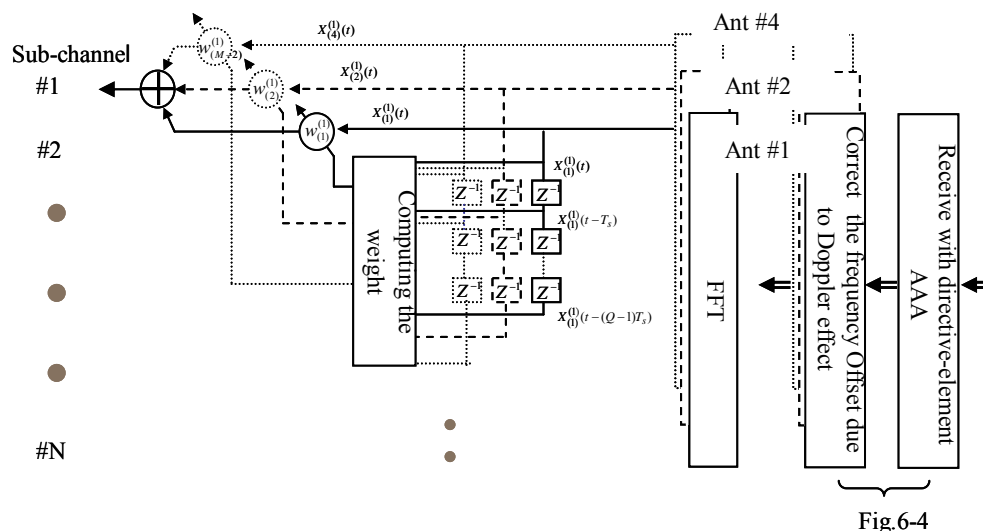


Fig. 6-5 Maximal Ratio Combining (MRC)

6.3 Simulations

A computer simulation is carried out to evaluate the performance of omni-directional and directional- element adaptive array antenna. The assumed propagation environment and the OFDM system are discussed in prior presenting the results.

6.3.1 Propagation Environment

A multipath propagation environment with exponential power delay profile is assumed in the simulation. The number of multipaths is set to 32 and allocated them in between the guard interval maintaining the time space between two multipaths is exactly to T , PSK symbol duration. The total received power and the delay spread are set to 0dB and $17\mu\text{s}$, respectively. The DOAs of multipath signals are set randomly ranging from 0° to 360° . A basic diagram of the assumed propagation environment is illustrated in Fig.6-6.

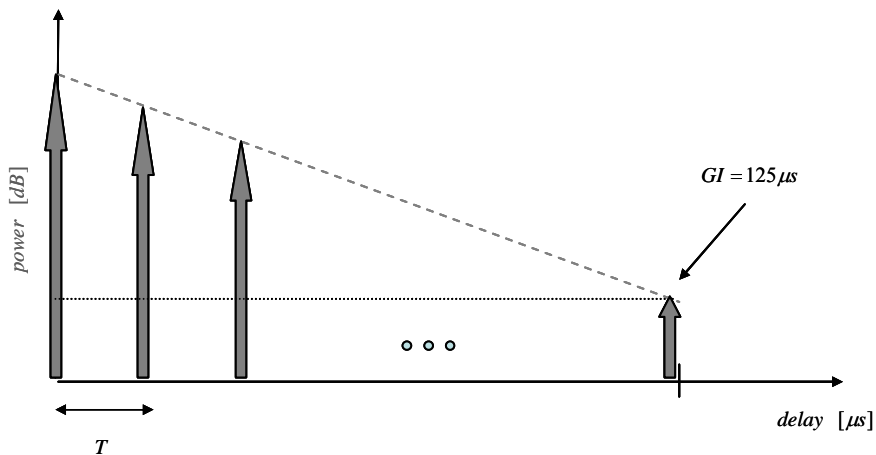


Fig. 6-6 Propagation environment (A discrete type exponential delay profile)

6.3.2 Assumed OFDM Scheme

Parameters of the assumed OFDM system are given in Table 6-1. Similar values to DTTB are used for the symbol period and guard interval, which are the fatal parameters when evaluating the influence of Doppler frequency spread and multipath propagation. Reduced number of subchannels is assumed to simplify the simulation. System performance is evaluated by bit error rate (BER) which is averaged over one million bits. Citing the result of $Q \geq 3$ is the optimum value when performing MRC from [33], $Q = 5$ is used in our simulation.

Table 6-1 System parameter

Number of bits transmitted	1,000,000
Number of sub-carriers ^(N)	256
Symbol period (without GI) ($T_s = 256 \times T$)	1 ms
Carrier frequency	600MHz
Modulation system	DQPSK
Guard interval (GI)	$32T$ (125 μ s)
Number of elements	2,4
Element spacing (l)	3λ (1.5m@600MHz)
Element spacing (w)	2λ (1.0m@600MHz)

6.4 Performance Evaluation

Simulations were carried out to optimize the degree of Doppler despreading for cosine-gain and equal-gain elements and to evaluate the performances of omni-directional-element and directional-element adaptive array antenna. A result for single omni-directional antenna is also presented as a reference. Further simulations were carried out to compare the performances of 2-element adaptive array antenna

6.4.1 Optimizing the despreading factor

Figure 6-7 illustrates the result of Doppler despreading effect as a function of despreading factor defined by $|\Delta f| / f_D$ to identify the most suitable value of the factor. Simulation is done at SNR=30dB and $f_D T_s = 0.05$. In the figure, *4-Cos-Element* and *4-Equal-Element* stand for four-element cosine-gain adaptive array antenna and four-element equal-gain adaptive array antenna, respectively and *w.DD* expresses that the Doppler despreading is applied for element number #1 and #3. Result shows that the optimum value lies in $\Delta f \approx \pm f_D / 2$ for equal-gain-directional elements and $\Delta f \approx \pm f_D$ for cosine-gain-directional elements. Here on we use the above value for simulation.

Further it should be noted that the velocity of the vehicle and the frequency of the received signal are assumed as known factors when despreading the Doppler frequency spread.

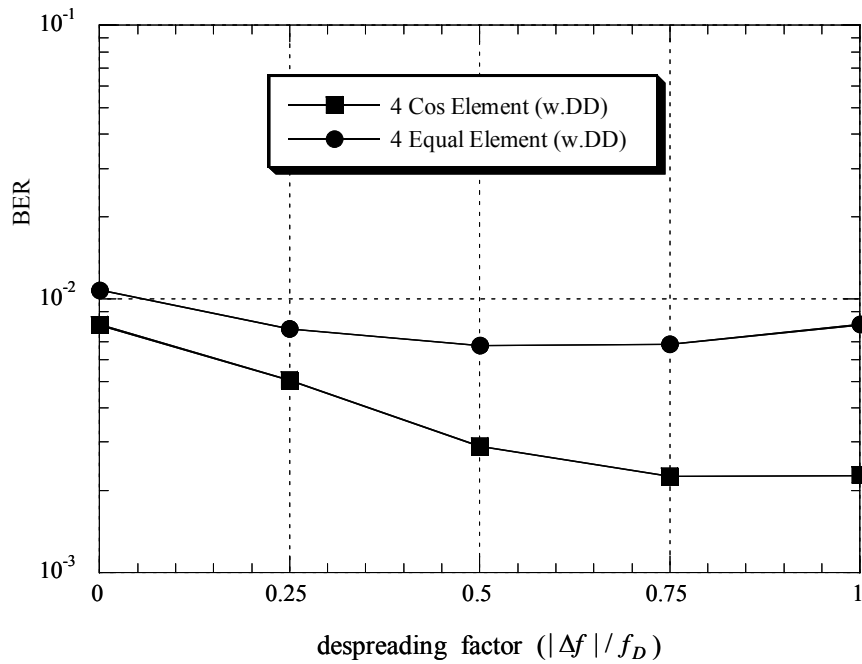
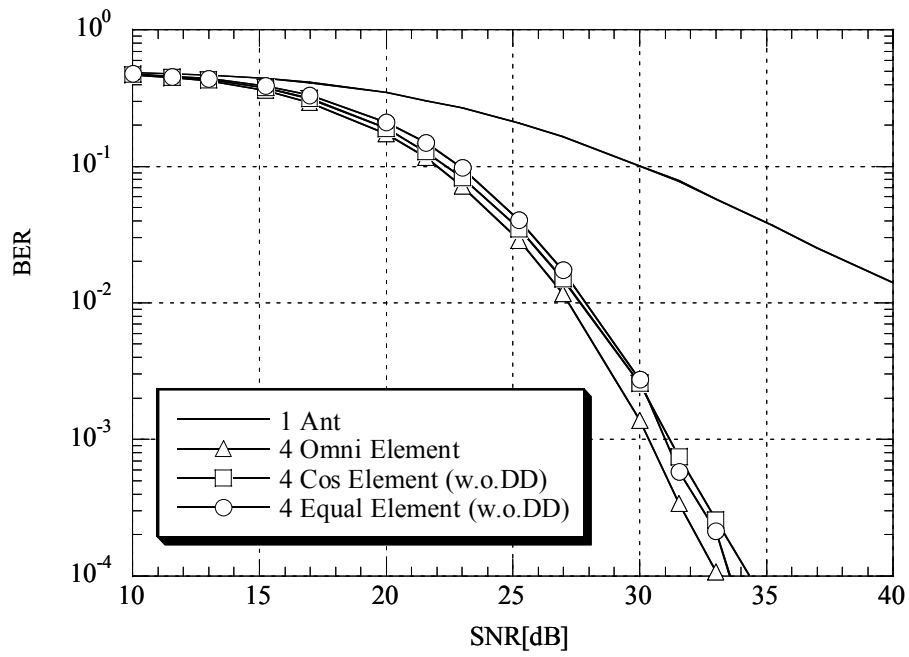


Fig. 6-7 Doppler despreading effect (SNR = 30dB , $f_D T_s = 0.05$)

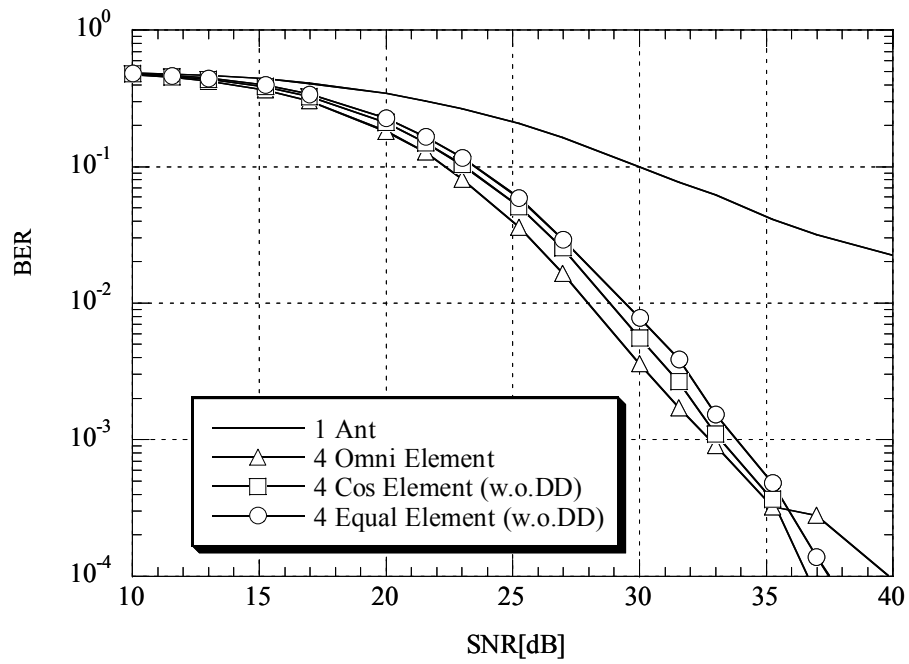
6.4.2 Four-Element Adaptive Array

Figure 6-8 illustrates the BER characteristic as a function of SNR for two different Doppler spread, $f_d T_s = 0.01$, which is negligible and $f_d T_s = 0.05$ which is considerably large. In the figure, *1 Ant* and *4-Omni-Element* stand for the results of single omni directional antenna and four-element omni-directional adaptive array antenna, respectively. Neither receiving scheme has applied Doppler despreading, which is expressed by *w.w.DD*. Result shows that for both the conditions, each adaptive array antenna gives similar performance confirming the use of directional element adaptive array antenna will not affect the receiving quality.

The characteristic of BER as a function of Doppler frequency spread is illustrated in Fig.6-9. The simulation is done under SNR of 40dB, where noise is negligible, and SNR of 30dB under an environment with practical level of noise.

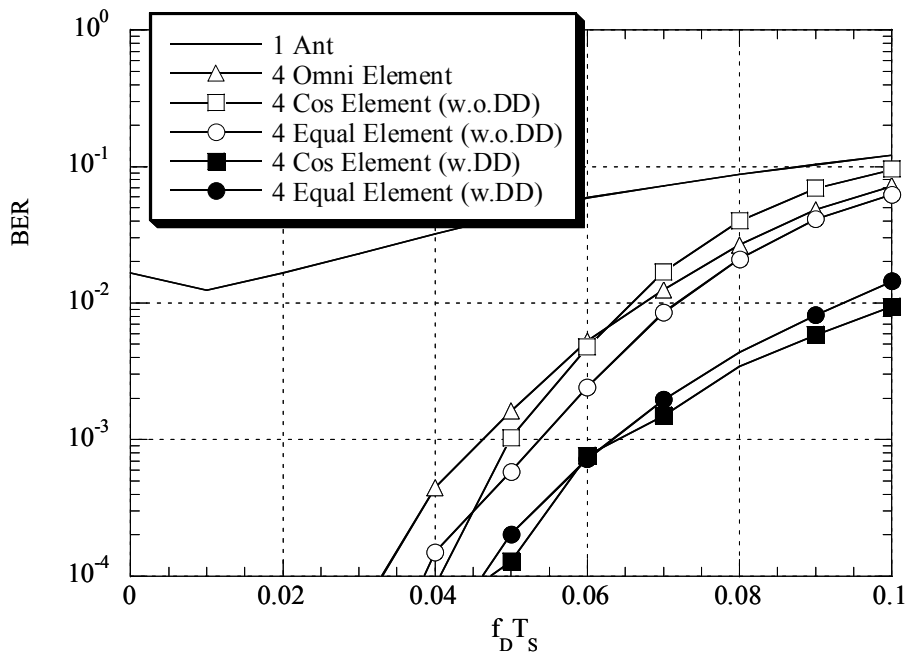


(a) $f_d T_s = 0.01$

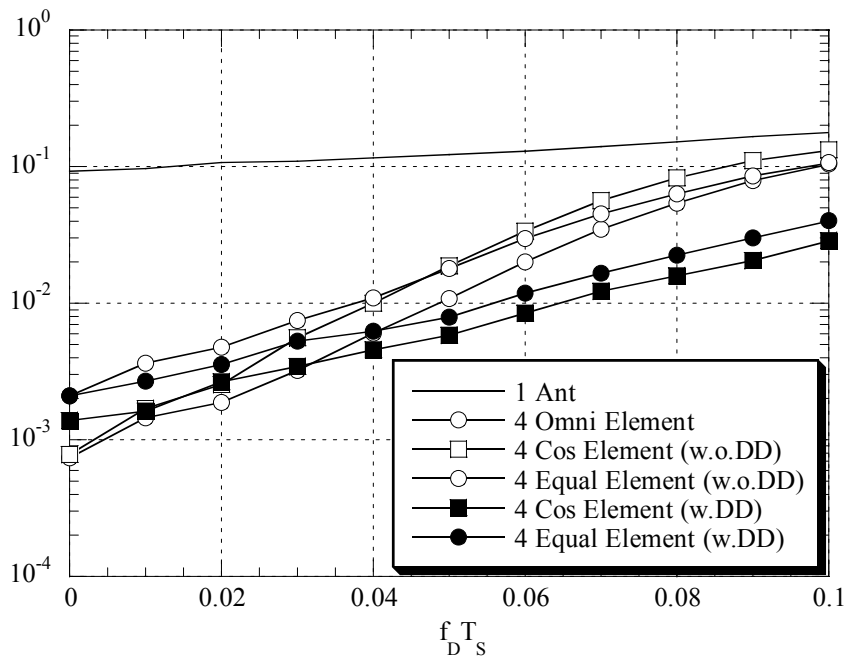


(b) $f_d T_s = 0.05$

Fig. 6-8 BER vs. SNR



(a) SNR = 40dB



(b) SNR = 30dB

Fig. 6-9 BER vs. Doppler frequency spread

These results too confirm that the use of directional element adaptive array antenna will not affect the receiving quality even without the application of Doppler despreading. Moreover, the results show that performance improvement can be obtained by means of Doppler despreading. Particularly cosine-gain-element adaptive array antenna gives the best performance under severe Doppler spreading environment.

6.4.3 Two-Element Adaptive Array

Figure 6-10 illustrates the BER characteristic for 2-directional-element adaptive array antenna. In figure, (1,3) and (2,4) denote the element pair that used in two element adaptive array antenna. Results clarifies allocating antennas on the front and rear side of the vehicle, which enables despreading Doppler frequency spread, gives better performance than allocating antennas on left and right sides. Further, cosine-gain-element adaptive array gives better performance here, too.

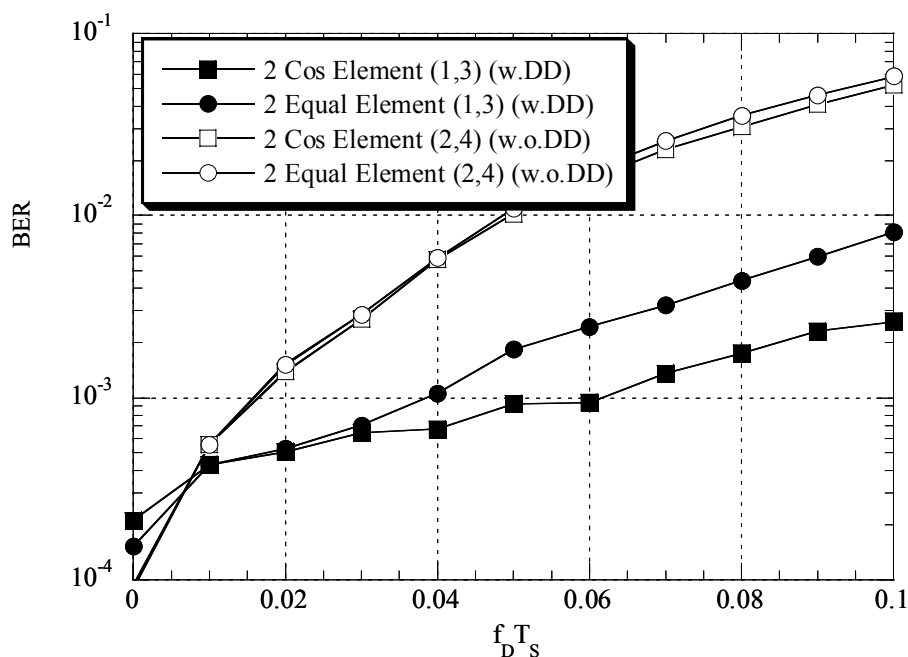


Fig. 6-10 Performance comparison between the use of element 2,4 and 1,3 (SNR = 40dB)

6.5 Summary

This chapter has evaluated the mobile receiving quality of omni-directional- and directional-element OFDM adaptive array antenna consisting of four elements which are

placed on the windows of a vehicle and confirms both omni-directional- and directional-element adaptive array give similar performance with the absence of Doppler despreading.

Further, this chapter proposes and confirms by computer simulation that remarkable performance improvement can be achieved with the application of Doppler despreading along with directional-element adaptive array antenna. Particularly, Doppler despreading applied cosine-gain-element adaptive array antenna gives the best BER characteristic.

The chapter also verifies that allocating directional-elements on front and rear side of the vehicle gives better performance than installing them on right and left sides when receiving signals only with two element adaptive array antenna.

Chapter 7

Eigenvalue-Decomposition-Based Recursive Least-Squares Algorithm for OFDM Communications over Fast Time-Varying Channels

This chapter introduces a method to reduce the convergence time of adaptive array antenna based on eigenvalue decomposition, which can be applicable for an environment with less number of interference signals along with any number of multipath signals of desired and interference signals. Further a method of applying the proposed adaptive algorithm to a post-FFT-type OFDM-AAA is presented.

7.1 Introduction

AAA has been introduced to OFDM in order to increase the adaptability of system for mobile communication systems because of the ability of AAA in increasing the system capacity without increasing the transmitted power or bandwidth [14-18]. AAA, consisting of a large number of elements along with a fast convergence rate would be an essential requirement to implement OFDM-based mobile radio systems such as MC-CDMA and OFDMA in fast time-varying channels. Even the fastest among MMSE adaptive algorithms, Recursive Least-Squares Algorithm (RLS), which takes 3, 4 times of steps of the number of weights it has to update to be converged [19], would not be suitable for such AAA applications with a large number of elements.

On the other hand we have experienced that MRC can be performed sufficiently by only referring to previous three samples [33], and hinted by [20], where Eigenvalue Decomposition has been introduced to AAA systems in the purpose of reducing the total computational load, we propose an adaptive algorithm call Eigenvalue-Decomposition-based Recursive Least-Squares (ED-RLS), where eigenvalue decomposition is been used to achieve a fast convergence rate in AAA.

After a discussion on the principals of the algorithm, a performance evaluation is done by computer simulations. Particularly we could gain an essential convergence in the seventh step in a 16-element array configuration, in an environment with -10dB of SNR and 10dB interference signal power, where more than 30 steps were taken corresponding to conventional RLS algorithm.

7.2 Eigenvalue Decomposition based RLS

Figure 7-1 illustrates the configuration of the proposed ED-RLS beamforming algorithm, which can be applicable in an environment where there is only one interference source, but both desired and interference signals having multipath. In the proposed scheme, first we calculate the correlation matrix among the array element signals by carrying out the sliding average of past K symbols. The correlation matrix of the array output signal at time t is given by

$$\mathbf{R}_{XX}(t) = \frac{1}{K} \sum_{i=0}^{K-1} \mathbf{X}(t-iT_s) \cdot \mathbf{X}^H(t-iT_s) \quad (7-1)$$

where T_s , and $\mathbf{X}(t)$ denote the symbol duration, and received array signal, respectively. Here $\mathbf{X}(mT_s)$ is defined as

$$\mathbf{X}(mT_s) = \mathbf{A} \cdot r^m + \mathbf{B} \cdot i^m + \mathbf{n} \quad (7-2)$$

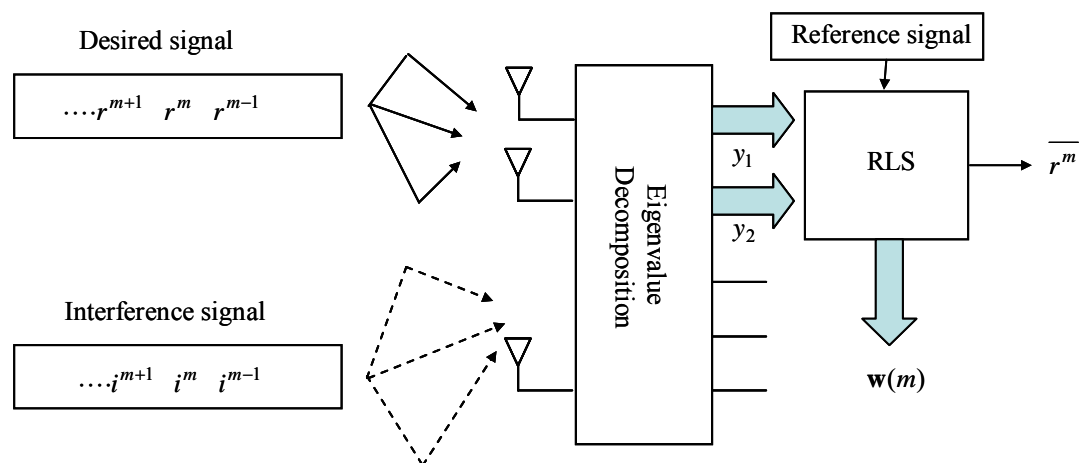


Fig. 7-1 Basic configuration of ED-RLS algorithm

where \mathbf{A} and \mathbf{B} denote the complex channel response vector of the desired and interference signals and r^m , i^m and \mathbf{n} denote the desired and interference signals and noise, respectively. Then we divide the received signal into two orthogonal components by eigenvalue decomposition. Here we use the eigenvectors of the highest and the second highest eigenvalues of the correlation matrix $\mathbf{R}_{XX}(t)$, as the orthogonal weight vectors.

Finally we extract the desired signal $\overline{r^m}$, by performing RLS estimation for only these two orthogonal components.

As it is well known that the number of convergence steps of RLS algorithm depends on the number of the weights, which have to be updated, by dividing the M -element array output signal only into two orthogonal streams, a fast convergence rate can be expected.

7.3 Simulation Results

To demonstrate the performance of the proposed scheme, computer simulations have been carried out and the system performance is measured by the mean-squared error, which is averaged over thousand bits. Further the desired signal itself has been used as the reference signal. A 16-element AAA is used as the receiver.

7.3.1 Simulation Conditions

System parameters and simulation conditions are shown in Table 7-1. We have assumed a simulation environment with considerable large noise power along with a strong interference signal. Propagation environment is illustrated in Fig.7-2, where the base station one (BS1), communicating with the mobile station one (MS1), receives interfering signals from mobile station two (MS2).

7.3.2 Simulation Results

Figure 7-3 illustrates the convergence characteristic for conventional RLS and ED-RLS algorithm. The number of past symbols that are used when performing eigenvalue decomposition, K is used as a parameter. The observation time is displayed on the horizontal axis and the mean-squared error is displayed on the vertical axis. Simulation result shows that the convergent time can be reduced very sharply by applying the proposed algorithm. Further, the result confirms that the influence of K to the convergent time is negligible.

Table 7-1 System parameter

	Power [dB]	Incident Angle
Desired signal	0dB	30°
Interference signal	10dB	40°
Noise Power	-10dB/element/desired signal power	
Number of Array elements	16	

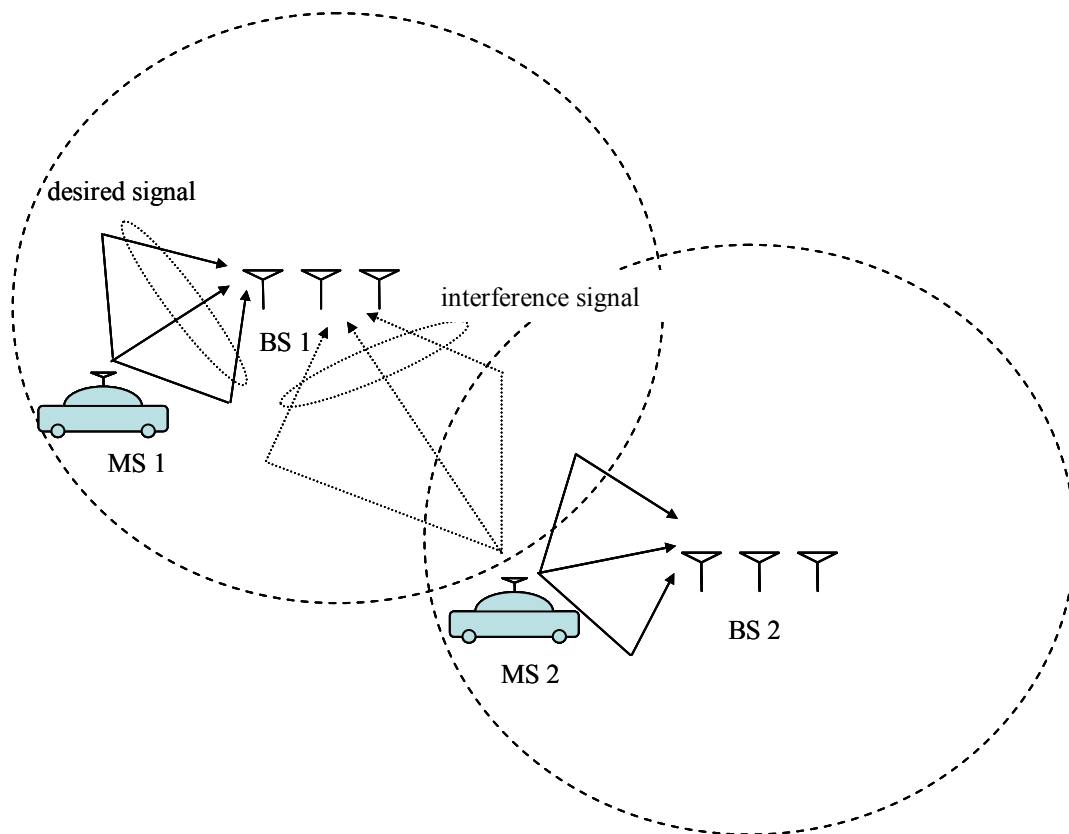


Fig. 7-2 OFDM mobile communications system

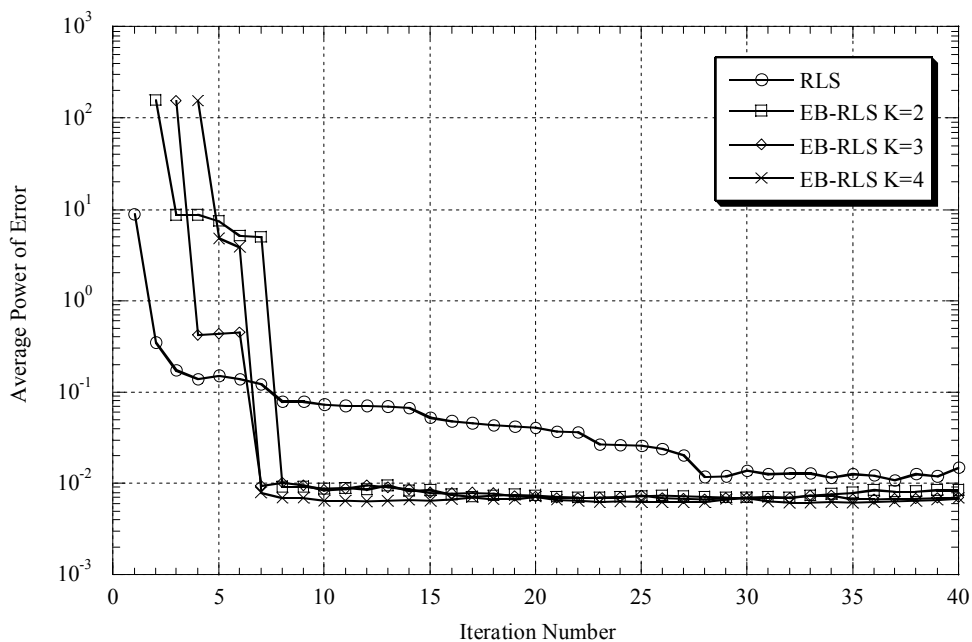


Fig. 7-3 Convergent characteristic for RLS and ED-RLS algorithm

7.4 ED-RLS based OFDM Communication

In similar to conventional MMSE adaptive algorithms, proposed ED-RLS adaptive algorithm converge the system using a reference signal. The necessity of a pilot signal means that there is no room to carry additional data but only have the ability to track the pilot. However, the application of proposed ED-RLS algorithm to a multicarrier communication system such as OFDM permits the scheme to hold pilot data stream as well as data stream simultaneously. Here we discuss the application of ED-RLS algorithm to an OFDM communication system.

7.4.1 Transmitted OFDM Signal

Figure 7-4 illustrates the transmitted signal of an OFDM communication system which is intended to be applied in proposed ED-RLS algorithm, where some subchannels are used as pilot signals. Here r_k^m denotes the k^{th} reference signal of the m^{th} symbol.

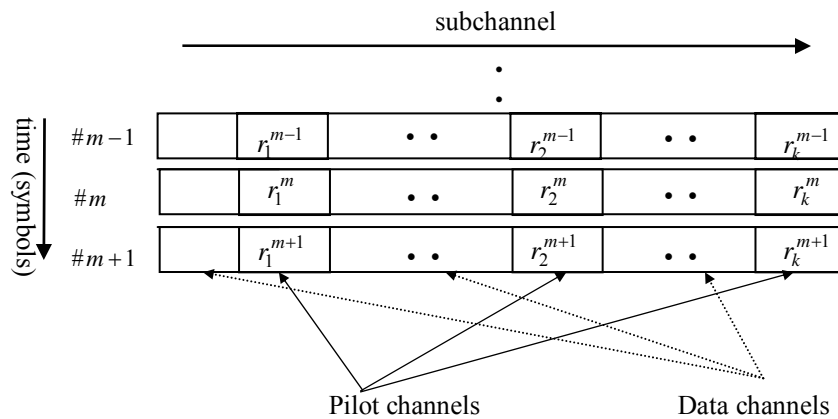


Fig. 7-4 Transmitted OFDM symbol

7.4.2 Receiving Scheme of OFDM Application

Figure 7-5 illustrates the receiving scheme of the proposed ED-RLS algorithm with application to OFDM system. In the receiver, first we demodulate the received signal of each array element separately. Secondly we combine the array output signals by performing ED-RLS algorithm. Here it should be noted that we perform ED-RLS only to the subchannels that are used as pilot channels, and interpolate the weight vectors of the data subchannels, which are in between the pilot subchannels. The method that used to interpolate data will be described in Chapter 8.

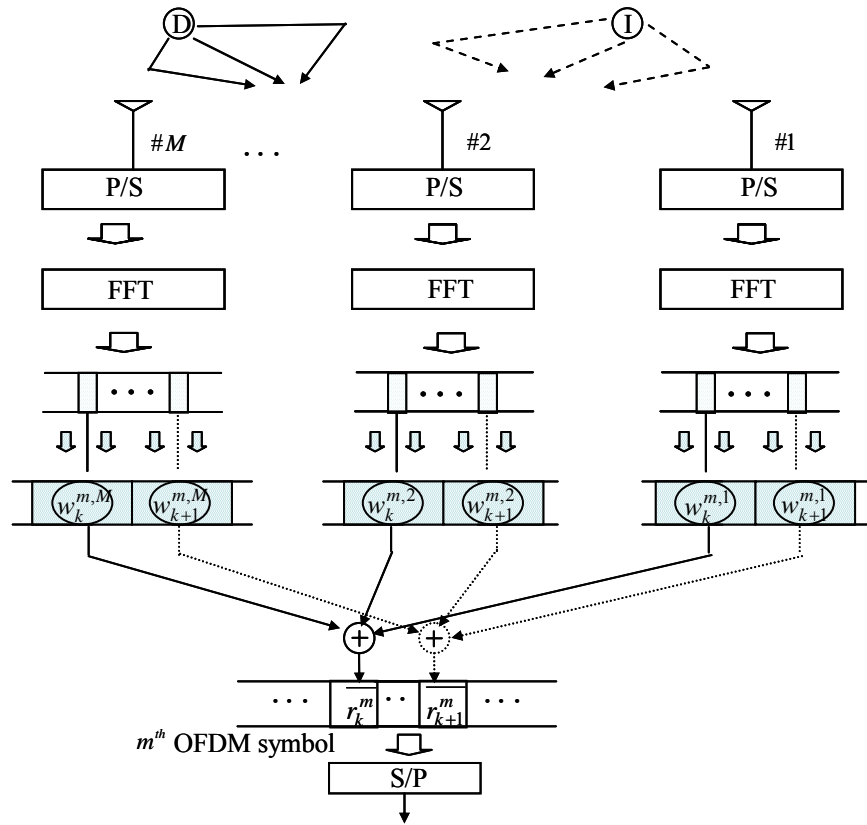


Fig. 7-5 Receiving scheme of the proposed OFDM system

7.5 Summary

In this chapter we proposed a beamforming algorithm, which has a fast convergence rate in a propagation environment with only one and strong interference source, but any number of multipaths of desired and interference signals exist.

In the proposed scheme we divide the array input signal into two orthogonal components by eigenvale decomposition first. Then extract the desired signal by performing RLS estimation for only these two orthogonal components. We name this algorithm as Eigenvalue Decomposition Recursive Least-Squares Algorithm (ED-RLS).

Further, we verified by computer simulation that the proposed scheme gives more rapid convergence comparing to conventional RLS algorithm in an environment with considerably large noise power along with a strong interference signal.

Particularly we could gain an essential convergence in the seventh step in a 16-element array configuration, in an environment with -10dB of SNR and 10dB interference signal power.

Finally the application of ED-RLS system to OFDM mobile communication system is discussed.

Chapter 8

Adaptive Algorithm Based on Accumulated Signal Processing for Fast Fading Channels with Application to OFDM Mobile Radio

In this chapter, we propose an adaptive algorithm based on accumulated signal processing, which could be applicable to Post-FFT-type OFDM adaptive array antennas. Proposed scheme calculates the weight of each element at a particular instant t , by considering both post- and pre-received symbols. Because of the use of additional forthcoming information on channel behavior in the weight calculation scheme, one can expect an improved performance in fast fading conditions by using the proposed adaptive algorithm. This paper also discusses the application of the proposed adaptive algorithm to OFDM adaptive array. In OFDM application, a few subchannels are being used to transmit pilot symbols, and at the receiver, the proposed adaptive algorithm is applied to those pilot subchannels, and interpolates the weights for the data subchannels which are allocated between the pilot subchannels. Finally, the system performance improvement with the application of the proposed adaptive algorithm is verified by computer simulation.

8.1 Introduction

Orthogonal frequency division multiplexing (OFDM) has already been applied to several digital communication and broadcasting systems such as Digital Video Broadcasting (DVB), Digital Audio Broadcasting (DAB), and Wireless Local Area Network (WLAN). Furthermore, OFDM is being considered to be applied in future generation mobile communication systems because of its ability to combat intersymbol interference (ISI), which is one of the major problems encountered in wideband transmission over multipath fading channels.

On the other hand, adaptive array antennas have been introduced to OFDM communication systems in order to suppress the Doppler frequency shift as well as to increase the system capacity without increasing the transmitted power or bandwidth [16, 18]. Post-FFT-type OFDM adaptive array has gained a particular concern regardless of its high computational load since it increases the robustness against frequency selective fading due to multipath delay spreading. Moreover, the use of the same weight for a number of subchannels or interpolation of weights have been introduced to reduce the high computational load of Post-FFT-type OFDM adaptive array [22, 23].

Comparing to the propagation environments of WLAN, where it exists only delay spread but no Doppler spread, and DVB, where both delay spread and Doppler spread

exist but no interference signal, the propagation environment of mobile radio system is more complicated with the existence of delay spread, Doppler spread and interference signals. Steering of adaptive array antennas would be a challenging task under these conditions. In this paper, we propose an adaptive algorithm based on accumulated signal processing, which could be applicable to Post-FFT-type OFDM adaptive array antennas, which will keep the system performance in fast fading channels. Proposed scheme calculates the weight of each element at a particular instant t , by considering both -post and pre-received symbols. Since this technique utilizes additional forthcoming information on channel behavior to the weight calculating scheme, one can expect performance improvement with the application of the proposed algorithm under fast fading conditions. This chapter also discusses the application of the proposed adaptive algorithm to OFDM adaptive array. When applying to OFDM adaptive array, first, we allocate a few subchannels to transmit pilot symbols. At the receiver, we perform the proposed adaptive algorithm to those pilot subchannels and interpolate the weights for the data subchannels, which are allocated between the pilot subchannels.

In next section, the principals of the proposed adaptive algorithm, which is based on accumulated signal processing is discussed. In section 8-3, temporal variation and cumulated distribution of SINR of the proposed algorithm are compared to that of a conventional MMSE adaptive algorithm where the weights are calculated considering only the post-received symbols. Results confirm that the proposed scheme suppresses the interference and Doppler spread more efficiently. Section 8-4 of the paper discusses on applying the proposed adaptive algorithm to OFDM adaptive array. Finally, some concluding remarks are given in section 8-5.

8.2 Adaptive Algorithm Based on Accumulated Signal Processing

The basic structure of the proposed adaptive algorithm based on accumulated signal processing is illustrated in Fig.8-1. In the proposed algorithm, a certain period of received symbol stream of each antenna is accumulated once, and then the array output is calculated by performing MMSE adaptive algorithm such as SMI, RLS or LMS. When calculating the weight of each element at a particular instant t , a number of pre-received symbols (that received after the instant t) as well as post-received symbols (that received before the instant t) are taken into account. By taking this forthcoming information of the channel behavior into the weight optimizing scheme, one can expect to achieve higher accuracy than using only the past information in fast fading conditions.

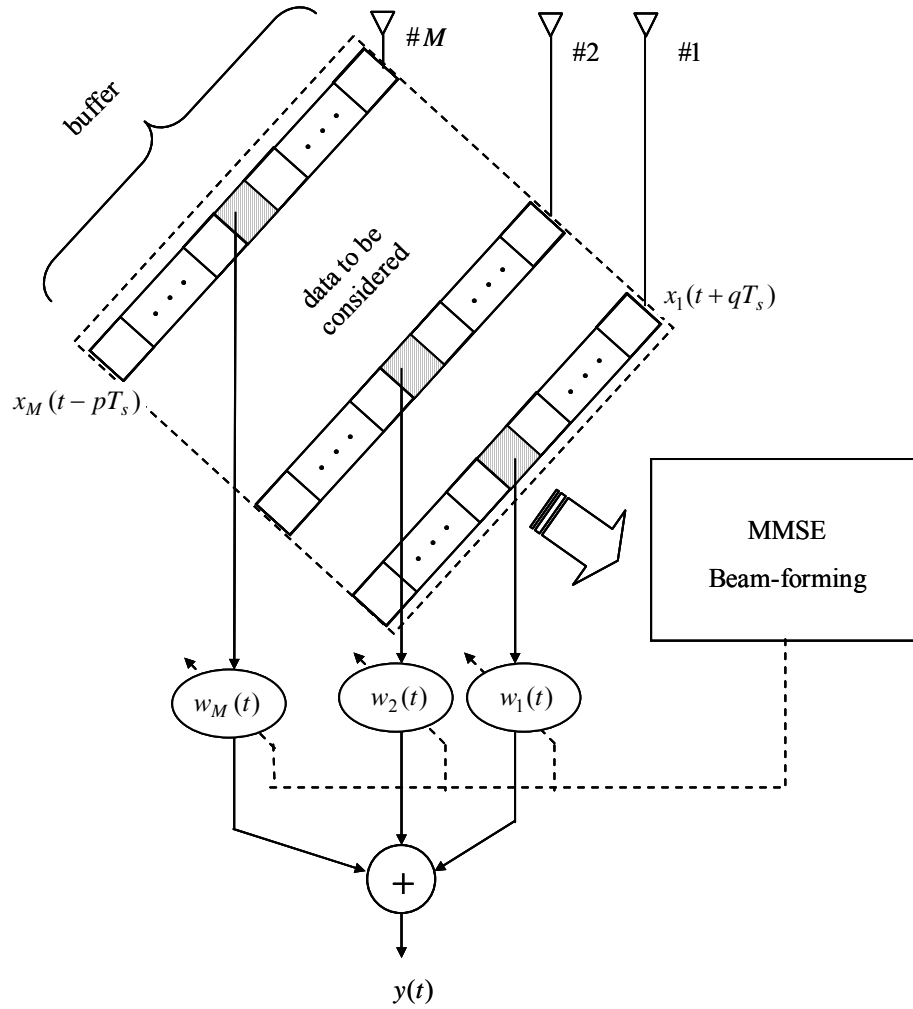


Fig. 8-1 Adaptive algorithm based on accumulated signal processing

In the proposed algorithm, the correlation matrix among the antennas is derived by

$$\mathbf{R}_{xx}(t) = \frac{1}{p+q+1} \sum_{i=-p}^q \beta^{|i|} \cdot \mathbf{x}(t+iT_s) \mathbf{x}^H(t+iT_s) \quad (8-1)$$

where, p and q denote the number of pre-received and post-received symbols, respectively. β is the forgetting factor which was applied to give more weight to the recent data symbols. $\mathbf{x}(t)$ is the received signal vector of antenna array at instant t , given by

$$\mathbf{x}(t) = [x_1(t), x_2(t), \dots, x_M(t)]^T \quad (8-2)$$

where, T_s and $x_m(t)$ denote the symbol period and the received signal of the m^{th} element at a particular instant t , respectively.

The correlation vector among the pilot signal and the accumulated received array signal is calculated by

$$\mathbf{r}_{xr}(t) = \frac{1}{p+q+1} \sum_{i=-p}^q \beta^{|i|} \cdot \mathbf{x}(t+iT_s) r^*(t+iT_s) \quad (8-3)$$

where $r(t)$ denotes the pilot signal at a particular instant t . The optimized weight vector of the proposed adaptive algorithm is derived by

$$\mathbf{w}_{opt}(t) = \mathbf{R}_{xx}^{-1}(t) \mathbf{r}_{xr}(t) \quad (8-4)$$

Finally the output signal of the adaptive array antenna is given by

$$y(t) = \mathbf{w}_{opt}^H(t) \cdot \mathbf{x}(t) \quad (8-5)$$

here it should be noted that the optimal weight is subject to change with the time in fast fading environments.

Because of the use of several pre-received data for the weight calculation, a small delay in data transmission could occur. This may be acceptable for real communication systems. On the other hand, we can expect higher accuracy in fast fading environment with the proposed adaptive algorithm. Although the proposed adaptive algorithm tracks a pilot signal even under a fast fading environment, there is no room to carry additional data since the algorithm works only under the existence of a pilot signal. However, multi-carrier communication systems, such as OFDM have the ability to provide both pilot and data signals simultaneously to the adaptive algorithm utilizing its enormous number of subchannels. Therefore the combination of the proposed adaptive algorithm with OFDM will allow the adaptive algorithm to communicate while tracking the pilot. Furthermore, the proposed algorithm will allow the adaptive array system to communicate continuously, which will enable the usage of the algorithm in both TDMA- and FDMA-based OFDM data communication systems.

8.3 Simulation Conditions and Results

A number of computer simulations are performed to verify the system performance of the proposed algorithm. In this section, the performance of the proposed adaptive algorithm is evaluated with a single carrier system.

8.3.1 Simulation Conditions

We have considered a propagation environment described in [34], where a number of multipath signals of both interfering and desired signals exist with different Doppler frequency shifts, and DOAs. Normal angular distribution of $N(DOA, 5^\circ)$ and randomly distributed Doppler frequency shift within $[0, f_d T_s]$ were assumed for the multipaths. Considered propagation environment is shown in Fig.8-2 and Table 8-1. Here, f_d and L denote the maximum Doppler frequency shift and the number of interference signals, respectively.

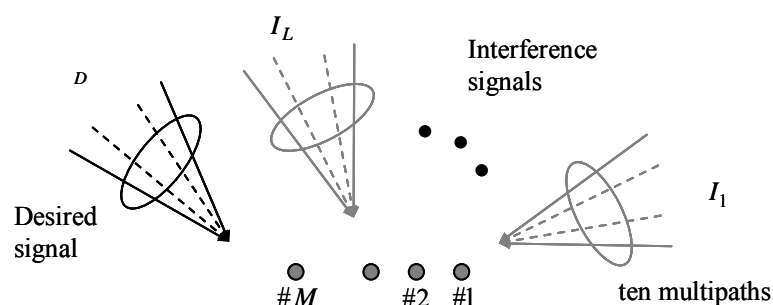


Fig. 8-2 Simulation environment

Table 8-1 Simulation environment

	Desired	Interfering
Total mean power (vs. noise)	20dB	20dB each
DOA (angular spread)	$30^\circ (5^\circ)$	$10^\circ, 80^\circ (5^\circ)$
No. of multipath	10	10 each
No. of Sources	1	2
Maximum Doppler ($f_d T_s$)	0.0 – 0.05	
Carrier frequency	1GHz	

Table 8-2 System parameters

No. of elements (M)	8
Forgetting factor (β)	0.75 - 1.0
Utilized post-symbols (P)	0 - 20
Utilized pre-symbols (q)	0 - 20
Modulation system	DQPSK

8.3.2 Simulation Results

In the simulation, SMI adaptive algorithm was used to calculate the weight. Here, $q = 0$ corresponds to the conventional SMI, where only post-received symbols are used to calculate the weight. We have considered two types of conventional SMI algorithms with (p, q) of $(10, 0)$ and $(20, 0)$, first one utilizes the same number of post-received symbols as the proposed algorithm while the second one equals the total number of utilized symbols with the proposed algorithm. System parameters are given in Table 8-2. In order to evaluate SINR accurately, SINR for hundred data symbols were averaged using the same weight vector at each iteration point. Cumulative distribution of SINR was calculated using ten thousand iteration points.

Figure 8-3 illustrates the time variant of the real part of the first element weight at $f_d T_s = 0.033$ and $\beta = 1.0$. Fig.8-3(a), (b) and (c) refer the result of $(p, q) = (0, 10)$, $(10, 0)$ and $(10, 10)$, respectively. It is apparent that Fig.8-3(b) is the time shift of Fig.8-3(a) by ten iteration periods. Though the results of $(p, q) = (0, 20)$ and $(20, 0)$ are not presented here, they resemble the time shift of $(10, 10)$ by twenty iteration periods.

When implementing SMI adaptive algorithm using only the past channel information under a time-variant propagation condition, the calculated channel characteristics will operate with a delay to that of the actual channel. On the other hand, the channel which is calculated using only future channel information will maintain a gain with the actual channel characteristics. This can be confirmed by previously described Fig.8-3(a) and Fig.8-3(b), which indicates that the weights of $(p, q) = (0, 10)$ and $(10, 0)$ contains a delay and a gain with the actual channel characteristic, respectively. On the other hand, the weight of the proposed algorithm, which considers both past and future channel information, is expected to be more closer to the actual channel characteristics and the expectation is confirmed by Fig.8-3(c), which weights remain between the weights of $(10, 0)$ and $(0, 10)$. Therefore a performance improvement with the application of the proposed adaptive algorithm to an adaptive array system under rapid fading conditions can be expected.

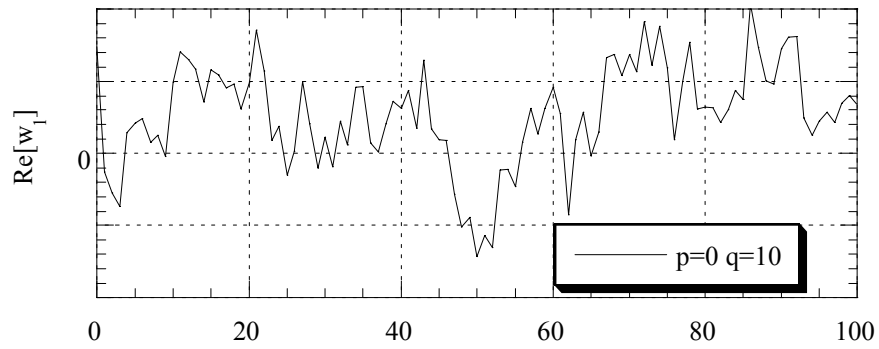
Figure 8-4 illustrates the temporal variation of SINR for both proposed and conventional SMI algorithm at $f_d T_s = 0.033$ and $\beta = 0.85$. Here the results for

$(p, q) = (0, 20)$, where only post-received symbols were used to calculate weight, is also illustrated as a reference. Result shows that the proposed algorithm gives a higher SINR compared to the conventional algorithms in this fast fading environment. Fig.8-5 shows the cumulative distribution of SINR for the same environment. This result quantitatively verifies the performance improvement with the application of the proposed adaptive algorithm.

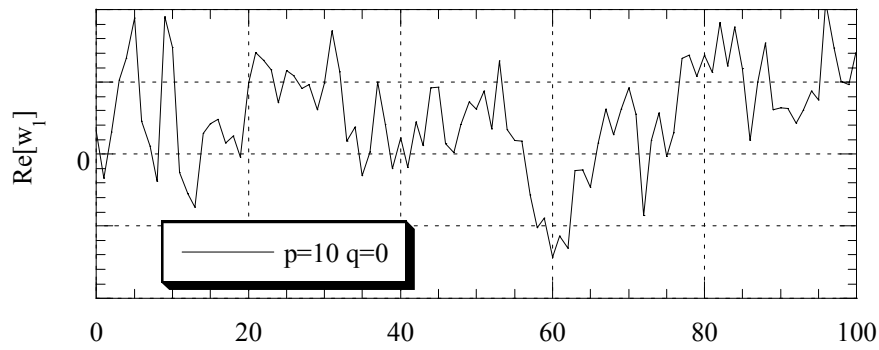
Furthermore simulations were carried out to optimize the system parameters given in Table 8-2. Fig.8-6 illustrates the relationship between the SINR and the number of utilized post- and pre-received symbols. Here the forgetting factor β is being used as a parameter. Ten thousand iteration points were considered when calculating the SINR for each combination of p , q and β . Figs.8-6(a) and (b) refer to the results at $f_d T_s = 0.001$ and $f_d T_s = 0.033$, respectively. Figure (a) shows that considerably higher values are suitable for p , q and β when the Doppler spread is fairly small. On the other hand, figure (b) shows that the performance of the algorithm increases with the decreasing the value of p , q and β when the Doppler spread becomes larger.

Above two results confirm that the optimal values of p , q and β are subject to vary with the environment. However, since the combination of $(p, q, \beta) = (10, 10, 0.85)$ gives a reasonable performance in both the environments, they can be considered as an appropriate combination.

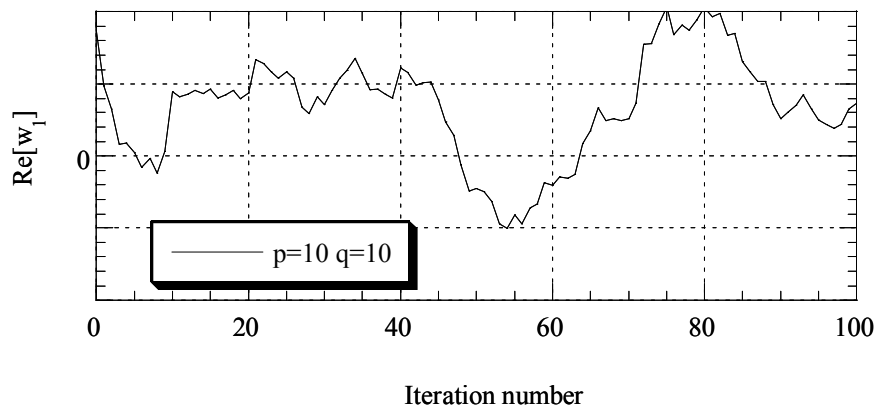
Figure 8-7 illustrates the relationship between SINR and Doppler frequency shift for proposed and conventional adaptive algorithms. Forgetting factor $\beta = 0.85$ was used in the simulation. Though the conventional (20,0) algorithm gives a similar SINR with the proposed (10,10) algorithm for $f_d T_s = 0$, its performance deteriorates with the increase of Doppler frequency. Conventional (10,0) algorithm could not reach the SINR value of proposed algorithm even at $f_d T_s = 0$, because of its less robustness against noise. The proposed algorithm maintains the best SINR for all Doppler values and verifies its ability to suppress the Doppler frequency shift and the influence of interference.



(a) $(p, q) = (0, 10)$



(b) $(p, q) = (10, 1)$



(c) $(p, q) = (10, 10)$

Fig. 8-3 Time variant of the real part of the first element weight at $f_d T_s = 0.033$ and $\beta = 1.0$

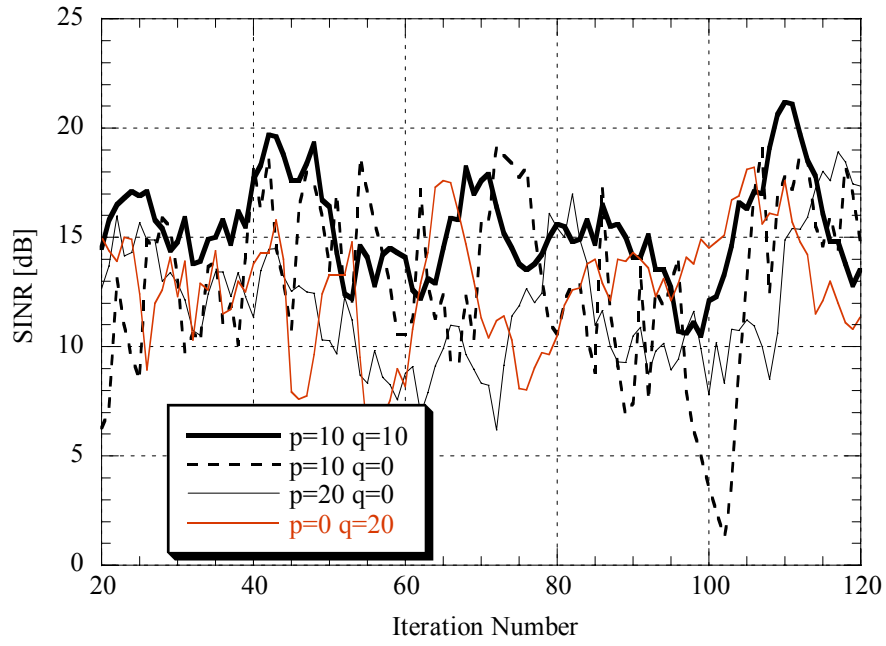


Fig. 8-4 Time variant of SINR at $f_a T_s = 0.033$ and $\beta = 0.85$

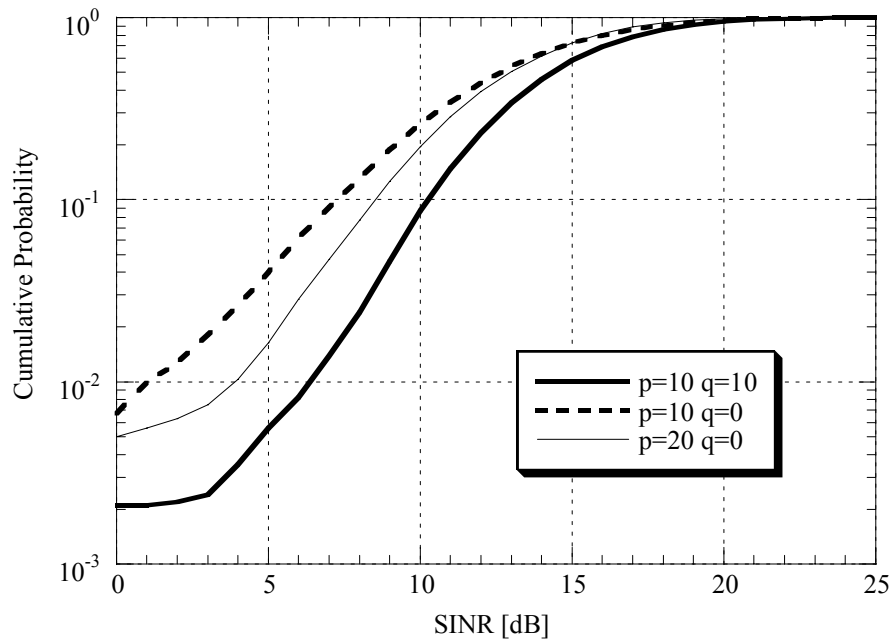
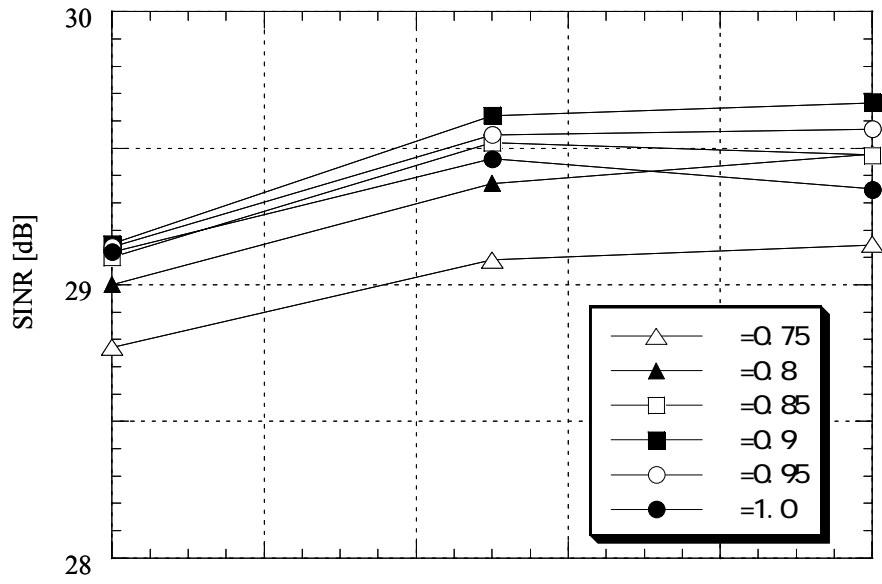
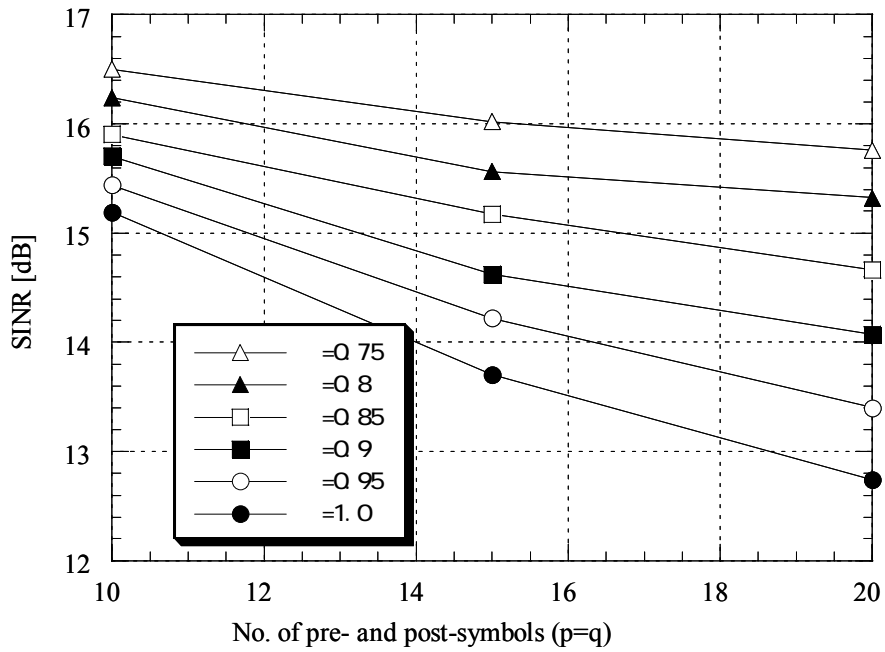


Fig. 8-5 Cumulative distribution of SINR at $f_a T_s = 0.033$ and $\beta = 0.85$



(a) $f_d T_s = 0.001$



(b) $f_d T_s = 0.033$

Fig. 8-6 SINR as a function of number of utilized pre- and post-received symbols ($p = q$)

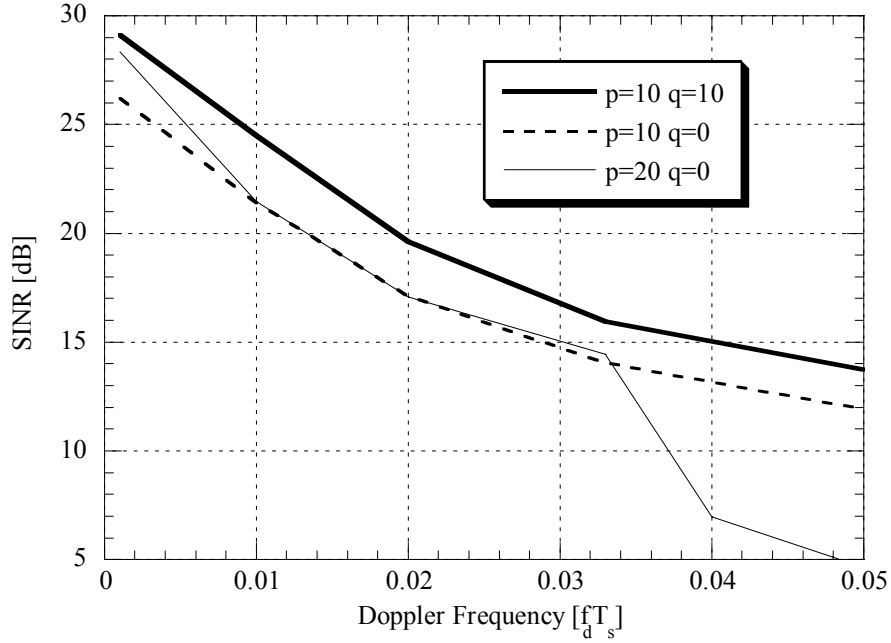


Fig. 8-7 SINR as a function of Doppler frequency shift ($\beta = 0.85$)

8.4 OFDM Application

As explained in section 8-2, the proposed adaptive algorithm only has the ability of tracking a pilot signal under a fast fading environment, but there is no room to carry additional data since the algorithm works only under the existence of a pilot signal. However, OFDM would be an appropriate application of our proposed algorithm since it has a large number of parallel subchannels. This will allow us to transmit a number of pilot channels and allocate the data subchannels between those pilot channels. In the receiver, proposed adaptive algorithm can be applied to the pilot subchannels and interpolate the weights for the data subchannels using the weights of the adjacent pilot subchannels.

8.4.1 OFDM Symbol

Figure 8-8 illustrates the OFDM symbol, which is intended to be applied in the proposed adaptive algorithm based on accumulated signal processing. As shown in the figure, a few subchannels are used as pilot channels, and a number of data subchannels are allocated between the pilot subchannels. Here r_i^k denotes the k^{th} pilot signal of the i^{th} OFDM symbol.

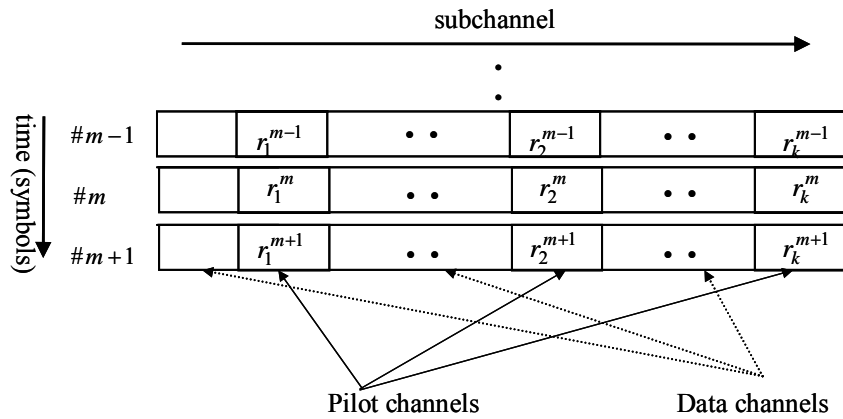


Fig. 8-8 OFDM symbol

8.4.2 Receiving Scheme of OFDM Application

Figure 8-9 illustrates the receiving scheme of the proposed adaptive algorithm based on accumulated signal processing with application to OFDM system. $w_m^k(i)$ denotes the weight of the k^{th} pilot subchannel of the m^{th} element for i^{th} OFDM symbol. In the receiver, first we demodulate the received OFDM signal of each array element separately. Secondly we combine the array output signals by performing the proposed adaptive algorithm. Here it should be noted that we perform the proposed algorithm only to the subchannels that are used as pilot channels, and interpolate the weight vectors for the data subchannels, which are allocated between the pilot subchannels.

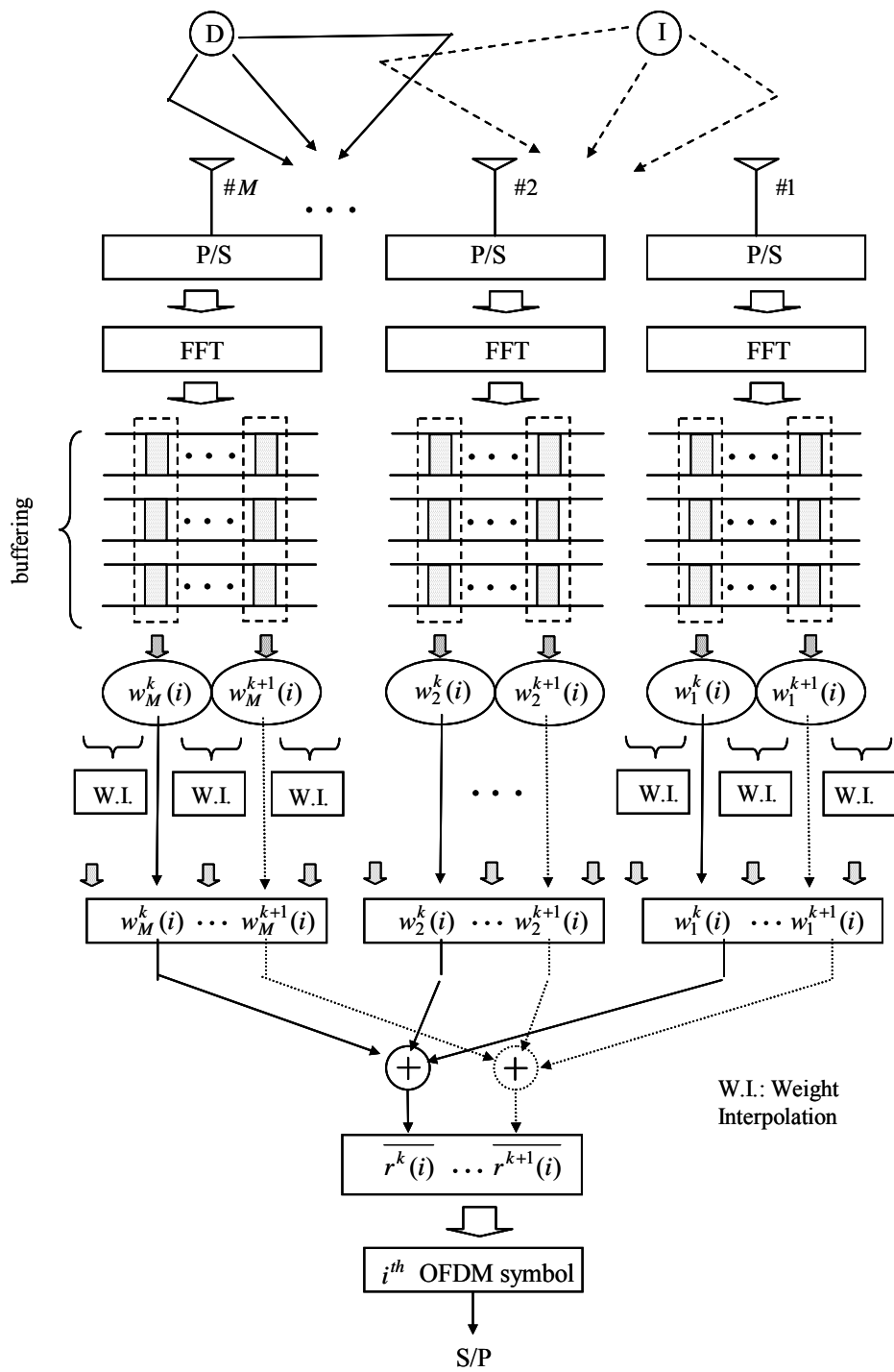


Fig. 8-9 Receiving scheme of OFDM application

8.4.3 Weight Interpolation

The weight vectors of the data subchannels, which are allocated between two pilot subchannels, have been interpolated using the weight vectors of those two pilot subchannels, as shown in Fig.8-10. The weight vector of the u^{th} data pilot subchannel from the k^{th} pilot symbol is given by

$$\mathbf{w}^{k,u}(i) = \mathbf{w}^k(i) + \frac{u}{U}(\mathbf{w}^{k+1}(i) - \mathbf{w}^k(i)) \quad (8-6)$$

where U and $\mathbf{w}^k(i)$ denote the number of data symbols allocated between two pilot symbols and the weight vector of the k^{th} pilot symbol of the i^{th} OFDM symbol, respectively.

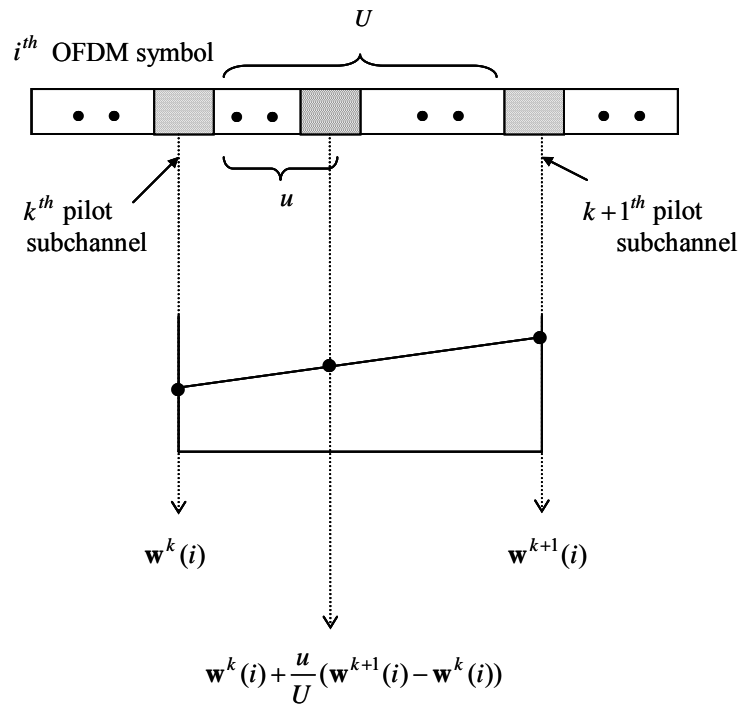


Fig. 8-10 Interpolation of weight vectors

8.4.4 Simulation Conditions and Results

After verifying the proposed adaptive algorithm with a single carrier system, we have adopted the algorithm to an OFDM communication system. Here too we have verified the system performance with a series of computer simulations.

The propagation model assumed here is as same as the one considered in the single carrier simulation. The DOA of the desired signal was set to 30° . The delay of the OFDM multipath signals were uniformly distributed within 0 to $3T_0$. In this simulation too we have considered two interfering sources located in the directions of 10° and 80° . Further, ten multipath signals from each interfering source reach to the antenna having angular spread of $N(DOA, 5^\circ)$ but no delay. OFDM system parameters are given in Table 8-3. Here T_0 denotes the duration of the original data symbol. Furthermore, SINR for each subchannel was calculated using hundred OFDM symbols.

Table 8-3 OFDM System parameters

Modulation System	DQPSK - OFDM
No. of subchannels	64
Guard Interval	$8T_0$
Data subchannels between two pilots(U)	4, 8

Figure 8-11 illustrates the Averaged SINR of each subchannel for proposed $(p, q) = (10, 10)$ algorithm, and conventional $(p, q) = (10, 0)$ and $(p, q) = (20, 0)$ SMI algorithms at $L = 2$ and $f_d T_s = 0.033$. Fig. 8-11(a) stands for the results of $U = 8$ and (b) for $U = 4$. The vertical lines in the graph indicate the locations of pilot subchannels. Result shows that the proposed algorithm gives a better SINR compared to the conventional algorithms. The SINR has deteriorated in data symbols, compared to the pilot subchannels in figure (a). On the other hand, the results in figure (b) confirms that the accuracy of the weight interpolation increases and maintains a stable SINR for each subchannel with the decrease of the number of data subchannels between two pilot subchannels, though it reduces the transmission efficiency. However the optimal number of data subchannels allocated between two pilot subchannels will depend on delay spread, symbol period, and number of subchannels. Further studies are required to optimize U .

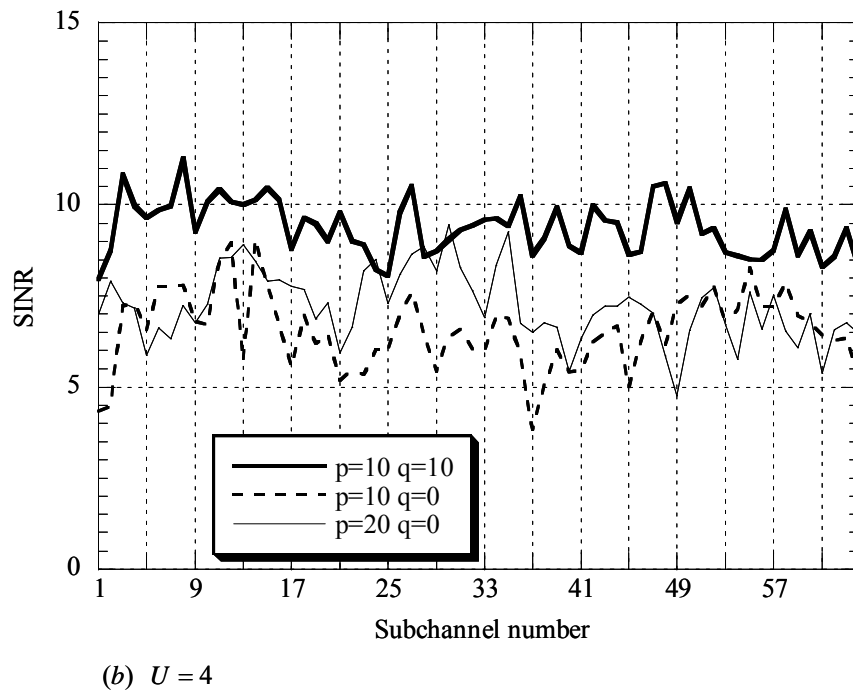
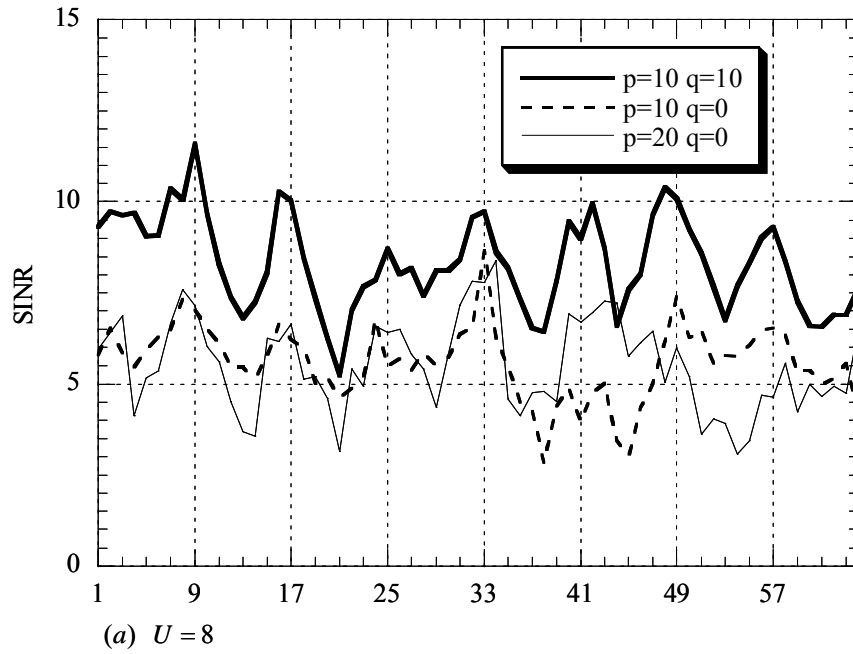


Fig. 8-11 Averaged SINR of each subchannel

8.5 Summary

This chapter has proposed an adaptive algorithm based on accumulated signal processing, which utilizes pre-received symbols as well as post-received symbols when optimizing the weight.

The proposed adaptive algorithm only tracks a pilot signal even under a fast fading environment, but there is no room to carry additional data since the algorithm works only under the existence of a pilot signal.

However, multi-carrier communication systems, such as OFDM have the ability of providing both pilot and data signals simultaneously to the adaptive algorithm utilizing its enormous number of subchannels. Therefore the combination of the proposed adaptive algorithm with OFDM will allow the adaptive algorithm to communicate while tracking the pilot.

The chapter has also discussed on applying the proposed algorithm to Post-FFT-type OFDM adaptive array by allocating a few subchannels as pilot channels and interpolating the weight vector of the data subchannels, which are allocated between the pilot subchannels.

Computer simulation has confirmed that the proposed algorithm gives a better SINR compared to the conventional algorithms in fast fading conditions.

Chapter 9

Conclusions and Future Work

This chapter concludes our work by summarizing the results and future work.

9.1 Conclusions

In this work, the fundamentals of OFDM, AAA and DTTB are described in chapter 2, 3 and 4, respectively. In chapter 5 BSAAA is introduced to suppress the Doppler frequency spread in mobile reception of OFDM signal. Chapter 6 proposes to use directional element AAA in mobile reception of DTTB. ED-RLS adaptive algorithm to achieve a fast convergent rate in AAA and accumulated signal processing based adaptive algorithm to improve the adaptability of AAA in fast fading environments are introduced in chapter 7 and 8, respectively.

Following are the concluding remarks that are obtained in this work

- ✓ A BSAAA receiver for OFDM mobile reception is proposed and system performances are verified by computer simulations. Particularly it has shown the possibility of efficient Doppler spread suppression for all incident angles by the use of 8-element BSAAA with element spacing of $(3/8)\lambda$.
- ✓ The influence of the iterative numbers of past OFDM symbols, when calculating the correlation matrix among the beam output signals for each subchannel in BSAAA-based OFDM mobile receiver is evaluated and it was verified by computer simulation that considering only 3 past symbols is sufficient to suppress the ICI due to Doppler spread.
- ✓ A receiving quality evaluation on omni-directional- and directional-element OFDM AAA is done and confirmed that both AAA give similar performances. However, further simulations showed that remarkable performance improvement can be achieved with the application of Doppler despreading along with directional-element AAA.
- ✓ Eigenvalue decomposition based adaptive algorithm, namely ED-RLS is introduced in order to achieve a fast convergence rate in environments with less number of interference sources but with any number of multipaths. Further, we verified by computer simulation that the proposed scheme gives rapid convergence compared to

conventional RLS algorithm in an environment with considerably large noise power along with a strong interference signal. Finally the application of ED-RLS algorithm to an OFDM modulation system is discussed.

- ✓ An accumulated signal processing based adaptive algorithm, which utilizes pre-received symbols as well as post-received symbols when optimizing the weight is introduced and confirmed by computer simulation that the proposed algorithm performs well under fast fading conditions compared to conventional algorithms. Further application of proposed algorithm to Post-FFT-type OFDM-AAA is discussed and evaluated by computer simulation.

9.2 Future Work

Following above mentioned concluding remarks, there are several areas that could be extended for future research.

- ✓ In our Doppler despreading method, the speed of the vehicle is considered as a known factor. However, this method could be extended by calculating the Doppler shift of each beam directly from the received signal using the pilots.
- ✓ Beam pattern of BSAAA that introduced in chapter 5 depends on the wavelength. This will affect the performance of Doppler despreading since the wavelength is different from DTTB channel to channel. An evaluation of this influence is essential to be done. Further, if the influence is countable, a scheme to overcome this is still open for further research.
- ✓ Although the application of ED-RLS algorithm to Post-FFT-type OFDM-AAA is discussed, a sufficient performance evaluation is yet to be done.
- ✓ Linear interpolation is used in weight calculation for data subchannels in introduction of proposed adaptive algorithms to OFDM communication system in Chapter 7 and 8. More appropriate method would improve the system performance.

References

- [1] R.W. Chang and R.A. Gabby, "A Theoretical Study of Performance of and Orthogonal Multiplexing Data Transmission Scheme," IEEE Trans. Commn., COM-16, pp.529-540, 1968.
- [2] S. B. Weinstein and P. W. Ebert, "Data Transmission by Frequency Division Multiplexing using the Discrete Fourier Transform," IEEE Trans. Commn., COM-19, pp.628-634, 1971
- [3] H. Sari, G. Karam, and I. Jeanclaude, "Transmission techniques for digital terrestrial TV broadcasting," IEEE Commun. Magazine, vol.33, pp.100-109, Feb. 1995
- [4] L. Hanzo, "Bandwidth-efficient wireless multimedia communications," Proc. IEEE, vol.86, no.7, pp.1342-1382, July 1998
- [5] H. Atarashi, N. Maeda, S. Abeta and M.Sawahashi, "Broadband packet wireless access based on VSF-OFCDM and MC/DS-CDMA," in Proceedings of the IEEE Int. Personal, Indoor and Mobile Radio Commun. (PIMRC 02), Portugal, pp.992-997, Sept. 2002.
- [6] A. Svensson, A. Ahlen, A. Brunstrom, T. Ottosson and M. Strenad, "An OFDM based system proposal for 4G downlinks," in Proceeding of the Int. Workshop pn Multi-Carrier Spread-Spectrum and Related Topics (MC-SS 03), pp.15-22, Sept. 2003
- [7] Paul H. Moose, "A Technique for Orthogonal Frequency Division Multiplexing Frequency Offset Correction," IEEE Trans. communication, vol.42, no.10, pp.2908-2914, Oct. 1994
- [8] H. Ohta, M Itami, A. Tsuzuku, "A Study on Mulatipath Channel Modeling for Mobile Reception with an OFDM and Equalization Method for Reducing Interference by Using Estimated Propagation Path Characteristics," ITE Tans., vol.52, No.11, pp.1667-1675, 1998
- [9] T.Pollet, M. van Bladel, and M.Moeneclay, "BER sensitivity of OFDM systems to carrier frequency offset and Wiener phase noise," IEEE Trans. Communication, vol.43, pp.191-193, Feb./Mar./Apr. 1995
- [10] C. Muschallik, "Improving an OFDM reception using an adaptive Nyquist windowing," IEEE Trans. Consumer Electron, vol. 42, Aug. 1996.
- [11] Y. Zhao and S.G. Haggman, "Sensitivity to Doppler shift and carrier frequency errors in OFDM systems – The consequences and solutions," in IEEE 46th Vehicular Technology Conf., Atlanta, GA, Apr. 1996, pp.1564-1568.

- [12] T. Wada, M. Okada, H. Yamamoto, "Adaptive Modulation with Fast Fading Compensation Using Space-Domain Interpolation Filtered Array Antenna," Technical report of IEICE, RCS 2000-158, Oct. 2000.
- [13] T. Suzuki, S. Sampei and N. Morinaga, "Directive antenna diversity reception scheme for an adoptive modulation system in high mobility land mobile communications," IEICE Trans. Commun. Vol. E79-B, No.3, pp. 335-341, March 1996.
- [14] A. F. Naguib and A. Paulraj, "Performance of wireless CDMA with M-ary orthogonal modulation and cell site antenna arrays", IEEE J. Selected Areas Comm., vol.14, no.9, pp.1770-1783, Dec. 1996
- [15] V. K. Garg and L. Huntingotn, "Application of adaptive array antenna to a TDMA cellular / PCS system," IEEE Comm. Magazine, vol.35, pp.148-152, Oct 1997
- [16] M. Budsabathon, S. Hane, Y. Hara and S. Hara, "On a novel pre-FFT OFDM adaptive antenna array for signal suppression," IEICE Trans. Commun., vol.E86-B, no.6, pp.1936-1945, June. 2003
- [17] C. K. Kim, K. Lee and Y. S. Cho, "Adaptive Beamforming Algorithm for OFDM Systems with Antenna Arrays," IEEE Trans. On Consumer Lectronics, vol.46, no.4 Nov. 2000
- [18] P.S. Wijesena, Y. Karasawa, "Beam-space adaptive array antenna for suppressing the Doppler spread in OFDM mobile reception," IEICE Trans. Commun., vol.E87-B, no.1, pp.20-28, Jan. 2004.
- [19] N. Kikuma, Adaptive Signal Processing with Array Antenna, Science and Technology Publishing Co., Ltd., Japan, 1999
- [20] Y. Kamiya, Y. Karasawa, S. Denno, and Y. Mizuguchi, "A Software Antenna: Reconfigurable Adaptive Arrays Based on Eigenvalue Decomposition," IEICE Trans. Commun., Vol. E82-B, NO. 12, pp. 2012-2019, Dec. 1999.
- [21] Y. Li and N. R. Sollenberger, "Adaptive antenna arrays for OFDM system with cochannel interference," IEEE Trans. Commun., vol.47, pp.217-229, Feb. 1999
- [22] P.S. Wijesena, T. Taniguchi and Y. Karasawa, "Eigenvalue Decomposition Based Recursive Least-Squares Algorithm for OFDM Communications over Fast Time-Varying Channels," IEEE Topical Conference on Communication Technology Conference, Hawaii, Oct.2003
- [23] K. Wong, R. Cheng and K. Letaief, "Adaptive antennas at the mobile and base stations in an OFDM/TDMA system," IEEE Trans. Commun., vol.49, no.1, pp.195-205, Jan. 2001

- [24] R.W. Chang, "Synthesis of Band Limited Orthogonal Signal for Multichannel Data Transmission," *Bell Syst. Tech. J.*, Vol. 45, pp. 1775-1796, Dec. 1996.
- [25] A. Sugimoto and T. Araseki, "Current Status of Digital Terrestrial Broadcasting," NEC Technical Report Vol.57, No.4, 2004
- [26] H. Asami, "Digital Broadcasting in Japan HDTV – HDTV and Mobile Reception as Key Applications," Document of Ministry of Public Management, Home Affairs, Posts and Telecommunications (MPHPT)" (<http://www.broadcastpapers.com/BcastAsia04/BAsia04MPHPTJapanHDTV.pdf>)
- [27] Terrestrial Intergrated Service Digital Broadcasting, Document of Digital Broadcasting Experts Group (DiBEG)" (http://www.dibeg.org/techp/Documents/Isdb-t_spec.PDF)
- [28] Thorton, S. T. and A. Rex. *Modern Physics for Scientists and Engineers*. 2nd ed. Florence: Thomson Learning, Inc., 2002.
- [29] H. Yamada, R. Hara, Y. Ogawa and Y. Yamaguchi "On Performance Comparison of Calibration Techniques for Mutual Coupling Effect in Array Antennas," Technical Report of IEICE Communication Society, pp. 179-186, March 2003
- [30] K. Tsuchida and S. Nakahara, "Mobile Reception of Digital Terrestrial HDTV," *Trans. ITE*, Vol.58, No.5, pp.618-620, 2004.
- [31] W.C. Jakes, Ed., *Microwave Mobile Communications*, NY:IEEE Press, 1993
- [32] Chang Qing Xu, Choi Look Law, "On the Doppler Power Spectrum at the Mobile Unit Employing a Directional Antenna," *Letter, IEEE Commun.* Vol.5 No.1, pp. 13-15, Jan, 2001.
- [33] P. S. Wijesena, Y. Karasawa, "Optimizing the MRC of OFDM Doppler Spread Suppressing Beam-Space Adaptive Array," IEICE general conference, B-5-81, Sept. 2002
- [34] H. Iwai and Y. Karasawa, "Wideband propagation model for the analysis of the effect of the multipath fading on the near-far problem in CDMA mobile radio systems," *IEICE Trans Comm.*, E76-B, 2, pp. 103-112, 1993.

List of Original Publications

Journal Papers

1. P.S. Wijesena, Y. Karasawa, "Beam-space adaptive array antenna for suppressing the Doppler spread in OFDM mobile reception," IEICE Trans. Commun., vol.E87-B, no.1, pp.20-28, Jan. 2004.
2. P.S. Wijesena, T. Taniguchi, Y. Karasawa, "Adaptive algorithm based on accumulated signal processing for fast fading channels with application to OFDM mobile radio," IEICE Trans. Commun., vol.E88-B, no2, pp.568-574, Feb.2005.

International Conference Papers

1. P. S. Wijesena and Y. Karasawa, "Beam-Space Adaptive Array Antenna for Suppressing the Doppler Spread in OFDM Mobile Reception," Interim International Symposium on Antennas and Propagation (ISAP), Yokosuka Research Park, Japan, pp.37-40, Nov.26-28, 2002.
2. P. S. Wijesena, T. Taniguchi and Y. Karasawa, "Eigenvalue Decomposition Based Recursive Least-Squares Algorithm for OFDM Communications over Fast Time-Varying Channels," IEEE Topical Conference on Communication Technology Conference, Hawaii, Oct.2003.
3. P. S. Wijesena, T. Taniguchi and Y. Karasawa, "Adaptive Algorithm Based on Accumulated Signal Processing for Fast Fading Channel," Interim International Symposium on Antennas and Propagation (ISAP'04), Sendai, Japan, vol.2, pp.653-656, Aug.17-21, 2004.
4. P. S. Wijesena, T. Taniguchi and Y. Karasawa, "Comparison of Isotropic and Directive Adaptive Array Antennas in OFDM Mobile Reception of Terrestrial Digital Television," Interim International Symposium on Antennas and Propagation (ISAP'05), Seoul, Korea, vol.2, pp.531-534, Aug.3-5, 2005.

Other Conference Papers

1. P. S. Wijesena, Y. Karasawa, "Beam-Space Adaptive Array Antenna for Suppressing the Doppler Spread in OFDM Mobile Reception," Technical Report of IEICE, AP2002-7, pp.37-42, 2002.4
2. P. S. Wijesena, Y. Karasawa, "Optimizing the MRC of OFDM Doppler Spread Suppressing Beam Space Adaptive Array Antenna," IEICE Society Conference2002.9
3. P. S. Wijesena, 唐沢好男, 谷口哲樹, "固有値分割によるアダプティブアレーの収束の高速化," 信学総大, B-5-188, p.647, 2003.3
4. P. S. Wijesena, T. Taniguchi, Y. Karasawa, "Adaptive Algorithm based on Accumulated Signal Processing for Fast Fading Channel," Technical Report of IEICE, WBS2003-129, AP2003-322, RCS2003-345, MoMuC2003-123, MW2003-291(2004-03), pp.69-73, 2004.3
5. P. S. Wijesena, 竹本淳, 唐沢好男, "地上デジタルテレビの移動受信シミュレータを用いたドップラー変動による受信劣化評価," 信学会ソサイエティ大会, B-5-62, 2004.9
6. 竹本淳, P. S. Wijesena, "唐沢好男, "デジタル放送波のトータルレコーディングと移動体受信特性評価シミュレータ," 第487回 URSI-F 分科会資料, 2004.9
7. 竹本淳, P. S. Wijesena, 唐沢好男, "地上デジタルテレビジョン放送波のトータルレコーディング," RCS2004-25, CQ2004-25, pp.7-12, 2004.4
8. P. S. Wijesena, 谷口哲樹, 唐沢好男, "Fast Fading 環境を対象とする蓄積信号処理型アダプティブアルゴリズム," 信学総大, B-5-10, p.497, 2004.3
9. P. S. Wijesena, A. Takemoto, Y. Karasawa, "Mobile Reception Simulator for Digital Terrestrial Television based on Total Recording," Technical Report of IEICE, A.P2004-179, RCS2004-200, pp.1-4, 2004.10
10. P. S. Wijesena, A. Takemoto, Y. Karasawa, "Directional-Element Adaptive Array Antenna for Mobile Reception of Digital Terrestrial Television," Technical Report of IEICE, A.P2005-60, pp.131-136, 2005.7
11. P. S. Wijesena, A. Takemoto, Y. Karasawa, "Pre-demodulated Frequency Domain OFDM Adaptive Array," IEICE Society Conference, B-5-33, 2005.9
12. 竹本淳, P. S. Wijesena, 唐沢好男, "地上デジタル放送波のトータルレコーディングにおけるクリティカルサンプリング," 信学ソ大, B-5-127, 2005.9.
13. P. S. Wijesena, A. Takemoto, A. Kanda, Y. Karasawa, "Digital Television Mobile Reception Simulator using Actual DTTB Signal," Technical Report of ITE, BCT2005-125, Vol.29, No.57, pp.5-8, 2005.10
14. 竹本淳, P. S. Wijesena, 神田明彦, 唐沢好男, "地上デジタル TV 放送波のトータルレコーディング—パソコン収録の現時点での実力を探る—," 映像情報メディア学会技術報告, BCT2005-124, Vol.29, No.57, pp.1-4, 2005.10

15. 神田明彦、竹本淳、P. S. Wijesena、唐沢好男，“地上デジタル放送波のトータルレコーディングによる実環境移動体受信特性評価,” 電子情報通信学会技術報告, 2006.02
16. 竹本淳、神田明彦、P. S. Wijesena、唐沢好男，“地上デジタルテレビジョン放送の移動体受信特性評価用トータルレコーディングシステム,” 電子情報通信学会技術報告, 2006.02

Author Biography

Pubudu Sampath Wijesena was born in Sri Lanka on the 31st October 1974. He obtained a Diploma in Electronic Engineering from Sendai National College of Technology in March 1999. He received the Bachelor of Engineering in Electronics from the University of Electro-Communications, Tokyo, Japan in 2001 and Master of Engineering in Electronics from the same university in 2003. From April 2003 to March 2006 he was a doctorate candidate in the Department of Electronic Engineering in the same university. He was also a research assistant at the same department from April 2005 to March 2006. His research interests are in the areas of Adaptive Array Antenna (AAA) with application to Orthogonal Frequency Division Multiplexing (OFDM). He is a student member of the Institute of Electronics, Information and Communications Engineering Japan (IEICE), and the Institute of Electrical and Electronics Engineers (IEEE).